NASA CR-132410-3

# RELATIVE MOTION OF ORBITING PARTICLES UNDER THE INFLUENCE OF PERTURBING FORCES

## Volume III

(Construction of Relative Motion Traces)



105

J.B. Eades, Jr.



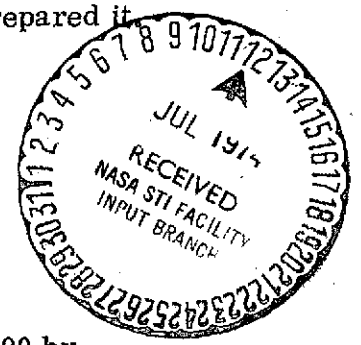


Prepared under Contract NAS1-11990 by
ANALYTICAL MECHANICS ASSOCIATES, INC.
(Report No. 73-39)

for

LANGLEY RESEARCH CENTER
August 1973


ANALYTICAL MECHANICS ASSOCIATES, INC.
10210 GREENBELT ROAD
SEABROOK, MARYLAND 20801

TABLE OF CONTENTS


| | | Page |
|---|---|---|
| SYMBOLS AND SELECTED EQUATIONS | | v |
| CONSTRUCTION OF RELATIVE MOTION TRACES | | 1 |
| I. | INTRODUCTION | 1 |
| II. | DISPLACEMENTS FOR THE ROTATING FRAME OF REFERENCE | 3 |
| | II.1 The Initial Values Problem | 3 |
| | II.2 The Non-Secular Initial Values Problem | 6 |
| | II.3 The Zero Initial Value Problem | 7 |
| III. | THE HODOGRAPH FOR A ROTATING FRAME OF REFERENCE | 12 |
| | III.1 The Initial Values Problem | 12 |
| | III.2 The Non-Secular Case | 13 |
| | III.3 The Zero Initial State Case | 14 |
| | III.4 Special Cases | 15 |
| IV. | DISPLACEMENTS IN THE INERTIAL FRAME OF REFERENCE | 18 |
| | IV.1 The Initial Values Problem | 18 |
| | IV.2 The Non-Secular Initial Values Problem | 21 |
| | IV.3 The Zero Initial Value Problem | 23 |
| V. | THE HODOGRAPH IN THE INERTIAL FRAME OF REFERENCE | 26 |
| | V.1 The Initial Values Problem | 26 |
| | V.2 The Non-Secular Initial Values Problem | 27 |

Page

V. THE HODOGRAPH IN THE INERTIAL FRAME OF REFERENCE (cont)

V.3 The Zero Initial State Case ..... 29

VI. THE INERTIALLY ALIGNED FORCE SYSTEM ..... 36

VII. DISPLACEMENTS FOR THE ROTATING FRAME OF REFERENCE ..... 37

VII.1 The Zero Initial State Problem ..... 37

VII.2 Special Cases ..... 40

VIII. THE HODOGRAPH FOR A ROTATING FRAME OF REFERENCE ..... 44

VIII.1 The Zero Initial Value Problem ..... 44

VIII.2 Special Cases ..... 46

IX. DISPLACEMENTS FOR THE INERTIAL FRAME OF REFERENCE ..... 50

IX.1 The Zero Initial Value Problem ..... 50

IX.2 Special Cases ..... 54

X. THE HODOGRAPH IN THE INERTIAL FRAME OF REFERENCE ..... 56

X.1 The Partial Solution due to $\bar{\tau}_I$ only ..... 56

X.2 Special Cases ..... 58

XI. OUT-OF-PLANE TRACE CONSTRUCTIONS ..... 63

XII. DISPLACEMENTS FOR THE INITIAL-VALUES PROBLEM ..... 65

(a) Local, Rotating Frame of Reference ..... 65

(b) The Inertial Frame of Reference ..... 68

Page

XIII. HODOGRAPHS FOR THE INITIAL VALUES PROBLEM ..... 70

(a) Local, Rotating Frame of Reference ..... 70

(b) Hodographs in the Inertial Frame of Reference ..... 72

XIV. ZERO INITIAL VALUE PROBLEMS ..... 75

(a) Local, Rotating Frame of Reference ..... 75

(b) The Inertial Frame of Reference ..... 77

XV. HODOGRAPHS FOR THE ZERO INITIAL VALUES PROBLEM ..... 80

(a) Local, Rotating Frame of Reference ..... 80

(b) Hodographs in the Inertial Frame of Reference ..... 80

XVI. OUT-OF-PLANE DISPLACEMENTS, DUE TO $\bar{\tau}_I$ ..... 84

(a) Local, Rotating Frame of Reference ..... 84

(b) Displacements in the Inertial Frame of Reference ..... 85

XVII. OUT-OF-PLANE HODOGRAPHS, DUE TO $\bar{\tau}_I$ ..... 91

(a) Local, Rotating Frame of Reference ..... 91

(b) Inertial Frame of Reference ..... 91

XVIII. SUMMARY ..... 97

## SYMBOLS

| | |
|---|---|
| A<br>$[A_a, A_{a_I}; (A_1, A_2)]$ | Matrix of constants (initial state quantities and specific force(s)) acquired in the analytical solution ($A_{1,2}$ formed by multiplication $J_i A_a$, $(i = 1, 2)$). |
| B<br>$[B_2]$ | An operator matrix; $B_2 \equiv \begin{bmatrix} 0 & -1 \\ 1 & 0 \end{bmatrix}$. |
| $I_j$ $(j \equiv 1, 2, 3)$ | The Idem matrix; subscript denotes order. |
| $J_i$ $(i = 1, 2, 3)$ | Special single non-zero element diagonal matrices; subscript denotes position of non-zero element, (e.g. $J_1 \equiv \begin{bmatrix} 1 & 0 \\ 0 & 0 \end{bmatrix}$, $J_2 \equiv \begin{bmatrix} 0 & 0 \\ 0 & 1 \end{bmatrix}$. |
| K<br>$[K_o, K_{o_I}; (K_1, K_2)]$ | Matrix composed of initial value quantities only; $(\sim)_I$ denotes quantities referred to the inertial frame of reference ($K_{1,2}$ obtained by multiplication, $J_i K_o$ $(i = 1, 2)$). |
| $T(\varphi^{\pm})$ | Transformation matrices; used to transfer vectors from one frame of reference to another. $(T(\varphi^{\pm}) \equiv I_2 \cos\varphi \mp B_2 \cos\varphi + J_3)$. |
| $\bar{h}$ , $\bar{h}'$ | Dimensionless relative state vectors, referred to the "local-rotating" frame of reference. |
| $\bar{R}$, $\bar{R}'$ | Dimensionless relative state vectors, referred to the inertial frame of reference. |
| $\varphi$ | Transfer angle measured on the base, circular orbit; also, the independent variable for the dimensionless expressions. |
| $\xi$, $\eta$, $\zeta$;<br>$\xi'$, $\eta'$, $\zeta'$ | Dimensionless cartesian relative "position" and "speed" scalars; referred to the local, rotating frame of reference ($\xi$ is the radial component; $\zeta$ is the out-of-plane component; $\eta$ completes the orthogonal triad). |

| | |
|---|---|
| $\Xi$, H, Z;<br>$\Xi'$, H', Z' | Dimensionless cartesian relative "position" and "speed" scalars; referred to the inertially aligned frame of reference ($\Xi$ is analogous to $\xi$; Z is parallel to $\zeta$; H completes the orthogonal triad). |
| $\bar{\tau}(\tau_i)$<br>$[\bar{\tau}_I]$ | The dimensionless specific force vector (scalars). Subscripts (i) are included to denote direction (relative to the triad of reference); $(\sim)_I$ designates the vector to be inertially aligned. |

Subscripts and Superscripts

| | |
|---|---|
| $(\sim)_o$ | Designates an initial value quantity. |
| $(\sim)_{i.v.}$ | Used to indicate the matrix, to which affixed, contains only initial valued quantities. |
| $(\sim)_\tau$ | Used to indicate the matrix, to which affixed, contains only $\bar{\tau}$ quantities. |
| $(\sim)^{(1)}$ | A specialization of the matrix to which affixed (specialized, as noted). |

## SELECTED EQUATIONS

1. $$A_a \equiv \frac{1}{2}\left\{3J_1\bar{\hbar}_o + \left[J_2 - 2J_1\right]B_2\bar{\hbar}'_o + \left[J_1 - 2J_2\right]\bar{\tau}\right\}$$

$$= \frac{1}{2}\begin{bmatrix} 3 & 0 \\ 0 & 0 \end{bmatrix}\begin{bmatrix} \xi_o \\ \eta_o \end{bmatrix} + \begin{bmatrix} 0 & 2 \\ 1 & 0 \end{bmatrix}\begin{bmatrix} \xi'_o \\ \eta'_o \end{bmatrix} + \begin{bmatrix} 1 & 0 \\ 0 & -2 \end{bmatrix}\begin{bmatrix} \tau_\xi \\ \tau_\eta \end{bmatrix} .$$

2. $$K_o \equiv \left[4J_1 + J_2\right]\bar{\hbar}_o - 2B_2\bar{\hbar}'_o$$

$$= \begin{bmatrix} 4 & 0 \\ 0 & 1 \end{bmatrix}\begin{bmatrix} \xi_o \\ \eta_o \end{bmatrix} + \begin{bmatrix} 0 & 2 \\ -2 & 0 \end{bmatrix}\begin{bmatrix} \xi'_o \\ \eta'_o \end{bmatrix} .$$

3. $$\Psi_\tau \equiv \left[J_1 + 4J_2\right] - \varphi\left[2B_2 + \frac{3}{2}J_2\varphi\right]$$

(equation continued on next page)

3. (cont)

$$= \begin{bmatrix} 1 & 0 \\ 0 & 4 \end{bmatrix} - \begin{bmatrix} 0 & -2\varphi \\ 2\varphi & \frac{3\varphi^2}{2} \end{bmatrix} .$$

4. $$\Psi'_\tau \equiv -\left[2B_2 + 3J_2\varphi\right]$$

$$= \begin{bmatrix} 0 & 2 \\ -2 & 0 \end{bmatrix} + \begin{bmatrix} 0 & 0 \\ 0 & -3\varphi \end{bmatrix} .$$

5. $$A_{a_I} \equiv \frac{1}{2}\left\{I_2 \bar{\Re}_o + \left[J_2 - 2J_1\right] B_2 \bar{\Re}'_o + \left[J_1 - 2J_2\right] \bar{\tau}\right\}$$

$$= \frac{1}{2} \begin{bmatrix} 1 & 0 \\ 0 & 1 \end{bmatrix} \begin{bmatrix} \Xi_o \\ H_o \end{bmatrix} + \begin{bmatrix} 0 & 2 \\ 1 & 0 \end{bmatrix} \begin{bmatrix} \Xi'_o \\ H'_o \end{bmatrix} + \begin{bmatrix} 1 & 0 \\ 0 & -2 \end{bmatrix} \begin{bmatrix} \tau_\xi \\ \tau_\eta \end{bmatrix} .$$

6. $$\Phi_\tau = \left[2J_1 + 5J_2\right]\left[T_2(\varphi^+) - I_2\right] + \frac{3\varphi}{2}\left[J_1 + 2J_2\right]\left[J_2B_2 + B_2T_2(\varphi^+)\right]$$

$$+ \frac{1}{4}\left[J_1 - 2J_2\right]\left[T_2(\varphi^-) - T_2(\varphi^+)\right]$$

$$= -\begin{bmatrix} 2(1-\cos\varphi) & 2\sin\varphi \\ 5\sin\varphi & 5(1-\cos\varphi) \end{bmatrix} + \frac{3\varphi}{2} \begin{bmatrix} \cos\varphi & -\sin\varphi \\ 2(1+\sin\varphi) & 2\cos\varphi \end{bmatrix}$$

$$- \frac{1}{2} \begin{bmatrix} 0 & \sin\varphi \\ 2\sin\varphi & 0 \end{bmatrix} .$$

7. $$\Phi'_\tau = -\left[2J_1 + 5J_2\right] B_2T_2(\varphi^+) + \frac{3}{2}\left[J_1 + 2J_2\right]\left[J_2B_2 + (I_2 - B_2\varphi)\, B_2T_2(\varphi^+)\right]$$

$$+ \frac{1}{4}\left[J_1 - 2J_2\right] B_2\left[T_2(\varphi^-) + T_2(\varphi^+)\right]$$

(equation continued on next page)

$$= -\begin{bmatrix} 2\sin\varphi & -2\cos\varphi \\ 5\cos\varphi & 5\sin\varphi \end{bmatrix} + \begin{bmatrix} 0 & 0 \\ 3 & 0 \end{bmatrix} + \frac{3}{2}\begin{bmatrix} \sin\varphi + \varphi\cos\varphi & -\cos\varphi + \varphi\sin\varphi \\ 2(\cos\varphi - \varphi\sin\varphi) & 2(\sin\varphi + \varphi\cos\varphi) \end{bmatrix}$$

$$- \frac{1}{2}\begin{bmatrix} 0 & \cos\varphi \\ 2\cos\varphi & 0 \end{bmatrix} .$$

8. $$J_1 B_2 = \begin{bmatrix} 0 & -1 \\ 0 & 0 \end{bmatrix} = B_2 J_2, \qquad J_2 B_2 = \begin{bmatrix} 0 & 0 \\ 1 & 0 \end{bmatrix} = B_2 J_1 .$$

9. $$B_2 \equiv \begin{bmatrix} 0 & -1 \\ 1 & 0 \end{bmatrix}, \quad B_2^{\,2} = -I_2 = \begin{bmatrix} -1 & 0 \\ 0 & -1 \end{bmatrix} .$$

10. $$T_2^{-} = I_2 \cos\varphi + B_2 \sin\varphi = \begin{bmatrix} \cos\varphi & -\sin\varphi \\ \sin\varphi & \cos\varphi \end{bmatrix} \equiv T_2(\varphi^{-}) ,$$

$$T_2(\varphi^{+}) = I_2 \cos\varphi - B_2 \sin\varphi = \begin{bmatrix} \cos\varphi & \sin\varphi \\ -\sin\varphi & \cos\varphi \end{bmatrix} .$$

# CONSTRUCTION OF RELATIVE MOTION TRACES

## I. INTRODUCTION

This report contains information on the construction of relative motion traces developed as a consequence of various input conditions. The formulae used here stem from analytical results acquired from a linearized set of governing ordinary differential equations. The inputs used in these solutions were the initial state values and a specific force system which was assumed to be aligned with either a local, rotating triad of reference or with an inertially aligned triad. Since the results for these inputs are independent of one another the traces represent: (1) an initial values problem, without specific forces present; and (2), the zero-initial values problem, where only the specific forces are considered. In order to retain a compact and concise system of notation, throughout, the state variables and the specific force(s) are manipulated and presented in a dimensionless format. For these representations the relative motion state variables have been normalized by the radius and speed, respectively, of the base, circular reference orbit. The specific force has been normalized by the specific centrifugal force experienced by a unit mass particle on the base orbit.

Since the analytical expressions used herein allow the in-plane state to be separated from the out-of-plane variables, it is convenient to study the in-plane cases first and then to examine the remaining situations. It will be seen that these are natural separations as provided by the analytical solutions; and, consequently, the in-plane cases may be described in rather elegant but simple forms. This simplicity does not carry over to the out-of-plane situations because the homogenity of coefficients which appeared initially is not retained. This leads to rather cumbersome mathematical statements for some of the trace descriptions; and, elegance is recaptured only when numerical constraints are placed on the values assigned to the coefficient parameters.

The trace geometries which are constructed, sketched and discussed herein arise (necessarily) from particular example cases. For all of these the input

parameters have been chosen as positive valued constants. The results, then, reflect this specification. Such selections do not alter the method of construction but could influence the "direction" for some vectors, and/or the "size" (magnitude) of some of the other quantities.

For the constructions described below, each trace has been formed by the summing of vector components. Each component has been developed in accord with natural separation of variables, or functions, from within the trace equations. In this fashion each vector defines a particular geometry (or set of point loci); and the ordered summing of these (geometries) leads directly to the final loci for each trace. Necessarily, the traces are acquired for a given plane, referred to a chosen triad of reference; hence there will be <u>one</u> in-plane trace and <u>two</u> out-of-plane traces for each of the problem discussions. Where it is convenient to do so these trace geometries are described by equations, geometric labels and by illustrative sketches. It must be remembered that the task undertaken here is primarily one of a tutorial nature. One should not expect these results to be all inclusive; rather this is more of a compendium of data with the essential results being graphic descriptions.

Each principal section of the report treats a separate problem segment and construction. The manner in which these are treated is obvious from each section headings. Explanatory comments are included to acquaint the reader with these various operations and their results.

## II. DISPLACEMENTS FOR THE ROTATING FRAME OF REFERENCE

According to the analytical expressions which describe the in-plane displacements, these are dependent on the initial values pertaining to any particular situation, and on the disturbance forces impressed on the system.

When one examines these expressions it is found that the influences which affect the motion can be separated. As a consequence, for the descriptions which follow the initial value problem ($\bar{\tau} \equiv 0$) and the zero-initial state cases will be discussed as separate and independent entities.

II.1 The Initial Values Problem. The analytical solution for this case has been obtained elsewhere as:

$$I_2 \bar{\lambda}(\varphi) = \left[I_2 + 3(J_2 - J_1)\right] T_2(\varphi^-) \left[A_a\right]_{i.v.} + \left[I_2 - \frac{3}{2}\varphi\,(B_2 J_1)\right] K_o , \tag{1}$$

wherein

$$\left[A_a\right]_{i.v.} \equiv \frac{1}{2}\left[3J_1 \bar{\lambda}_o + (J_2 - 2J_1) B_2 \bar{\lambda}'_o\right], \tag{2}$$

and

$$K_o \equiv (4J_1 + J_2)\, \bar{\lambda}_o - 2B_2 \bar{\lambda}'_o . \tag{3}$$

In order to reduce these expressions to a more useful and meaningful form, the scalar quantities noted below will be introduced.

For present purposes let $\left[A_a\right]_{i.v.} \equiv A_a(A_1, A_2)$, and $K_o \equiv K_o(K_1, K_2)$ where each scalar is symbolically defined by:

$$N_i \equiv J_i N,$$

with

$$N \equiv (A, K); \quad i = 1, 2$$

In this regard it can be shown that:

$$A_1 \equiv J_1\left[A_a\right]_{i.v.} = \frac{1}{2}\left[3J_1 \bar{\lambda}_o - 2J_1 B_2 \bar{\lambda}'_o\right] = \frac{1}{2}\left[K_1 - J_1 \bar{\lambda}_o\right],$$

$$A_2 = \frac{1}{2}\left[J_2 B_2 \bar{\lambda}'_o\right],$$

$$K_1 = 2J_1 (2\bar{\lambda}_o - B_2 \bar{\lambda}'_o),$$

and $$K_2 = J_2(\bar{\kappa}_o - 2B_2\bar{\kappa}'_o). \tag{4}*$$

An inspection of Eq. (1) will indicate that the displacement vector can be more conveniently discussed in terms of the three vector sum represented there. Following this, then, the construction of a displacement locus, onto the $(\xi, \eta)$-plane, will be obtained using the vectors $(\equiv \delta_i I_2 \bar{\kappa}\ ;\ i = 1, 2, 3)$ noted below:

(1) First, let $\delta_1 [I_2 \bar{\kappa}(\varphi)] \equiv [I_2 + 3(J_2 - J_1)]\, T_2(\varphi^-)\, [A_a]_{i.v.}$. This is equivalent to the matrix equation:

$$\begin{bmatrix} \delta_1 \xi \\ \delta_1 \eta \end{bmatrix} = 2 \begin{bmatrix} -\cos\varphi & \sin\varphi \\ 2\sin\varphi & 2\cos\varphi \end{bmatrix} \begin{bmatrix} A_1 \\ A_2 \end{bmatrix} . \tag{5a}$$

Equation (5a) describes a (2:1) ellipse whose principal axes are proportional to the magnitude of $[A_a]_{i.v.}$. These axes are parallel to the reference frame's coordinate directions; and the quadric equation for this figure is:

$$\left(\frac{\delta_1 \xi}{2\sqrt{A_1^2 + A_2^2}}\right)^2 + \left(\frac{\delta_1 \eta}{4\sqrt{A_1^2 + A_2^2}}\right)^2 = 1. \tag{5b}$$

(2) The component of $[I_2 \bar{\kappa}(\varphi)]$ expressed in terms of $K_o$ leads to the following two vectors:

$$\delta_2 \left[I_2 \bar{\kappa}(\varphi)\right] + \delta_3 \left[I_2 \bar{\kappa}(\varphi)\right] \equiv \left\{I_2 K_o\right\} + \left\{-\frac{3}{2}\varphi \left[B_2 J_1\right] K_o\right\} . \tag{6a}$$

This equation describes a fixed locus and a moving point. The corresponding matrix relations for these two vectors are:

$$\begin{bmatrix} \delta_2 \xi \\ \delta_2 \eta \end{bmatrix} \equiv \begin{bmatrix} 1 & 0 \\ 0 & 1 \end{bmatrix} \begin{bmatrix} K_1 \\ K_2 \end{bmatrix} . \tag{6b}$$

and

$$\begin{bmatrix} \delta_3 \xi \\ \delta_3 \eta \end{bmatrix} \equiv -\frac{3\varphi}{2} \begin{bmatrix} 0 & 0 \\ 1 & 0 \end{bmatrix} \begin{bmatrix} K_1 \\ K_2 \end{bmatrix} . \tag{6c}$$

*See See SELECTED EQUATIONS for the scalar form of these expressions.

Since Eqs. (5) and (6) represent vector components of the complete in-plane relative position vector, then it follows that the required vector addition can be performed in any convenient manner whatsoever. For instance, if the vectors $\bar{\delta}_1$ and $\bar{\delta}_2$ are considered, first, one finds as the geometry a (2:1) ellipse with its center shifted to the point locus $\bar{\delta}_2$. Adding to this the vector $\bar{\delta}_3$ it is seen that a general point on the displacement trace is described by this simple mathematical operation.

On Fig. (1) a typical construction is shown, in sketch. There $\bar{\delta}_2$ is the fixed component vector, locating the geometric center of the ellipse ($\bar{\delta}_1$). Consequently, the vector sum ($\bar{\delta}_1 + \bar{\delta}_2$) defines typical loci for the "shifted ellipse". Adding vector $\bar{\delta}_3(\varphi)$ leads to position loci $P(\varphi)$, for this completed in-plane trace. (For clarity the $\varphi = 0$ vector, $\bar{\delta}_1(0)$, is also shown. This locates an "origin" for the trace on the displacement plane).

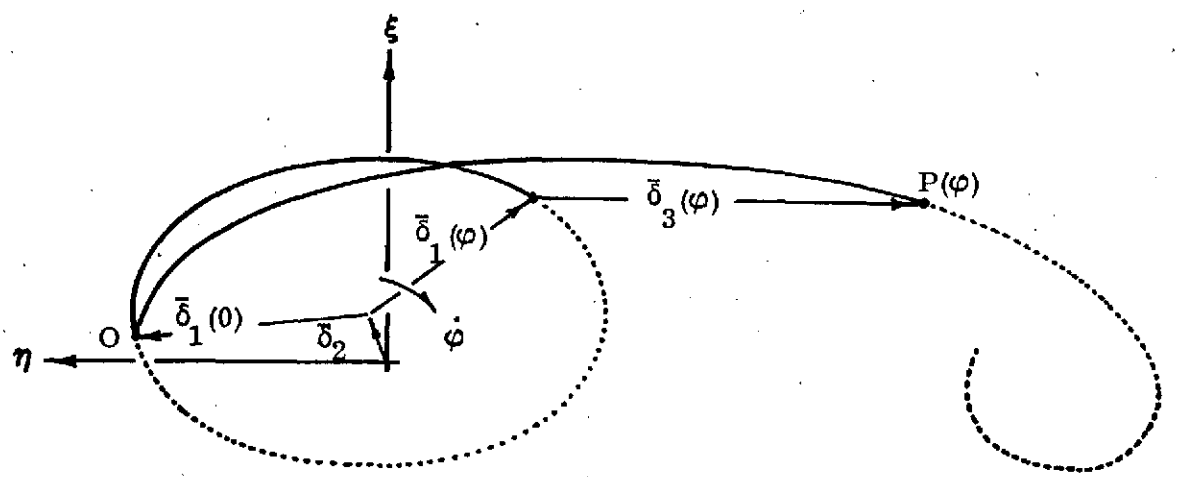


FIG. 1. A typical construction for the in-plane displacements trace referred to a rotating frame of reference. Here $\bar{\delta}_1(0)$ denotes the initial trace position, on the ellipse; $\bar{\delta}_2$ locates a fixed point; and, $\bar{\delta}_3(\varphi)$ defines the secular influence from the solution.

II.2 The Non-Secular Initial Values Problem. In order to remove the secular, or divergent, character from this solution it is necessary (see Eq. (6c)) that $K_1$ be removed. In general this can be accomplished by either of two means; namely, by initiating the motion so that: (1), $\xi_o = \eta'_o = 0$; or by, (2), $\eta'_o = 2\xi_o$ (see Eq. (4).

For purposes of this discussion, it is sufficient, simply, to let $K_1 = 0$ and to examine the resulting trace(s). Here, then:

$$A_1^{(1)} = -\frac{1}{2} J_1 \bar{\lambda}_o, \quad A_2 = \frac{1}{2}\left[J_2 B_2 \bar{\lambda}'_o\right]; \quad K_1 = 0; \quad K_2 = J_2(\bar{\lambda}_o - 2B_2 \bar{\lambda}'_o). \tag{7}$$

As a consequence of this constraint, Eqs. (5) and (6) reduce to:

$$\begin{bmatrix} \delta_1\xi \\ \delta_1\eta \end{bmatrix} = 2 \begin{bmatrix} -\cos\varphi & \sin\varphi \\ 2\sin\varphi & 2\cos\varphi \end{bmatrix} \begin{bmatrix} A_1^{(1)} \\ A_2 \end{bmatrix}, \tag{8a}$$

$$\begin{bmatrix} \delta_2\xi \\ \delta_2\eta \end{bmatrix} = \begin{bmatrix} 1 & 0 \\ 0 & 1 \end{bmatrix} \begin{bmatrix} 0 \\ K_2 \end{bmatrix}, \tag{8b}$$

and

$$\begin{bmatrix} \delta_3\xi \\ \delta_3\eta \end{bmatrix} = \begin{bmatrix} 0 \\ 0 \end{bmatrix}. \tag{8c}$$

According to Eqs. (8): the vector $\bar{\delta}_1$ describes (again) a (2:1) ellipse (but with some reduction in size, due to $A_a^{(1)}$). Also, the vector $\bar{\delta}_2$ (again) describes the fixed locus, $(\xi, \eta)_2$, but without an $\xi$-component.

Necessarily, this modified trace is a closed curve with a geometric center shifted away from the coordinate origin. In particular, Eqs. (8) define, for $\bar{\delta}_1$, the (2:1) ellipse:

$$\left(\frac{\delta_1\xi}{2\sqrt{A_1^{(1)2} + A_2^2}}\right)^2 + \left(\frac{\delta_1\eta}{2\sqrt{A_1^{(1)2} + A_2^2}}\right)^2 = 1, \tag{9a}$$

and, for $\bar{\delta}_2$, the fixed locus

$$\delta_2 \eta - K_2 = 0. \tag{9b}$$

A sketch for this solution is shown on Fig. (2), below. There $(\bar{\delta}_1(0) + \bar{\delta}_2)$ locates the "initial position" for this problem, while $P(\varphi)$ is a general trace point for this (hypothetical) relative motion.

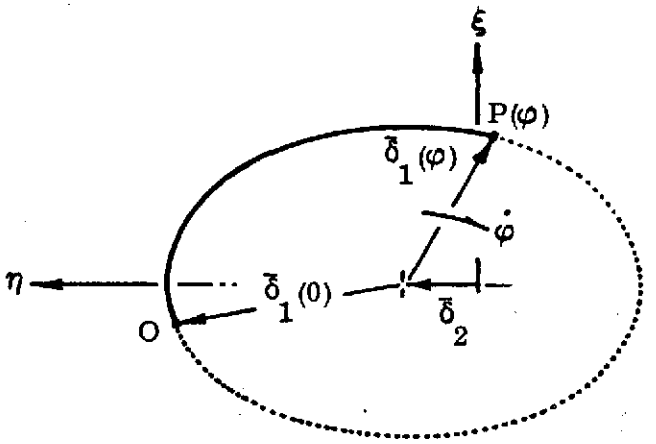


FIG. 2. A sketch depicting the Non-Secular Initial Values Problem geometry for the in-plane motion referred to a rotating reference frame. The vector $\bar{\delta}_1(0)$ locates the trace's initial position while the sum $(\bar{\delta}_1 + \bar{\delta}_2)$ defines any general locus; e.g. $P(\varphi)$.

II.3 The Zero Initial Value Problem. Continuing with the construction of in-plane displacements, the zero-initial-value problem which is described next infers a situation where "thrusting" (or an externally applied force) is present. For this discussion the assumption is that these motions originate from a zero relative motion state (i.e., $\bar{\mathcal{R}}_o = \bar{\mathcal{R}}'_o = 0$).

The analytical solution for this problem, with $\bar{\tau} \equiv \bar{\tau}(\tau_\xi, \tau_\eta, \tau_\zeta)$, leads to motion traces described from:

$$I_2 \bar{h}(\varphi) \equiv \left\{ \left[ I_2 + 3(J_2 - J_1) \right] T_2(\varphi^-) \left[ A_a \right]_\tau + \Psi_\tau \right\} \bar{\tau} , \tag{10}$$

wherein

$$\left[ A_a \right]_\tau \equiv \frac{1}{2} \left[ J_1 - 2J_2 \right] , \tag{11}$$

and

$$\Psi_\tau \equiv \left[ J_1 + 4J_2 \right] - \varphi \left[ 2B_2 + \frac{3}{2} J_2 \varphi \right] . \tag{12}*$$

As a suggestion, for illustrating the vector composition according to Eq. (10), the recommendation is that the overall position vector be viewed as being formed from three component vectors. One of these given in terms of $[A_a]_\tau$; while $\Psi_\tau$ will contribute a pair of vectors - one for the constants, and another proportional to the secular terms. In this regard the component vectors will be defined as follows:

$$\delta_1 \left[ I_2 \bar{h}(\varphi) \right] \equiv \left\{ \left[ I_2 + 3(J_2 - J_1) \right] T_2(\varphi^-) \left[ A_a \right]_\tau \right\} \bar{\tau} , \tag{13a}$$

$$\delta_2 \left[ I_2 \bar{h}(\varphi) \right] \equiv \left[ J_1 + 4J_2 \right] \bar{\tau} , \tag{14a}$$

and

$$\delta_3 \left[ I_2 \bar{h}(\varphi) \right] \equiv - \varphi \left[ 2B_2 + \frac{3}{2} J_2 \varphi \right] . \tag{15a}$$

Expressed in matrix form the above equations are:

$$\begin{bmatrix} \delta_1 \xi \\ \delta_1 \eta \end{bmatrix}_\tau = \begin{bmatrix} -\cos\varphi & \sin\varphi \\ 2\sin\varphi & 2\cos\varphi \end{bmatrix} \begin{bmatrix} \tau_\xi \\ -2\tau_\eta \end{bmatrix} , \tag{13b}$$

$$\begin{bmatrix} \delta_2 \xi \\ \delta_2 \eta \end{bmatrix}_\tau = \begin{bmatrix} 1 & 0 \\ 0 & 4 \end{bmatrix} \begin{bmatrix} \tau_\xi \\ \tau_\eta \end{bmatrix} , \tag{14b}$$

and

$$\begin{bmatrix} \delta_3 \xi \\ \delta_3 \eta \end{bmatrix}_\tau = \varphi \begin{bmatrix} 0 & 2 \\ -2 & -\frac{3\varphi}{2} \end{bmatrix} \begin{bmatrix} \tau_\xi \\ \tau_\eta \end{bmatrix} . \tag{15b}$$

*See SELECTED EQUATIONS for the scalar form of this expression.

It is obvious that the first vector ($\bar{\delta}_1$) describes a (2:1) ellipse:

$$\left(\frac{\delta_1 \xi}{\sqrt{\tau_\xi^2 + 4\tau_\eta^2}}\right)^2 + \left(\frac{\delta_1 \eta}{2\sqrt{\tau_\xi^2 + 4\tau_\eta^2}}\right)^2 = 1; \tag{13c}$$

while the second ($\bar{\delta}_2$) is indicative of a "fixed position" in the plane of motion. Lastly, $\bar{\delta}_3$ suggests a parabolic relationship between the in-plane displacements:

$$\delta_3 \eta = -\left[\delta_3 \xi \frac{\tau_\xi}{\tau_\eta} + \frac{3}{8} \frac{(\delta_3 \xi)^2}{\tau_\eta}\right]. \tag{15c}$$

Here, the sum ($\bar{\delta}_1 + \bar{\delta}_2$) defines those positional loci which are on the ellipse with its center shifted away from the coordinate origin. Adding to this the secular component ($\bar{\delta}_3$), it is found that the resulting trace acquires more of the parabola's character than that of the elliptic. (Primarily this is due to the influence of the $\varphi^2$-term in Eqs. (15)). A typical sketch for this trace is found on Fig. (3) below.

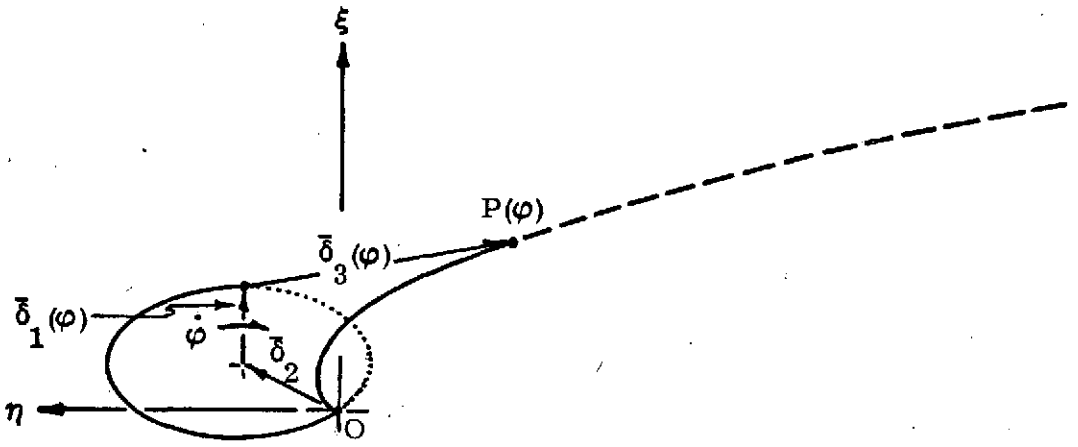


FIG. 3. A sketch showing the construction for an in-plane trace geometry representing the Zero Initial Value Problem, $\bar{\tau} \equiv \bar{\tau}(\tau_\xi, \tau_\eta, \tau_\zeta)$. Here $\bar{\delta}_1$ locates a point on the ellipse; $\bar{\delta}_2$ defines a fixed locus; and, $\bar{\delta}_3$ describes the secular influence. The arc (O to P) illustrates trace loci for this problem.

Interestingly, the secular influence provided by the $\tau_\eta$-terms is more pronounced than that for the $\tau_\xi$-terms. Consequently, the trace geometry which developes when $\tau_\eta = 0$ is most significantly altered. As a matter of fact, for this condition the trace equations reduce to:

$$\delta\xi = \tau_\xi (1 - \cos\varphi),$$

and (15d)

$$\delta\eta = -2\tau_\xi (\varphi - \sin\varphi).$$

These expressions describe a cycloid on the displacement plane (see Fig. 4). By constrast, the basic geometry which is developed for $\tau_\xi = 0$ is parabolic in character. Again, this is largely due to the $\varphi^2$-terms present in the parametric equations.

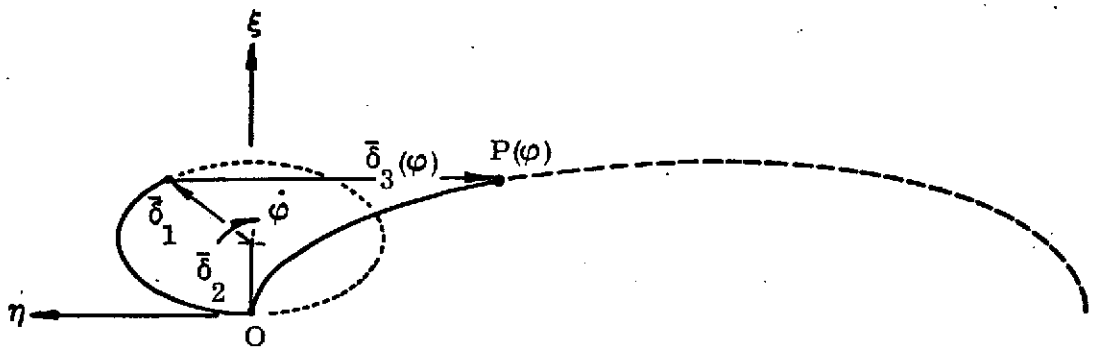


FIG. 4. Sketch of the displacement geometry for a Zero-Initial-Value Problem when $\tau_\eta = 0$. The locus $P(\varphi)$ is described by $\bar{\delta}_1(\varphi)$, $\bar{\delta}_2$ and $\bar{\delta}_3(\varphi)$. The trace (here) is a regular cycloid.

From the above discussion it is evident that divergence in these traces cannot be as simply removed as it was for the initial values problem. Of course this is to be expected since these impressed accelerations do not allow the velocity to be cyclic in character. This, in turn, takes away the possibility of cyclic variations in the displacements. Hence, the only means by which this divergent characteristic can be removed is to eliminate the in-plane $\tau$-terms completely.

## III. THE HODOGRAPH FOR A ROTATING FRAME OF REFERENCE

To complete these discussions on construction of state variable traces, as they arise from these problem types, the traces on corresponding hodograph planes must be described. This is the topic for the following paragraphs.

Once again the two disturbing influences will be examined separately. Thus, the hodographs described below will correspond directly to the displacement traces discussed above.

III.1 The Initial Values Problem. The analytical solution pertinent to this part of the investigation has been obtained as:

$$I_2\bar{h}'(\varphi) = \left[I_2 + 3(J_2 - J_1)\right]\left[B_2 T_2(\varphi^-)\right]\left[A_a\right]_{i.v.} - \frac{3}{2}\left[B_2 J_1\right]K_o \,, \tag{16}$$

wherein $\left[A_a\right]_{i.v.}$ and $K_o$ are the coefficients defined in Eqs. (2), (3), and (4).

Taking the contributions from $A_a$ and $K_o$ separately, it is found that point loci on the $(\xi', \eta')$ hodograph plane are composed from the two vectors:

$$\delta_1\left[I_2\bar{h}'(\varphi)\right] \equiv \left[I_2 + 3(J_2 - J_1)\right]B_2 T_2(\varphi^-)\left[A_a\right]_{i.v.} \,, \tag{17a}$$

and

$$\delta_2\left[I_2\bar{h}'(\varphi)\right] \equiv -\frac{3}{2}\left[B_2 J_1\right]K_o \,. \tag{17b}$$

These equations can be recast as the following matrices:

$$\begin{bmatrix}\delta_1\xi' \\ \delta_1\eta'\end{bmatrix} = 2\begin{bmatrix}\sin\varphi & \cos\varphi \\ 2\cos\varphi & -2\sin\varphi\end{bmatrix}\begin{bmatrix}A_1 \\ A_2\end{bmatrix} \,, \tag{18a}$$

and

$$\begin{bmatrix}\delta_2\xi' \\ \delta_2\eta'\end{bmatrix} = \frac{3}{2}\begin{bmatrix}0 & 0 \\ -1 & 0\end{bmatrix}\begin{bmatrix}K_1 \\ K_2\end{bmatrix} \,. \tag{18b}$$

Here one sees that Eqs. (18) represent; (1), a (2:1) ellipse $(\bar{\delta}_1)$; and (2), a fixed point locus $(\bar{\delta}_2)$. A combining of the vectors $(\bar{\delta}_2 + \bar{\delta}_1(\varphi))$ would describe the (2:1)

ellipse but with its geometric center shifted to the position $(\bar{\delta}_2)$. A sketch of this geometry and its construction is found on Fig. 5. below (note curve "I").

III.2 The Non-Secular Case. It was mentioned earlier that the secular character of this problem could be eliminated by setting the constant coefficient, $K_1$, to zero. When this condition is imposed on the hodograph equations then (in place of Eqs. (18)) one finds:

$$\begin{bmatrix} \delta_1\xi' \\ \delta_1\eta' \end{bmatrix} \equiv 2 \begin{bmatrix} \sin\varphi & \cos\varphi \\ 2\cos\varphi & -2\sin\varphi \end{bmatrix} \begin{bmatrix} A_1^{(1)} \\ A_2 \end{bmatrix} , \tag{19a}$$

and

$$\begin{bmatrix} \delta_2\xi' \\ \delta_2\eta' \end{bmatrix} \equiv \frac{3}{2} \begin{bmatrix} 0 & 0 \\ -1 & 0 \end{bmatrix} \begin{bmatrix} 0 \\ K_2 \end{bmatrix} = \begin{bmatrix} 0 \\ 0 \end{bmatrix} . \tag{19b}$$

where the constants $A_1^{(1)}$, $A_2$ are those described in Eq. (7).

It is apparent that for this hodograph trace $(\bar{\delta}_1)$ is, again, a (2:1) ellipse, however, it has its geometric center located at the coordinate origin, $(\bar{\delta}_2 = \bar{0})$. The major dimensions of the figure are proportional to the magnitude of the present initial value matrix $(A_a)$.

A sketch of this hodograph also appears on Fig. 5, (note curve "II").

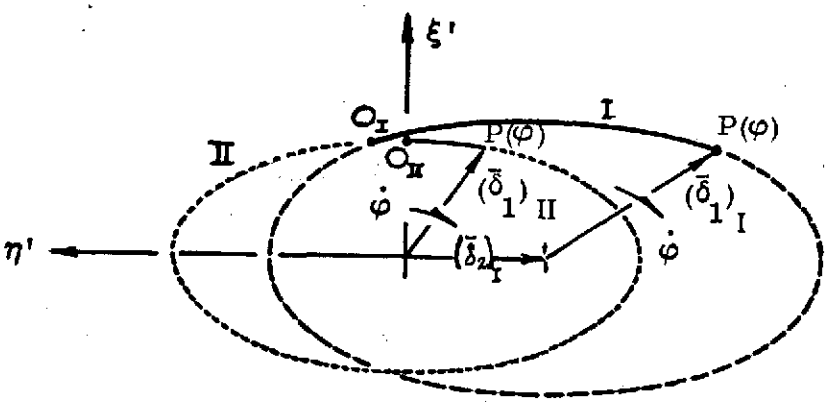


FIG. 5. Sketch of the hodograph for a general Initial-Value Problem (I), and for the non-secular case (II). Note the general trace loci are described by $(\bar{\delta}_1 + \bar{\delta}_2)$; and, that for the non-secular case $\bar{\delta}_2 = \bar{0}$. Motion over both traces occurs at a rate, $\dot{\varphi}$.

III.3 The Zero-Initial State Case. The hodograph to be described next is due solely to the applied specific force $\bar{\tau} \equiv \bar{\tau}(\tau_\xi, \tau_\eta, \tau_\zeta)$. Here the initial state is set to zero, again. A physical interpretation for this problem could be that of a mass particle being propelled from a spacecraft by a fixed, continuous thrusting action.

The analytical solution for this case is given by:

$$I_2 \bar{k}'(\varphi) = \left\{ \left[ I_2 + 3(J_2 - J_1) \right] B_2 T_2(\varphi^-) \left[ A_a \right]_\tau + \Psi'_\tau \right\} \bar{\tau} \; ; \tag{20}$$

wherein

$$\left[ A_a \right]_\tau = \frac{1}{2} \left[ J_1 - 2J_2 \right], \tag{21a}$$

and

$$\left[ \Psi' \right]_\tau = - \left[ 2B_2 + 3J_2 \varphi \right]. \tag{21b}*$$

When these expressions are recast into matrix form and allowed to represent vector components (one due to $A_a$, and two arising from $\Psi'_\tau$) it can be shown that:

$$\begin{bmatrix} \delta_1 \xi' \\ \delta_1 \eta' \end{bmatrix} \equiv \begin{bmatrix} \sin\varphi & \cos\varphi \\ 2\cos\varphi & -2\sin\varphi \end{bmatrix} \begin{bmatrix} \tau_\xi \\ -2\tau_\eta \end{bmatrix}, \tag{22a}$$

$$\begin{bmatrix} \delta_2 \xi' \\ \delta_2 \eta' \end{bmatrix} \equiv \begin{bmatrix} 0 & 2 \\ -2 & 0 \end{bmatrix} \begin{bmatrix} \tau_\xi \\ \tau_\eta \end{bmatrix}, \tag{22b}$$

and

$$\begin{bmatrix} \delta_3 \xi' \\ \delta_3 \eta' \end{bmatrix} \equiv \begin{bmatrix} 0 & 0 \\ 0 & -3\varphi \end{bmatrix} \begin{bmatrix} \tau_\xi \\ \tau_\eta \end{bmatrix}. \tag{22c}$$

Here one sees the three vectors which describe all trace points for the $(\xi', \eta')$-hodograph. The first vector's loci $(\bar{\delta}_1)$ define a (2:1) ellipse whose dimensions are proportional to $\sqrt{\tau_\xi^2 + 4\tau_\eta^2}$. The second vector $(\bar{\delta}_2)$ locates a fixed point, while the third $(\bar{\delta}_3)$ represents a moving point - one which moves parallel to the $\eta'$-axis at a rate proportional to $\tau_\eta$.

*See SELECTED EQUATIONS for the scalar form of this expression.

To describe a representative point on the hodograph by the (vector) sum $\bar{\delta}_2 + \bar{\delta}_1 + \bar{\delta}_3$, the construction sketched onto Fig. 6 is appropriate to this case. On the sketch "O" is the initial locus (the origin) while $P(\varphi)$ is a general hodograph point.

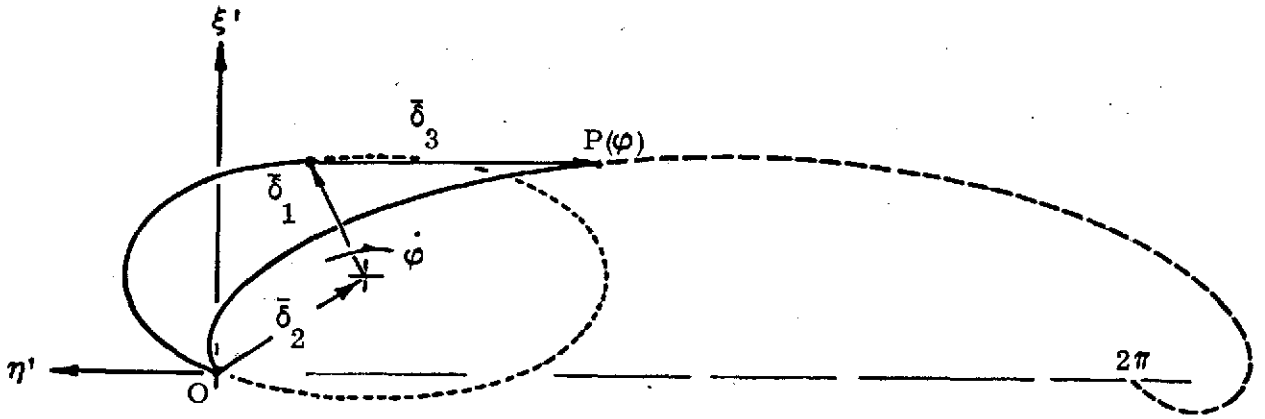


FIG. 6. A sketch depicting the construction for a Zero-Initial-Values Problem hodograph. Here $\bar{\delta}_2$ locates a fixed point (ellipse center); $\bar{\delta}_1$ describes loci on the ellipse, and $\bar{\delta}_3$ adds the secular influence. These $\delta_i$ combine to define trace points, $P(\varphi)$.

III.4 Special Cases. As a first special case, for this hodograph construction, suppose that $\tau_\eta \equiv 0$. The consequence of this condition is that the loci $(\bar{\delta}_1)$ describe a (2:1) ellipse, again; however, this one is defined by the quadric expression:

$$\left(\frac{\delta_1 \xi'}{\tau_\xi}\right)^2 + \left(\frac{\delta_1 \eta'}{2\tau_\xi}\right)^2 = 1. \tag{23a}$$

In a like manner the fixed vector locus ($\bar{\delta}_2$) above reduces to the simple relation:

$$\delta_2 \eta' = -2\tau_\xi . \tag{23b}$$

Finally, for this case, the component vector ($\bar{\delta}_3$) is reduced to a null vector; thus, the construction can be represented by the sketch on Fig. 7. That is, the loci here are located on the (2:1) ellipse with the originating point at the coordinate origin (point "O"). Note that the ellipse has its center shifted to the position defined by the fixed vector ($\bar{\delta}_2$), Eq. (23b).

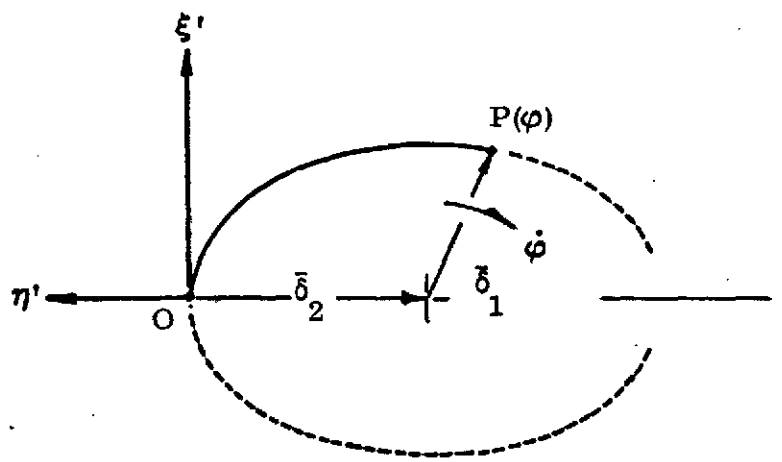


FIG. 7. A typical "special" Zero Initial State Hodograph.
This in-plane trace is for $\tau_\eta = 0$.

The second special case is a direct consequence of the imposed condition, $\tau_\eta = 0$. When this constraint is applied the ellipse ($\bar{\delta}_1$), described in Eq. (22a), it becomes a new (2:1) ellipse, defined by:

$$\left(\frac{\delta_1 \xi'}{2\tau_\eta}\right)^2 + \left(\frac{\delta_1 \eta'}{4\tau_\eta}\right)^2 = 1. \qquad (24a)$$

Similarily, the vector $\bar{\delta}_2$, from Eq. (22b), is replaced by:

$$\begin{bmatrix} \delta_2 \xi' \\ \delta_2 \eta' \end{bmatrix} \equiv \begin{bmatrix} 0 & 2 \\ -2 & 0 \end{bmatrix} \begin{bmatrix} 0 \\ \tau_\eta \end{bmatrix} \quad ;$$

note that here the line vector $(\bar{\delta}_3)$ is retained and is apparent to the hodograph's description; however, now it parallels the $\xi'$-axis.

The trace which is found here can be described as a "moving (2:1) ellipse", which has its geometric center shifted (by $\bar{\delta}_2$), and whose peripherial loci are additively displaced (parallel to the $\eta'$-axis) by the vector, $\bar{\delta}_3$. (This geometry is not reproduced by sketch, here, since it is basically the same as that developed from Eqs. (22). It should be evident that this figure is akin to the cycloid).

In the continuation of these construction descriptions, the next few paragraphs will outline the vector compositions for traces in the inertial frame of reference.

## IV. DISPLACEMENTS IN THE INERTIAL FRAME OF REFERENCE

In the foregoing paragraphs the discussions on displacement and velocity traces were referred to a rotating frame of reference. In the next few paragraphs similar constructions and discussions for traces in an inertial frame of reference will be undertaken.

For these next studies the sequence of cases to be examined will be the same as those used previously. In this fashion a direct comparison of the various traces can be made. Such a procedure should enhance the reader's understanding and knowledge of these relative motion situations.

IV.1 The Initial Values Problem. Recalling that for this case the external force system is set to zero then the motion traces are determined from the initial state alone.

The analytical solution which describes these in-plane displacements is:

$$I_2\bar{R}(\varphi) = \left[3(J_2 - J_1) + T_2(2\varphi^-)\right]\left[A_{a_I}\right]_{i.v.} + T_2(\varphi^-)\left[I_2 - \frac{3}{2}\varphi B_2 J_1\right]K_{o_I}, \tag{25}$$

wherein the coefficient matrices (A, K) are defined by:

$$\left[A_{a_I}\right]_{i.v.} \equiv \frac{1}{2}\left[I_2\bar{R}_o + (J_2 - 2J_1)B_2\bar{R}'_o\right], \tag{26}*$$

and

$$K_{o_I} \equiv (2J_1 - J_2)\bar{R}_o - 2B_2\bar{R}'_o\,. \tag{27}*$$

For the purpose of describing these particular motion traces the matrix constants (A, K) will be symbolically separated to conform with the general notation in use here. That is, the coefficients will be represented as:

$$\left[A_{a_I}\right]_{i.v.} \equiv A_{a_I}(A_1, A_2), \tag{26b}$$

and

$$K_{o_I} \equiv K_{o_I}(K_1, K_2); \tag{27b}$$

*See SELECTED EQUATIONS for a matrix definition of this quantity.

where it can be shown that:

$$A_1 \equiv J_1\left[A_{a_I}\right]_{i.v.} = \frac{1}{2}J_1\left[\bar{R}_o - 2B_2\bar{R}'_o\right] = \frac{1}{2}J_1\left[\frac{1}{2}K_{o_I} - B_2\bar{R}'_o\right],$$

$$A_2 = \frac{1}{2}J_2\left[\bar{R}_o + B_2\bar{R}'_o\right] = -\frac{1}{2}J_2\left[K_{o_I} + B_2\bar{R}'_o\right],$$

$$K_1 \equiv J_1 K_{o_I} = 2J_1\left[\bar{R}_o - B_2\bar{R}'_o\right],$$

and

$$K_2 = -J_2\left[\bar{R}_o + 2B_2\bar{R}'_o\right]. \tag{28}$$

The grouping of terms in Eq. (25) suggests that these in-plane displacements may be constructed from the four vectors seen there. Of these, one will describe a fixed locus while the others are all functionally dependent on the independent variable ($\varphi$).

Separating terms so that the matrices (A, K) are treated individually then the following component vectors are defined: First, for $A_{a_I}$:

$$\delta_1\left[I_2\bar{R}(\varphi)\right] + \delta_2\left[I_2\bar{R}(\varphi)\right] \equiv \left\{\left[3(J_2 - J_1)\right] + \left[T_2(2\varphi^-)\right]\right\}\left[A_{a_I}\right]_{i.v.}; \tag{29a}$$

wherein

$$\begin{bmatrix}\delta_1\Xi(\varphi)\\ \delta_1 H(\varphi)\end{bmatrix} \equiv \begin{bmatrix}-3 & 0\\ 0 & 3\end{bmatrix}\begin{bmatrix}A_1\\ A_2\end{bmatrix}, \tag{29b}$$

and

$$\begin{bmatrix}\delta_2\Xi(\varphi)\\ \delta_2 H(\varphi)\end{bmatrix} \equiv \begin{bmatrix}\cos 2\varphi & -\sin 2\varphi\\ \sin 2\varphi & \cos 2\varphi\end{bmatrix}\begin{bmatrix}A_1\\ A_2\end{bmatrix}. \tag{29c}$$

Similarily, the partial solutions involving $K_{o_I}$ lead to the matrix components:

$$\begin{bmatrix}\delta_3\Xi(\varphi)\\ \delta_3 H(\varphi)\end{bmatrix} \equiv \begin{bmatrix}\cos\varphi & -\sin\varphi\\ \sin\varphi & \cos\varphi\end{bmatrix}\begin{bmatrix}K_1\\ K_2\end{bmatrix}, \tag{29d}$$

and

$$\begin{bmatrix} \delta_4 \Xi(\varphi) \\ \delta_4 H(\varphi) \end{bmatrix} \equiv -\frac{3\varphi}{2} \begin{bmatrix} -\sin\varphi & 0 \\ \cos\varphi & 0 \end{bmatrix} \begin{bmatrix} K_1 \\ K_2 \end{bmatrix} \quad . \tag{29e}$$

After studying these matrix expressions it is seen that:

(1) The vector in Eq. (29b) locates a point in the displacement plane, while the vector loci from Eq. (29c) describe a circle, with radius $\sqrt{A_1^2+A_2^2} \equiv \left|\left[A_{a_I}\right]_{i.v.}\right|$. This circle has a double orbit frequency for its description.

(2) The loci defined from Eq. (29d) describe a second circle, but one whose radius is $|K_{0_I}|$. This figure has a frequency matching that of the base orbit, $(\dot{\varphi})$.

(3) The last expression can be recognized as an archimedian spiral, for the trace figure.

The consequence drawn from these observations is that the full in-plane trace, for this motion (on the ($\Xi$, H)-plane), is composed as the sum of these four vectors. In retrospect, it is known that the dominant characteristic for this trace is the spiral; hence, as a general classification, the geometry can be referred to as "spiral-like". A sketch depicting this construction is found on Fig. 8 below (this figure is only approximate in its scaling).

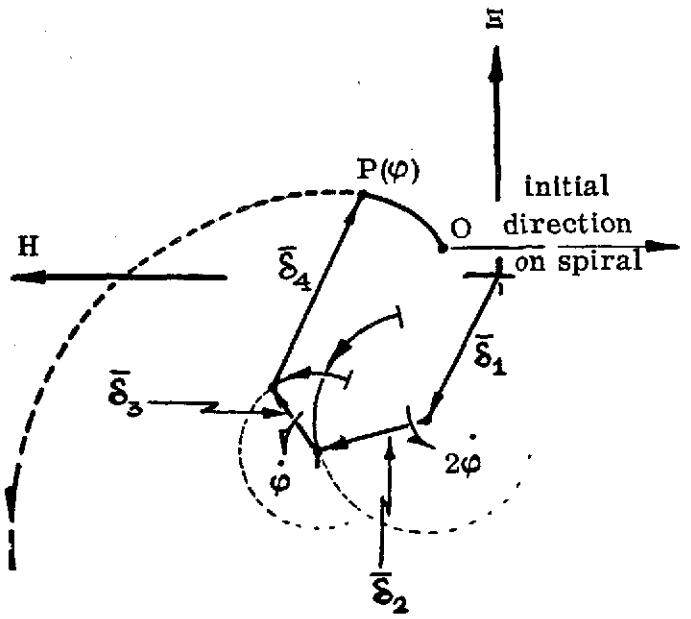


FIG. 8. Inertial plane trace construction for an Initial Values Problem. A typical point P($\varphi$) is located by the vector sum of: $\bar{\delta}_1$ (a fixed locus), plus $\bar{\delta}_2$, $\bar{\delta}_3$ and $\bar{\delta}_4$ (all $\varphi$ dependent). Vectors $\bar{\delta}_2$ and $\bar{\delta}_3$ describe circles; $\bar{\delta}_4$ traces an archimedian spiral.

On the sketch "C" and "P" represent the initial and a general locus, respectively. The circles shown there depict loci for the vectors $\bar{\delta}_2$ and $\bar{\delta}_3$; the arcs drawn on each are representative of the segments traversed for these partial constructions. Lastly the $\bar{\delta}_4$-component vector is indicative of the contribution provided by the spiral, to the final point locus, (P).

IV.2 The Non-Secular Initial Values Problem. The condition to be imposed (next) is that which will remove the divergent nature of the displacement trace. From Eqs. (29) it is apparent that this is accomplished when the scalar $K_1 \equiv 0$. Necessarily the implication of such a constraint is felt elsewhere in the solution (see Eq. (28)). Also, the means by which this condition ($K_1 = 0$) occurs has an added ramification. (Note that when $K_1$ is zero, then either: (1), $J_1 \bar{\mathcal{R}}_o = J_1 B_2 \bar{\mathcal{R}}'_o$; or, (2) $J_1 \bar{\mathcal{R}}_o = J_1 B_2 \bar{\mathcal{R}}'_o = 0$).

For illustration purposes, here, it will be assumed that $K_1 = 0$ without any specification of which constraint is implied regarding the initial values. In this regard the coefficient scalars (A, K) are now altered as follows:

$$A_1^{(1)} \equiv -\frac{1}{2} J_1 B_2 \bar{\mathcal{R}}'_o, \quad A_2 \equiv -\frac{1}{2} J_2 \left[ K_{o_I} + B_2 \bar{\mathcal{R}}'_o \right], \quad K_1 \equiv 0, \quad K_2 \equiv -J_2 \left[ \bar{\mathcal{R}}_o + 2 B_2 \bar{\mathcal{R}}'_o \right].$$

Next, rewriting Eqs. (29) to reflect these constraints, one finds that the trace component vectors are modified to read:

$$\begin{bmatrix} \delta_1 \Xi(\varphi) \\ \delta_1 H(\varphi) \end{bmatrix} \equiv \begin{bmatrix} -3 & 0 \\ 0 & 3 \end{bmatrix} \begin{bmatrix} A_1^{(1)} \\ A_2 \end{bmatrix}, \tag{30a}$$

$$\begin{bmatrix} \delta_2 \Xi(\varphi) \\ \delta_2 H(\varphi) \end{bmatrix} \equiv \begin{bmatrix} \cos 2\varphi & -\sin 2\varphi \\ \sin 2\varphi & \cos 2\varphi \end{bmatrix} \begin{bmatrix} A_1^{(1)} \\ A_2 \end{bmatrix}, \tag{30b}$$

and

$$\begin{bmatrix} \delta_3 \Xi(\varphi) \\ \delta_3 H(\varphi) \end{bmatrix} \equiv \begin{bmatrix} \cos\varphi & -\sin\varphi \\ \sin\varphi & \cos\varphi \end{bmatrix} \begin{bmatrix} 0 \\ K_2 \end{bmatrix}. \tag{30c}$$

with $\bar{\delta}_4 = \bar{0}$, necessarily.

The graphical interpretation of these vector expressions remains the same as previously; that is, $\bar{\delta}_1$ defines a fixed point locus, while $\bar{\delta}_2$ and $\bar{\delta}_3$ each describe circles -- $\bar{\delta}_2$ having double frequency, but $\bar{\delta}_3$ retains its single frequency in trace motion. Of course, the size of these geometric figures will be altered due to the removal of the scalar $K_1$. Combining the vectors $\bar{\delta}_1$ and $\bar{\delta}_2$ it is seen that these produce loci generated from a double circulating trace vector, not originating from the origin. Adding to this the vector $\bar{\delta}_3$ it is found that the final trace geometry is a limacon. In order to illustrate this study case more clearly, a sketch is provided on Fig. 9. This shows the appropriate constructions.

On Fig. 9 one can see a slight asymmetry, in the trace geometry, about the H-axis. After examining the governing expressions for this particular case it is found that when the speed component $H_o' \equiv 0$ this asymmetry is removed.

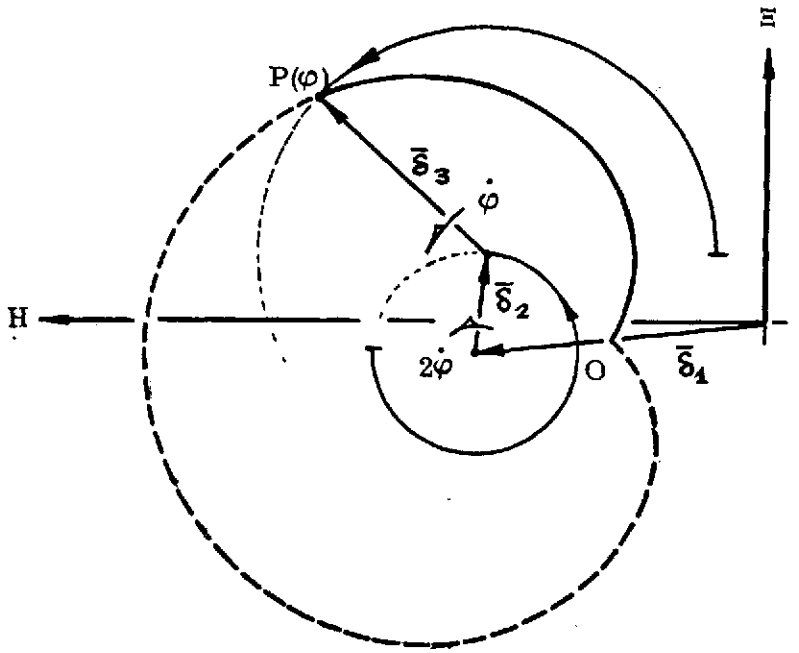


FIG. 9. In-plane displacement construction for a typical non-secular Initial-Values Problem, referred to an inertially oriented frame of reference. The figure is a limacon, developed from two circles ($\bar{\delta}_2$, $\bar{\delta}_3$). Solid arcs, on circles, correspond to the solid arc on the limacon (arc O to P). Position vector $\bar{\delta}_1$ locates a fixed point on the plane.

IV.3 The Zero Initial Value Problem. In this case the initial state conditions are set to zero and the motion is developed solely from the influence of the applied force system. The specific forces here are those having fixed components in the directions of the rotating axes; i.e., $\bar{\tau} \equiv \bar{\tau}\,(\tau_\xi,\ \tau_\eta,\ \tau_\zeta)$.

For the discussion of these in-plane motion traces an appropriate analytical expression to be manipulated is:

$$I_2 \bar{R}(\varphi) \equiv \left[3(J_2 - J_1) + T_2(2\varphi^-)\right]\left[A_{a_I}\right]_\tau + T_2(\varphi^-)\ \Psi_\tau \bar{\tau}; \tag{31}$$

wherein

$$\left[A_{a_I}\right]_\tau \equiv \frac{1}{2}\left[J_1 - 2J_2\right]\bar{\tau}, \tag{32}$$

and

$$\Psi_\tau \equiv \left[J_1 + 4J_2\right] - \varphi\left[2B_2 + \frac{3}{2} J_2 \varphi\right]. \tag{33}*$$

As with earlier studies this trace vector will be constructed from the several vector components arising from the matrix coefficients (A, $\Psi$). The most obvious selection for these vectors requires five components -- two and three, respectively, associated with the coefficient matrices (A, $\Psi$). Note that in this total there is one fixed vector; all others are dependent on the position variable ($\varphi$).

Expressing these vectors in matrix form one finds:

$$\begin{bmatrix} \delta_1 \Xi(\varphi) \\ \delta_1 H(\varphi) \end{bmatrix} \equiv 3 \begin{bmatrix} -1 & 0 \\ 0 & 1 \end{bmatrix}\begin{bmatrix} A_1 \\ A_2 \end{bmatrix} = \begin{bmatrix} -3 & 0 \\ 0 & 3 \end{bmatrix}\begin{bmatrix} \frac{1}{2}\tau_\xi \\ -\tau_\eta \end{bmatrix}, \tag{34a}$$

$$\begin{bmatrix} \delta_2 \Xi(\varphi) \\ \delta_2 H(\varphi) \end{bmatrix} \equiv \begin{bmatrix} \cos 2\varphi & -\sin 2\varphi \\ \sin 2\varphi & \cos 2\varphi \end{bmatrix}\begin{bmatrix} \frac{1}{2}\tau_\xi \\ -\tau_\eta \end{bmatrix}, \tag{34b}$$

$$\begin{bmatrix} \delta_3 \Xi(\varphi) \\ \delta_3 H(\varphi) \end{bmatrix} \equiv \begin{bmatrix} \cos\varphi & -4\sin\varphi \\ \sin\varphi & 4\cos\varphi \end{bmatrix}\begin{bmatrix} \tau_\xi \\ \tau_\eta \end{bmatrix}, \tag{34c}$$

*A matrix definition is found in the SELECTED EQUATIONS listing.

$$\begin{bmatrix} \delta_4 \Xi(\varphi) \\ \delta_4 H(\varphi) \end{bmatrix} \equiv 2\varphi \begin{bmatrix} \sin\varphi & \cos\varphi \\ -\cos\varphi & \sin\varphi \end{bmatrix} \begin{bmatrix} \tau_\xi \\ \tau_\eta \end{bmatrix} , \tag{34d}$$

and

$$\begin{bmatrix} \delta_5 \Xi(\varphi) \\ \delta_5 H(\varphi) \end{bmatrix} \equiv \frac{3\varphi^2}{2} \begin{bmatrix} 0 & \sin\varphi \\ 0 & -\cos\varphi \end{bmatrix} \begin{bmatrix} \tau_\xi \\ \tau_\eta \end{bmatrix} . \tag{34e}$$

The first vector ($\bar{\delta}_1$) describes a fixed locus, while the vector, $\bar{\delta}_2$, represents a circle having double orbital frequency. The third component vector ($\bar{\delta}_3$) also represents a circle; however, this one has a single frequency of motion. Also, it has a radius $=\sqrt{\tau_\xi^2 + (4\tau_\eta)^2}$ . The last two vectors ($\bar{\delta}_4$ and $\bar{\delta}_5$) contribute the secular effect found for this (analytical) trace description. Since both $\tau$-terms contribute to the trace's divergent character, it is obvious that there is no simple means (other than nulling the force system) by which this effect can be removed. (For reference purposes, $\bar{\delta}_4$ describes an archimedian spiral while $\bar{\delta}_5$ describes "spiral-like" loci on the plane of motion).

Since the two spirals will quickly dominate the motion's trace, then it is appropriate to classify this total geometry as "spiral-like".

Because the construction for this trace would be rather cluttered it is felt that little can be gained by attempting to develop this complicated figure from its several components. Accordingly, a sketch of the construction is not included.

Since the specific force component, $\tau_\eta$, has the greater secular influence on this trace it is informative to examine the situation when $\tau_\eta \equiv 0$. This specialization removes the last vector component ($\bar{\delta}_5$); but, additionally, the other components are affected. In general, the other loci are not changed, geometrically, even though the magnitude of the various influences may be altered. The general trace still will have a divergent character; this is brought out by the archimedian spiral ($\bar{\delta}_4$). The other vectors will most likely produce a figure which would appear as a limacon (this is developed from $\bar{\delta}_1$, $\bar{\delta}_2$ and $\bar{\delta}_3$).

If one compares this problem with its counterpart, appearing on the local-rotating-frame of reference, it is evident that the present situation is (geometrically) more complicated. A review of all trace geometries described in this frame of reference will quickly point to the fact that, basically, these traces lead to spiral-like figures while those found in the "rotating frame" would likely be of a more varied geometry. What is most important here, as seen from the several examples studied so far, is the unusual nature of the traces, and the inherent difficulty one would have in attempting to "guess" these shapes, a priori.

Continuing with the pattern established earlier, the hodograph traces corresponding to the displacement diagrams,above, are to be determined and discussed next. These are found in the paragraphs to follow.

## V. THE HODOGRAPH IN THE INERTIAL FRAME OF REFERENCE

In a discussion of hodograph traces for the inertial frame of reference, as these are determined from an analytical solution to this relative motion problem, the in-plane traces will be examined first. In keeping with the philosophy established earlier, the Initial Values Problems will be separated from the "thrusting" case and each studied independently. However, these two situations must be recognized to be additive so that the complete evaluations, involving all contributions, may be obtained simply by summing results.

V.1. The Initial Values Problem. The expression from which the hodograph traces are drawn is:

$$I_2\bar{R}'(\varphi) = B_2\left\{2T_2(2\varphi^-)\left[A_{a_I}\right]_{i.v.} + T_2(\varphi^-)\left[I_2 - \frac{3}{2}B_2J_1\varphi\right]K_{o_I}\right\} - \frac{3}{2}T_2(\varphi^-)\left[B_2J_1\right]K_{o_I}, \tag{35a}$$

where the coefficient matrices (A, K) are those defined in Eqs. (26) and (27). As in the discussions on displacement traces, these coefficients are expressed in terms of their scalars ($A_i$, $K_i$), obtained by matrix multiplication. As a consequence the trace geometries are developed from three vector components -- one involving $A_a$, and two obtained from the matrix, $K_{o_I}$. (See Eqs. (28) for a description of the scalars $A_i$, $K_i$).

Forming the three vectors noted above, then as matrices, define:

$$\begin{bmatrix}\delta_1\Xi'(\varphi)\\ \delta_1H'(\varphi)\end{bmatrix} = 2\begin{bmatrix}-\sin 2\varphi & -\cos 2\varphi\\ \cos 2\varphi & -\sin 2\varphi\end{bmatrix}\begin{bmatrix}A_1\\ A_2\end{bmatrix}, \tag{35b}$$

$$\begin{bmatrix}\delta_2\Xi'(\varphi)\\ \delta_2H'(\varphi)\end{bmatrix} = \begin{bmatrix}\frac{1}{2}\sin\varphi & -\cos\varphi\\ -\frac{1}{2}\cos\varphi & -\sin\varphi\end{bmatrix}\begin{bmatrix}K_1\\ K_2\end{bmatrix}, \tag{35c}$$

and

$$\begin{bmatrix}\delta_3\Xi'(\varphi)\\ \delta_3H'(\varphi)\end{bmatrix} = \frac{3\varphi}{2}\begin{bmatrix}\cos\varphi & \sin\varphi\\ \sin\varphi & -\cos\varphi\end{bmatrix}\begin{bmatrix}K_1\\ 0\end{bmatrix}. \tag{35d}$$

Geometrically these vectors describe: (1), a circle ($\bar{\delta}_1$) whose radius is $\sqrt{A_1^2 + A_2^2}$ (the magnitude of $\left[A_{a_I}\right]_{i.v.}$); note that this trace has double orbital frequency. The second vector (2), ($\bar{\delta}_2$) is also a circle, but this one has a frequency of motion matching that of the base orbit; and, its radius is $\sqrt{\left(\frac{1}{2}K_1\right)^2 + K_2^2}$. Lastly, the loci described from $\bar{\delta}_3$ form an archimedian spiral whose constant of proportionality is (3/2) $K_1$. Obviously, as the trace progresses (in time) this last characteristic will play the dominant role; hence, (again) a general classification for this hodograph would be "spiral-like".

As an aid to understanding the composition for these loci (P), on the hodograph plane, a sketch (typical of this case) has been prepared (see Fig. 10). There, several points are described using the appropriate vectors ($\bar{\delta}_i$). The purpose in detailing this construction is to give more explicit diagramming information regarding the makeup of each locus.

V.2 The Non-Secular Initial Values Problem. The elimination of secular effects for this part of the relative motion, and in particular on the hodograph, can be achieved by setting $K_1 = 0$. When this is done the spiral ($\bar{\delta}_3$) disappears and the subsequent trace, on the ($\Xi'$, H')-plane, is formed from the component vectors $\bar{\delta}_1$ and $\bar{\delta}_2$. Actually, the elimination of $K_1$ has more of an influence than what is explicitly seen. There is an added implied effect since the matrix $A_{a_I}$ is related to $K_{o_I}$ directly, (see Eq. (28)). The consequence of this action is such that the relationship between the scalars ($A_i$, $K_i$) and the state variables is (for the non-secular traces):

$$A_1 \equiv \frac{1}{2} H'_o, \quad A_2 = \frac{1}{2}(H_o + \Xi'_o), \quad K_1 = 0, \quad K_2 = -(H_o + 2\Xi'_o). \tag{36}$$

With these reductions in hand the component vectors (Eq. (35)) reduce to the following set:

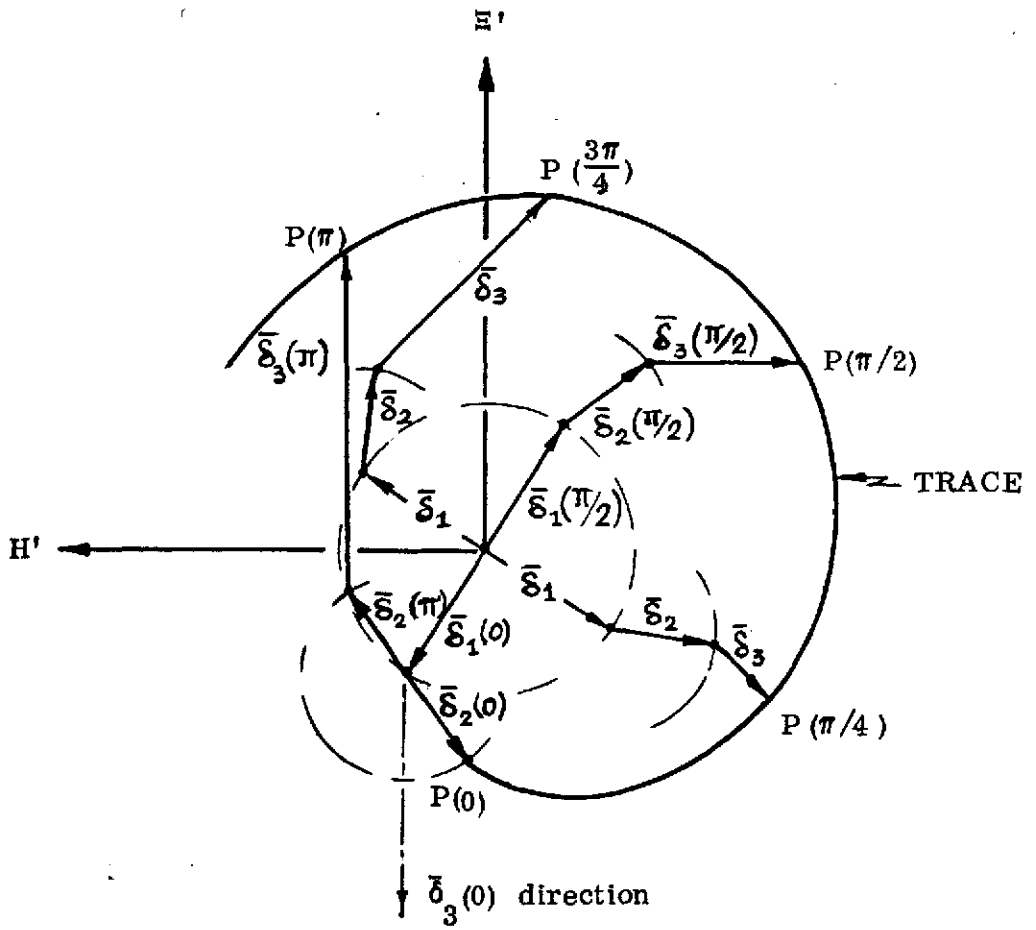


FIG. 10. A typical construction of the hodograph ($\Xi'$, H') for an Initial-Values Problem. Each point (P) is located by an appropriate sum of the position vectors ($\bar{\delta}_i$). For convenience, this trace has been sketched assuming positive valued scalars ($A_i$, $K_i$).

$$\begin{bmatrix} \delta_1 \Xi' \\ \delta_1 H' \end{bmatrix} = \begin{bmatrix} -\sin 2\varphi & -\cos 2\varphi \\ \cos 2\varphi & -\sin 2\varphi \end{bmatrix} \begin{bmatrix} H'_o \\ H_o + \Xi'_o \end{bmatrix} , \tag{37a}$$

and

$$\begin{bmatrix} \delta_2 \Xi' \\ \delta_2 H' \end{bmatrix} = \begin{bmatrix} \frac{1}{2}\sin\varphi & -\cos\varphi \\ -\frac{1}{2}\cos\varphi & -\sin\varphi \end{bmatrix} \begin{bmatrix} 0 \\ -(H_o + 2\Xi'_o) \end{bmatrix} ; \tag{37b}$$

with (necessarily) $\bar{\delta}_3 = \bar{0}$.

As noted above these expressions describe two circles -- one with double orbit frequency ($\bar{\delta}_1$), and one with single orbit frequency (for their trace motion). Typically, the trace generated by these vectors describes a limacon. It should be mentioned that when $H'_o \equiv 0$, the limacon is symmetric about the $\Xi'$-axis (see Figs. 11). However, if the motion is so restricted that $\bar{\mathcal{R}}_o = \bar{0}$ and $\bar{\mathcal{R}}'_o \equiv \bar{\mathcal{R}}'_o(\Xi'_o, 0, 0)$ then the limacon assumes the form of a cardioid (see Fig. 11(a)). As an aid in clarifying this construction, a limacon is developed, using the vectors ($\bar{\delta}_1$, $\bar{\delta}_2$), on Fig. 11(b). There the point "O" locates the initial position for the trace; this is described by $\bar{\delta}_1(0) + \bar{\delta}_2(0)$. Corresponding to the initial positions, $O_1$ defines the point, $\bar{\delta}_1(0)$, and the vector connecting O to $O_1$ would be $\bar{\delta}_2(0)$. The several tic marks on the various curves are to indicate corresponding $\varphi$-positions on each component trace. Also these same marks will imply a direction of traverse along each arc.

V.3 The Zero-Initial State Case. The hodograph equation referred to the inertial frame of reference for this situation is given as:

$$I_2 \bar{\mathcal{R}}'(\varphi) = B_2 \left\{ \left[ 2T_2(2\varphi^-) \right] \left[ A_{a_I} \right]_\tau + T_2(\varphi^-) \left[ \Psi_\tau \right] \right\} \bar{\tau} + T_2(\varphi^-) \Psi'_\tau \bar{\tau} , \tag{38}$$

wherein the coefficient matrices are:

$$\left[ A_{a_I} \right]_\tau \equiv \frac{1}{2} \left[ J_1 - 2J_2 \right] ,$$

$$\Psi_\tau \equiv \left[ J_1 + 4J_2 \right] - \varphi \left[ 2B_2 + \frac{3}{2} J_2 \varphi \right] ,$$

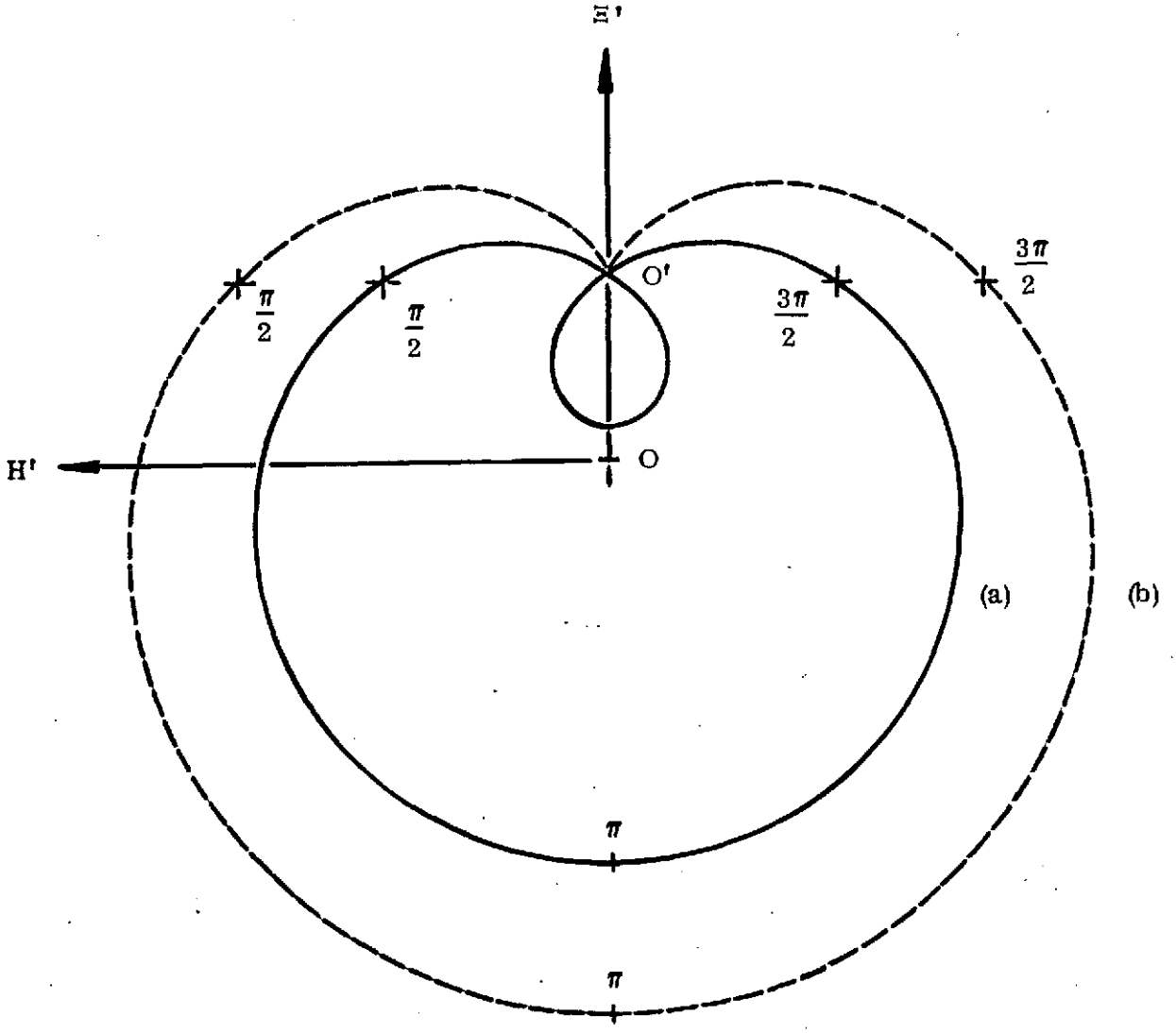


FIG. 11a. The hodograph ($\Xi'$, H') for a typical non-secular Initial-Values Problem. Curve (a), the symmetric limacon, is due to the constraint, $H'_o = 0$; curve (b) occurs when $\Xi'_o$ is the only initial state value acting. Note: O is origin for curve (a), while O' is for curve (b); scaling is not consistent for the two curves.

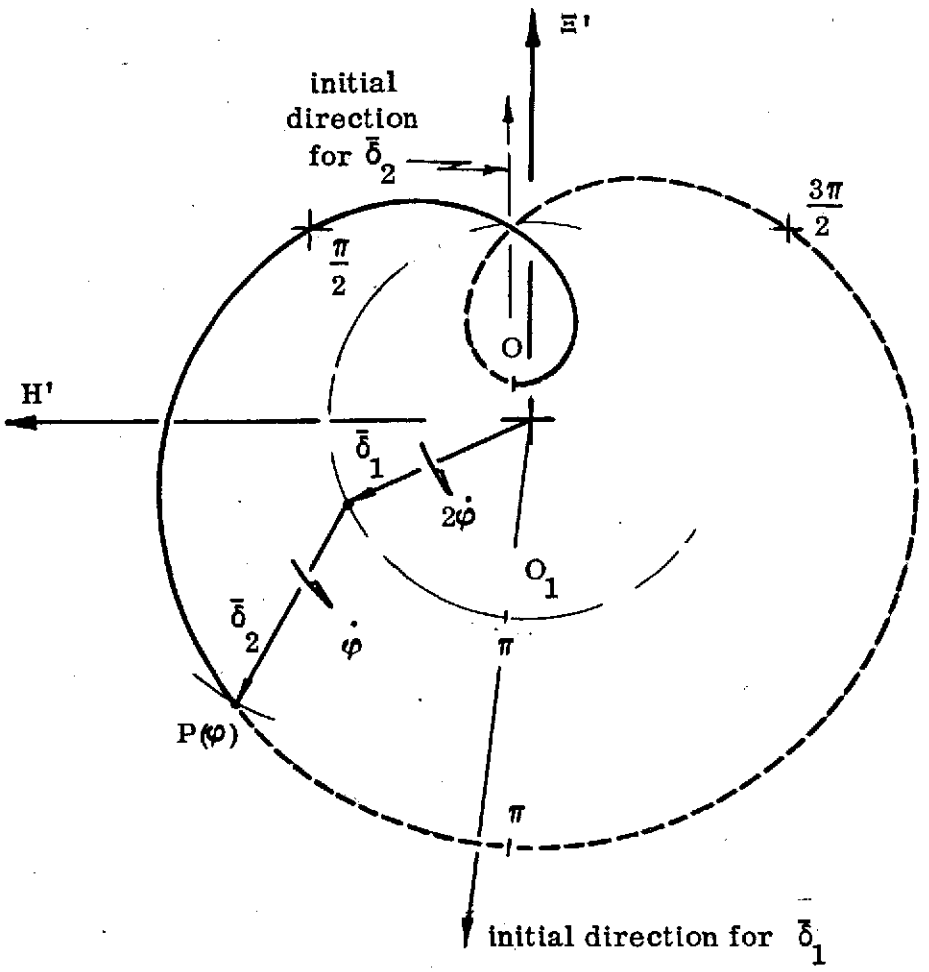


FIG. 11b. Typical construction for a general locus (P) on the non-secular Initial-Values Problem Hodograph. These loci are defined by $(\bar{\delta}_1 + \bar{\delta}_2)$, where $\bar{\delta}_1$ describes the circle of double orbit frequency; $\bar{\delta}_2$ defines points on the one of single orbit frequency. Initial position $(O_1)$ is for the circle $(\bar{\delta}_1)$; point O is the originating locus for the trace; O is described by $(\bar{\delta}_1(0) + \bar{\delta}_2(0))$.

and

$$\Psi'_{\tau} \equiv -\left[2B_2 + 3J_2\varphi\right]. \tag{39}*$$

Reviewing the overall composition of Eq. (38), it is seen that the more expedient means to describe the trace $(\Xi', H')$ is in terms of four vectors. The separation for these vectors is such that each one is homogenous in the variable, $\varphi$. As a consequence, one vector will involve the coefficient $A_{a_I}$ alone. Then, from $\Psi_{\tau}$ and $\Psi'_{\tau}$, there will be vectors involving powers of $\varphi$ (from the zeroth through the second). These vectors are defined as follows: first,

$$\delta_1\left[I_2\bar{R}'(\varphi)\right] \equiv 2B_2 T_2(2\varphi^-)\left[A_{a_I}\right]_{\tau}\bar{\tau}. \tag{40a}$$

This can be rewritten as the matrix equation:

$$\begin{bmatrix}\delta_1\Xi'(\varphi)\\ \delta_1 H'(\varphi)\end{bmatrix} = 2\begin{bmatrix}-\sin 2\varphi & -\cos 2\varphi\\ \cos 2\varphi & -\sin 2\varphi\end{bmatrix}\begin{bmatrix}A_1\\ A_2\end{bmatrix}, \tag{40b}$$

wherein $A_1 \equiv \frac{1}{2}\tau_{\xi}$, $A_2 \equiv -\tau_{\eta}$, and $\left[A_{a_I}\right]_{\tau} \equiv A_{a_I}(A_1, A_2)$.

Next, the vector for $\varphi^0$ is described. It is:

$$\begin{aligned}\delta_2\left[I_2\bar{R}'(\varphi)\right] &\equiv T_2(\varphi^-)\left[B_2(J_1 + 4J_2) - 2B_2 I_2\right]\bar{\tau}\\ &= T_2(\varphi^-)\left[B_2(2J_2 - J_1)\right]\bar{\tau};\end{aligned}$$

or, as a matrix expression:

$$\begin{bmatrix}\delta_2\Xi'(\varphi)\\ \delta_2 H'(\varphi)\end{bmatrix} = \begin{bmatrix}\sin\varphi & -2\cos\varphi\\ -\cos\varphi & -2\sin\varphi\end{bmatrix}\begin{bmatrix}\tau_{\xi}\\ \tau_{\eta}\end{bmatrix}. \tag{40c}$$

The first order secular terms appear in the equation:

$$\delta_3\left[I_2\bar{R}'(\varphi)\right] \equiv -\left[T_2(\varphi^-)\right]\varphi\left[2B_2^2 + 3J_2\right]\bar{\tau} = T_2(\varphi^-)\left[(2J_1 - J_2)\,\varphi\right]\bar{\tau},$$

*A matrix form of the equation is found in the SELECTED EQUATIONS listing.

which is alternately expressed by:

$$\begin{bmatrix} \delta_3 \Xi'(\varphi) \\ \delta_3 H'(\varphi) \end{bmatrix} = \varphi \begin{bmatrix} 2\cos\varphi & \sin\varphi \\ 2\sin\varphi & -\cos\varphi \end{bmatrix} \begin{bmatrix} \tau_\xi \\ \tau_\eta \end{bmatrix} . \tag{40d}$$

Finally, the expression involving $\varphi^2$ is noted to be:

$$\delta_4 \left[ I_2 \bar{R}'(\varphi) \right] \equiv -\frac{3}{2}\varphi^2 \left[ B_2 T_2(\varphi^-) \right] \left[ J_2 \bar{\tau} \right];$$

or

$$\begin{bmatrix} \delta_4 \Xi'(\varphi) \\ \delta_4 H'(\varphi) \end{bmatrix} = +\frac{3}{2}\varphi^2 \begin{bmatrix} \sin\varphi & \cos\varphi \\ -\cos\varphi & \sin\varphi \end{bmatrix} \begin{bmatrix} 0 \\ \tau_\eta \end{bmatrix} . \tag{40e}$$

In these four equations one finds two circles and two spirals. The first expression, Eq. (40b) describes a circle of double orbit frequency, having a radius equal to twice the magnitude of $\left[ A_{a_I} \right]_\tau$. The second circle, acquired from $\bar{\delta}_2$, has single frequency and a radius of $\sqrt{\tau_\xi^2 + (2\tau_\eta)^2}$ . The third equation ($\bar{\delta}_3$) describes an archimedian spiral ($r = k\varphi$), whose coefficient, $k \equiv \sqrt{(2\tau_\xi)^2 + \tau_\eta^2}$ . Lastly, Eq. (40c) is recognized to be a spiral-like curve symbolically expressed as $r = k\varphi^2$. Here the constant is seen to be, $k \equiv \frac{3}{2}\tau_\eta$.

It is evident that the spiral-like contributions to this total trace will quickly dominate the geometry; hence, the curve is obviously classified as "spiral-like".

The component makeup here is somewhat confusing to see in its construction; therefore, the component composition will not be illustrated below. Instead the sketch of a typical trace is given on Fig. 12. As an aid to the visualization of this construction the initial directions for the component vectors ($\bar{\delta}_i$) are indicated below. There the parathetic zero infers $\varphi = 0$; this describes an initial position referred to the base orbit.

Initial directions are obtained from Eqs. (40), these are:

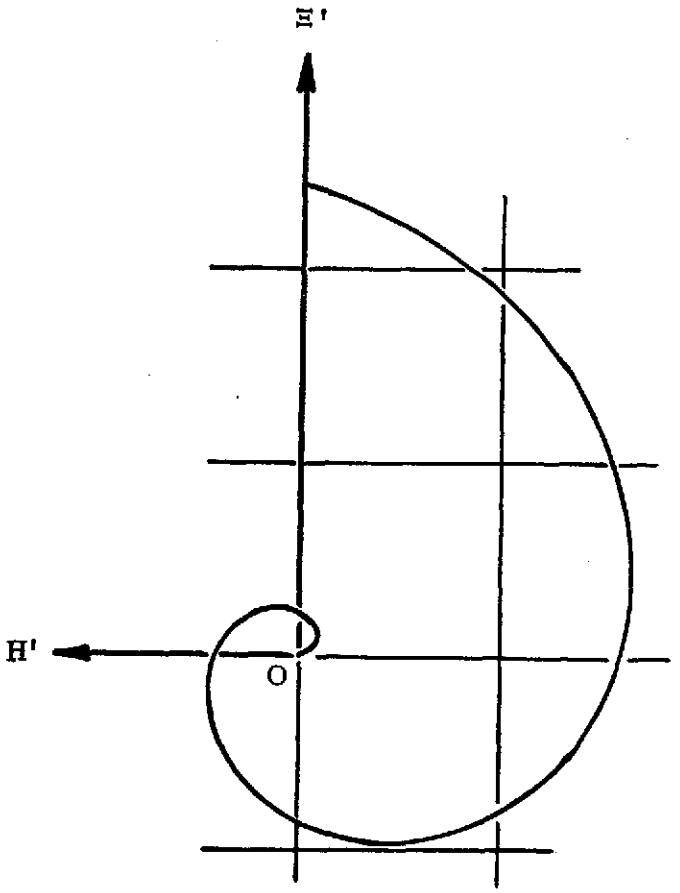


FIG. 12. A schematic of the trace for a typical Zero-Initial-Values Problem. This is for the specific force vector $\bar{\tau} \equiv \bar{\tau}(\tau_\xi, \tau_\eta)$.

$$\bar{\delta}_1(0) = (2\tau_\eta,\ \tau_\xi);\ \bar{\delta}_2(0) = (-2\tau_\eta,\ -\tau_\xi);\ \bar{\delta}_3(0) \propto (2\tau_\xi,\ -\tau_\eta);$$

and

$$\bar{\delta}_4(0) \propto \left(\frac{3}{2}\tau_\eta,\ 0\right). \tag{40f}$$

As an added aid to the construction description, the "vectors" at $\varphi = 2\pi$ are defined as follows:

$$\bar{\delta}_1(2\pi) = (2\tau_\eta,\ \tau_\xi);\ \bar{\delta}_2(2\pi) = (-2\tau_\eta,\ -\tau_\xi);\ \bar{\delta}_3(2\pi) = (4\pi\tau_\xi,\ -2\pi\tau_\eta);$$

and

$$\bar{\delta}_4(2\pi) = (6\pi^2\tau_\eta,\ 0). \tag{40g}$$

Note, also, that the elimination of $\tau_\eta$ would cause the trace to be obtained as a three vector sum for the construction of each point locus. Here the loci would be given from the two circles and the archimedian spiral; consequently this curve is akin to an involute of a circle.

The completes the description(s) for both the initial values problem and the case of a disturbing force system aligned with the rotating frame of reference. Yet to be analyzed is that case where the force system is assumed to be parallel to the inertial frame of reference. The descriptions for that system will be the subject for study in the next paragraphs.

## VI. THE INERTIALLY ALIGNED FORCE SYSTEM

The hodograph and displacement traces to be analyzed here are the consequence of an inertial aligned force system. That is, the specific applied force will be assumed to have fixed components parallel to an inertial frame of reference directions. Of course, the traces will be described in both the inertial and the "local rotating" frames of reference, as before.

It is not necessary here to redefine the initial values problem ($\bar{\tau} = 0$; and $\bar{R}_1, \bar{R}_o \neq 0$) since that solution is independent of any such force system applied; and, too, that solution has been examined earlier.

Therefore, in these paragraphs the traces are developed as a response to the particular force system applied. Following the pattern established earlier, traces in the local rotating frame will be examined first; then analogous cases for the inertially aligned frame will follow.

## VII. DISPLACEMENTS FOR THE ROTATING FRAME OF REFERENCE

In keeping with the work pattern established earlier the displacement diagrams below are those to appear on the $(\xi, \eta)$-plane; that is, the plane of motion for the reference particle.

VII.1 The Zero Initial State Problem. An equation for in-plane displacements referred to a local, rotating frame of reference, attached to the base particle is:

$$I_2 \bar{\mathcal{R}}(\varphi) = \left[I_2 + 3(J_2 - J_1)\right] T_2(\varphi^-) \left[A_a\right]_{i.v.} + \left[I_2 - \frac{3}{2}(B_2 J_1)\varphi\right] K_o + \Phi_\tau \bar{\tau}_I , \tag{41}$$

wherein $\left[A_a\right]_{i.v.}$ and $K_o$ are the quantities defined earlier (see Eq. (1)). The term $(\Phi_\tau \bar{\tau}_I)$ represents the (partial) solution of interest here. This expression analytically describes the influence of an applied force system $(\bar{\tau}_I)$ on the displacements, per se. For clarity, and for information, a mathematical description of the component terms is given below:

(1). $\bar{\tau}_I \equiv \bar{\tau}_I(\tau_\Xi, \tau_H, \tau_z)$; these scalars are presumed to be constants for this analysis. Each component bears a subscript to indicate its direction, in the inertial frame of reference.

$$(2).\ \Phi_\tau \equiv \left[2J_1 + 5J_2\right]\left[T_2(\varphi^+) - I_2\right] + \frac{3\varphi}{2}\left[J_1 + 2J_2\right]\left[J_2 B_2 + B_2 T_2(\varphi^+)\right]$$
$$+ \frac{1}{4}\left[J_1 - 2J_2\right]\left[T_2(\varphi^-) - T_2(\varphi^+)\right]; \tag{42}*$$

here $T_2(\varphi^\pm)$ denotes the transformation matrices used to transform any vector quantity from one triad of reference to another. The matrix operators $(J_i, B_2, I_2)$ has been defined elsewhere and should be well known.

To a small degree the transformation operators, $T_2(\varphi^\pm)$, as used here, are artifical; that is, they have been employed to describe certain trigonometric terms which came about in the mathematical analysis. This ploy has been used also to retain uniformity in notation throughout this study.

*See SELECTED EQUATIONS for an equivalent form of this resultant.

From Eq. (42) it appears that trace loci from that expression can be best constructed as the sum of five component vectors ($\bar{\delta}_i$); each vector selected to describe a particular geometry. It will be shown that these vectors determine: (1), a fixed point,($\delta_1$); an ellipse,($\delta_2$); a moving (line) point,($\bar{\delta}_3$); an oscillating (line) point,($\bar{\delta}_4$); and, a spiral,($\bar{\delta}_5$). Adding these vectors will obviously describe each representative point on the in-plane displacement trace.

Now, identifying each vector mentioned above:

(1). The fixed point ($\bar{\delta}_1$) is described by:

$$\delta_1\left[I_2\,\bar{\hbar}\,(\varphi)\right] \equiv \left[2J_1 + 5J_2\right](-I_2)\,\bar{\tau}_I\;;$$

or, as a matrix expression:

$$\begin{bmatrix}\delta_1\xi\\ \delta_1\eta\end{bmatrix} = -\begin{bmatrix}2 & 0\\ 0 & 5\end{bmatrix}\begin{bmatrix}\tau_\Xi\\ \tau_H\end{bmatrix}\quad . \tag{43a}$$

This locus is a fixed point expressed in terms of the in-plane components of $\bar{\tau}_I$.

(2). The elliptic loci are obtained from:

$$\delta_2\left[I_2\,\bar{\hbar}\,(\varphi)\right] \equiv \left\{\left[2J_1 + 5J_2\right]T_2(\varphi^+)\right\}\,\bar{\tau}_I\;;$$

which is the same as:

$$\begin{bmatrix}\delta_2\xi\\ \delta_2\eta\end{bmatrix} = \begin{bmatrix}2\cos\varphi & 2\sin\varphi\\ -5\sin\varphi & 5\cos\varphi\end{bmatrix}\begin{bmatrix}\tau_\Xi\\ \tau_H\end{bmatrix}\quad , \tag{43b}$$

and represents the (2:5) ellipse,

$$\left(\frac{\delta_2\xi}{2\sqrt{\tau_\Xi^2+\tau_H^2}}\right)^2 + \left(\frac{\delta_2\eta}{5\sqrt{\tau_\Xi^2+\tau_H^2}}\right)^2 = 1. \tag{43c}$$

When vectors $\bar{\delta}_1$ and $\bar{\delta}_2$ are added the resulting trace is a (2:5) ellipse with its geometric center shifted to the $\bar{\delta}_1$-locus.

(3). Next, the moving point ($\bar{\delta}_3$) is acquired from:

$$\delta_3\left[I_2\bar{\mathcal{K}}(\varphi)\right] \equiv \frac{3\varphi}{2}\left[J_1+2J_2\right]\left[J_2 B_2\right]\bar{\tau}_I \ ;$$

or,

$$\begin{bmatrix}\delta_3\xi\\ \delta_3\eta\end{bmatrix} = \begin{bmatrix}0 & 0\\ 3\varphi & 0\end{bmatrix}\begin{bmatrix}\tau_\Xi\\ \tau_H\end{bmatrix} \quad . \tag{43d}$$

This point moves parallel to the $\eta$-axis -- its direction of motion depends on sgn ($\tau_\Xi$), and the motion rate is $3\,|\tau_\Xi|$ .

(4). The oscillating line point is a consequence of:

$$\delta_4\left[I_2\bar{\mathcal{K}}(\varphi)\right] \equiv \frac{1}{4}\left[J_1-2J_2\right]\left[T_2(\varphi^-)-T_2(\varphi^+)\right]\bar{\tau}_I \ ;$$

or, in matrix form:

$$\begin{bmatrix}\delta_4\xi\\ \delta_4\eta\end{bmatrix} = \begin{bmatrix}0 & -\frac{1}{2}\sin\varphi\\ -\sin\varphi & 0\end{bmatrix}\begin{bmatrix}\tau_\Xi\\ \tau_H\end{bmatrix} \quad . \tag{43e}$$

This trace originates at an origin; it oscillates through that origin, and has an amplitude of motion, $|\bar{\delta}_4|_{max} \equiv \sqrt{\tau_\Xi^2+(\frac{\tau_H}{2})^2}$ .

(5). Finally, the spiral motion, here, is obtained from:

$$\delta_5\left[I_2\bar{\mathcal{K}}(\varphi)\right] \equiv \frac{3\varphi}{2}\left[J_1+2J_2\right]\left[B_2 T_2(\varphi^+)\right]\bar{\tau}_I \ ;$$

or,

$$\begin{bmatrix}\delta_5\xi\\ \delta_5\eta\end{bmatrix} = \frac{3\varphi}{2}\begin{bmatrix}-\sin\varphi & -\cos\varphi\\ 2\cos\varphi & -2\sin\varphi\end{bmatrix}\begin{bmatrix}\tau_\Xi\\ \tau_H\end{bmatrix} \quad . \tag{43f}$$

This describes an archimedian spiral ($r = k\varphi$), but one given in terms of a "reduced" set of coordinates; that is,

$$|\bar{\delta}_5|_{spiral} \equiv \sqrt{(\delta_5\xi)^2+\left(\frac{\delta_5\eta}{2}\right)^2} = \frac{3}{2}\sqrt{\tau_\Xi^2+\tau_H^2}\ \varphi \ . \tag{43g}$$

(Note that this spiral exists in the $(\xi, \frac{\eta}{2})$ displacement space rather than the true displacement space $(\xi, \eta)$).

Due to the rather cumbersome nature of this construction, only a composite (sketch) is shown below; see Fig. 13. It is evident that this trace originates at the coordinate origin and has a radius increasing in a secular (divergent) manner as the motion progresses.

Initial directions for each of the vectors $(\bar{\delta}_i)$ are noted below as an aid in visualizing the construction (an equality here is an explicit symbol; the proportionality sign infers direction; each such vector is expressed in the coordinates $(\xi, \eta)$). The initial vector "directions" are: $\bar{\delta}_1(0) \equiv (-2\tau_\Xi, -5\tau_H)$, which is invariant with $\varphi$; $\bar{\delta}_2(0) \equiv (2\tau_\Xi, 5\tau_H)$; $\bar{\delta}_3(0) \propto (0, \tau_H)$, a "direction" parallel to $\eta$, but described by sgn $(\tau_H)$; $\bar{\delta}_4(0) \propto (-\tau_H/2, -\tau_\Xi)$, this is a "pointing direction" for this vector; and, $\bar{\delta}_5(0) \propto (-3\tau_H/2, 3\tau_\Xi)$.

At the completion of one base orbit revolution ($\varphi \equiv 2\pi$) these component vectors will have loci determined from the vectors $(\bar{\delta}_i)$ as: $\bar{\delta}_1(2\pi) \equiv (-2\tau_\Xi, -5\tau_H)$, the invariant locus; $\bar{\delta}_2(2\pi) = (2\tau_\Xi, 5\tau_H)$; $\bar{\delta}_3(2\pi) = (0, 6\pi\tau_\Xi)$; $\bar{\delta}_4(2\pi) = (0, 0)$; and $\bar{\delta}_5(2\pi) = (-3\pi\tau_H, 6\pi\tau_\Xi)$. According to this description it is very easy to locate the point $(P(2\pi))$ in the displacement plane. Actually $P(2\pi)$ is seen to be the locus: $P(2\pi) \equiv (-3\pi\tau_H, 12\pi\tau_\Xi)$.

A general examination of these vectors (Eqs. (43)) finds a monotonic divergence for the loci of this motion. Of course, this is not an unexpected result in view of the physical interpretation of what is happening here. The interesting aspect of all that is shown is the overall character of this motion.

VII.2. Special Cases. The special cases of interest are those where $\tau_\Xi$ and $\tau_H$ are each set to zero, separately and independently. The trivial case, occurring when both components are nulled, is not of interest since this would not produce a displacement at all.

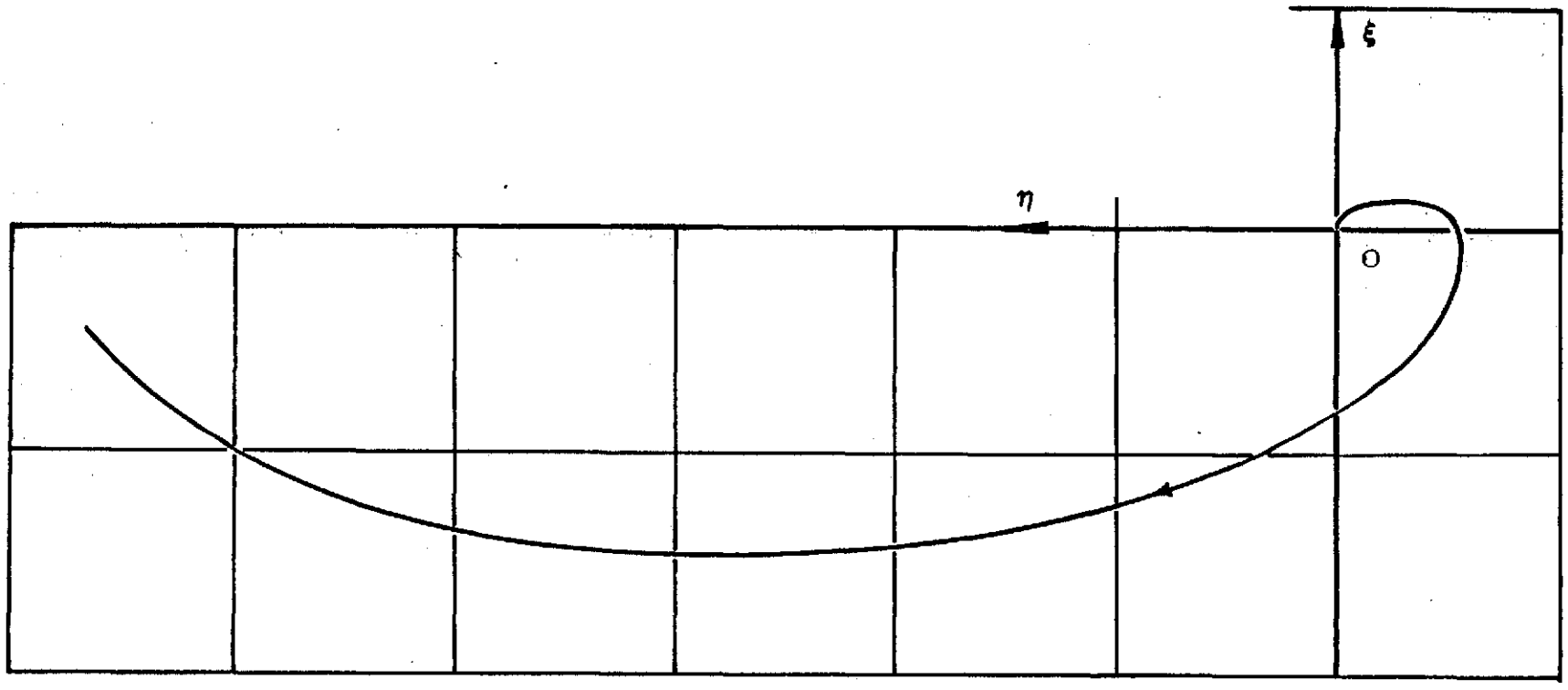


FIG. 13. A sketch of an overall typical in-plane trace for a Zero-Initial-Values Problem where the disturbance force is $\bar{\tau}_I \equiv \bar{\tau}_I(\tau_\Xi, \tau_H, \tau_Z)$. The figure is not scaled, however smallest scale divisions in the vicinity of the origin are for equal displacement increments.

When each force component is separately zeroed, the basic geometric character for each trace is not altered even though some size reductions are apparent. The one major alteration which does occur is the following: When $\tau_{\Xi} \equiv 0$, the line vector $\bar{\delta}_3$ is not in evidence. However, when $\tau_H \equiv 0$, the vector, $\bar{\delta}_3$, reappears -- actually, it is the <u>same</u> as the vector found for the general case.

It is not necessary to set down formulae for these special expressions since they are easily acquired from Eqs. (43). However, to clarify the trace geometries -- as they would occur for each special situation noted herein -- a sketch has been prepared. This is found on Fig. 14.

In the next paragraphs an examination of the corresponding hodograph traces will be undertaken. Once again the descriptions there will be limited to in-plane coordinates as a matter of convenience and compatibility with the prior presentations.

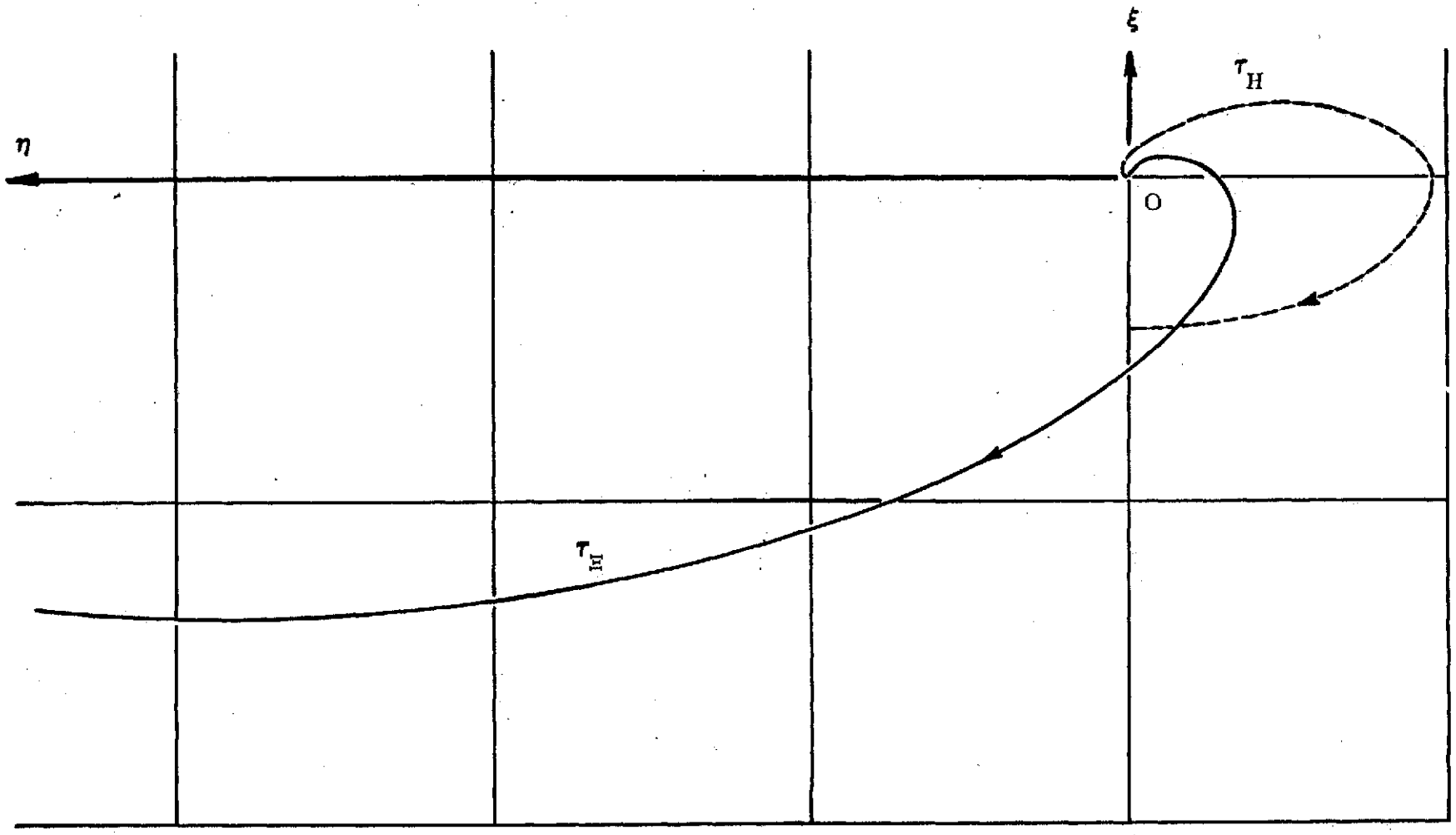


FIG. 14. Sketch for an in-plane, Zero-Initial-Values Problem showing the influence of $\tau_H$ and $\tau_H$ acting separately. Equal scale divisions imply equal displacement increments. (The numerical scaling is deleted for convenience and generalization).

## VIII. THE HODOGRAPH FOR A ROTATING FRAME OF REFERENCE

The in-plane hodographs which will be studied next are to be a consequence of the applied force system $\bar{\tau}_I \equiv \bar{\tau}_I(\tau_\Xi, \tau_H, \tau_z)$. This force acts on the test particle and produces a motion which is described in the local "rotating" reference space. The analytic expression which describes these hodographs has been developed earlier; however, that resultant obtained is:

$$I_2\bar{k}'(\varphi) = \left\{\left[I_2 + 3(J_2 - J_1)\right]B_2 T_2(\varphi^-)\right\}\left[A_a\right]_{i.v.} - \frac{3}{2}\left[B_2 J_1\right]K_o + \Phi'_\tau \bar{\tau}_I ; \tag{44}$$

wherein

$$\Phi'_\tau \equiv -\left[2J_1 + 5J_2\right]B_2 T_2(\varphi^+) + \frac{3}{2}\left[J_1 + 2J_2\right]\left[J_2 B_2 + (I_2 - B_2\varphi)\, B_2 T_2(\varphi^+)\right]$$
$$+ \frac{1}{4}\left[J_1 - 2J_2\right]B_2\left[T_2(\varphi^-) + T_2(\varphi^+)\right]. \tag{45}*$$

VIII.1 The Zero-Initial Value Problem. Equation (44) is the complete expression for the hodograph. However, all of this equation is not to be studied now since present interest is only in the partial solution, $\Phi'_\tau \bar{\tau}_I$. In this regard, then, attention will be given to Eq. (45), primarily.

To analyze this partial solution, and to propose a construction for the hodograph loci, the above expression will be examined as a four vector result. In the work to follow it will be shown that these vectors describe: (1), a point locus ($\bar{\delta}_1$); (2), an ellipse ($\bar{\delta}_2$); (3), an oscillating-line locus ($\bar{\delta}_3$); and (4), an archimedian spiral ($\bar{\delta}_4$).

A description for each of these contributing vectors is found below:

(1) The fixed (in-plane) point locus is described by:

$$\delta_1\left[I_2\bar{k}'(\varphi)\right] \equiv \frac{3}{2}\left[J_1 + 2J_2\right]\left[J_2 B_2\right]\bar{\tau}_I ;$$

or,

$$\begin{bmatrix}\delta_1\xi' \\ \delta_1\eta'\end{bmatrix} = \begin{bmatrix}0 & 0 \\ 3 & 0\end{bmatrix}\begin{bmatrix}\tau_\Xi \\ \tau_H\end{bmatrix} . \tag{46a}$$

*This expression appears in a matrix form, in with the SELECTED EQUATIONS.

This vector locates a point on the $\eta'$-axis.

(2). The ellipse is described by the vector:

$$\delta_2\left[I_2\,\bar{\kappa}'(\varphi)\right] \equiv \left\{-\left[2J_1+5J_2\right]+\frac{3}{2}\left[J_1+2J_2\right]\right\}\left[B_2\,T_2(\varphi^+)\right]\bar{\tau}_I\,;$$

which can be expressed in matrix form as:

$$\begin{bmatrix}\delta_2\xi'\\ \delta_2\eta'\end{bmatrix} = \begin{bmatrix}-\frac{1}{2}\sin\varphi & +\frac{1}{2}\cos\varphi\\ -2\cos\varphi & -2\sin\varphi\end{bmatrix}\begin{bmatrix}\tau_\Xi\\ \tau_H\end{bmatrix}\quad . \tag{46b}$$

A manipulation of these expressions defines the (4:1) ellipse,

$$\left(\frac{\delta_2\xi'}{\frac{1}{2}\sqrt{\tau_\Xi^2+\tau_H^2}}\right)^2+\left(\frac{\delta_2\eta'}{2\sqrt{\tau_\Xi^2+\tau_H^2}}\right)^2=1. \tag{46c}$$

Obviously when $\bar{\delta}_1$ and $\bar{\delta}_2$ are combined the subsequent trace appears as the ellipse with its center <u>shifted</u> by $\bar{\delta}_1$.

(3). The oscillating-line locus is obtained from the vector, $\bar{\delta}_3$; i.e.:

$$\delta_3\left[I_2\,\bar{\kappa}'(\varphi)\right] \equiv \left\{\frac{1}{4}\left[J_1-2J_2\right]\left[B_2\,T_2(\varphi^-)+B_2\,T_2(\varphi^+)\right]\right\}\bar{\tau}_I\,;$$

or

$$\begin{bmatrix}\delta_3\xi'\\ \delta_3\eta'\end{bmatrix} = \begin{bmatrix}0 & -\frac{1}{2}\cos\varphi\\ -\cos\varphi & 0\end{bmatrix}\begin{bmatrix}\tau_\Xi\\ \tau_H\end{bmatrix}\quad . \tag{46d}$$

This line oscillates at orbital frequency, passing through the origin each half cycle. Its initial direction (away from the origin) is in agreement with sgn $(\tau_i)$; and, the amplitude of these displacements is $\left|\bar{\delta}_3\right|_{max} \equiv \sqrt{\tau_\Xi^2+(\tau_H/2)^2}$.

(4). The last of these component vectors describes an archimedian spiral, but in a transformed coordinate space. That is:

$$\delta_4\left[I_2\,\bar{\kappa}'(\varphi)\right] \equiv \left\{+\frac{3}{2}\,\varphi\left[J_1+2J_2\right]T_2(\varphi^+)\right\}\bar{\tau}_I\,,$$

or, in an expanded format;

$$\begin{bmatrix} \delta_4\xi' \\ \delta_4\eta' \end{bmatrix} = \frac{3\varphi}{2} \begin{bmatrix} \cos\varphi & \sin\varphi \\ -2\sin\varphi & 2\cos\varphi \end{bmatrix} \begin{bmatrix} \tau_\Xi \\ \tau_H \end{bmatrix} \quad . \tag{46e}$$

The resultant here defines a spiral ($r = k\varphi$), expressed as:

$$\left[ (\delta_4\xi')^2 + \left( \frac{\delta_4\eta'}{2} \right)^2 \right]^{\frac{1}{2}} \equiv |\bar{\delta}_{4_{spiral}}| = \frac{3\varphi}{2} \sqrt{\tau_\Xi^2 + \tau_H^2} \quad . \tag{46f}$$

This figure is described in the $(\xi', \eta'/2)$-space; it has as the constant multiplier, $k \equiv \frac{3}{2}\sqrt{\tau_\Xi^2 + \tau_H^2}$ .

It is apparent that the divergent nature of this full trace comes about through the vector, $\bar{\delta}_4$. Also, it is obvious that this influence cannot be removed unless the complete (in-plane) force is eliminated. Of course, to do so would produce a rather trivial result.

When the four vector system is coupled, by means of vector addition, then the complete hodograph trace $(\xi', \eta')$ is acquired. As an illustration of this the plot on Fig. (15) is presented below. There, in its general appearance, the sketch appears as "spiral-like". This illustrates that the spiral, or secular nature, of the solution quickly dominates this geometry.

VIII.2 Special Cases. The special cases to be discussed here correspond to those situations described in the "displacements" section above. There, the two $\bar{\tau}_I$ cases considered were those where the force component scalars were zeroed separately and independently. These are the situations to be discussed below.

Setting either of the scalar force components to zero does not significantly alter the geometric character of any one of the component arcs. That is, the oscillating line trace remains a line; the ellipse retains its shape, and, so do the spirals. The main notable change occurs when $\tau_\Xi = 0$; then, the fixed locus vanishes (i.e., $\bar{\delta}_1 = \bar{0}$). This does not occur when $\tau_H = 0$.

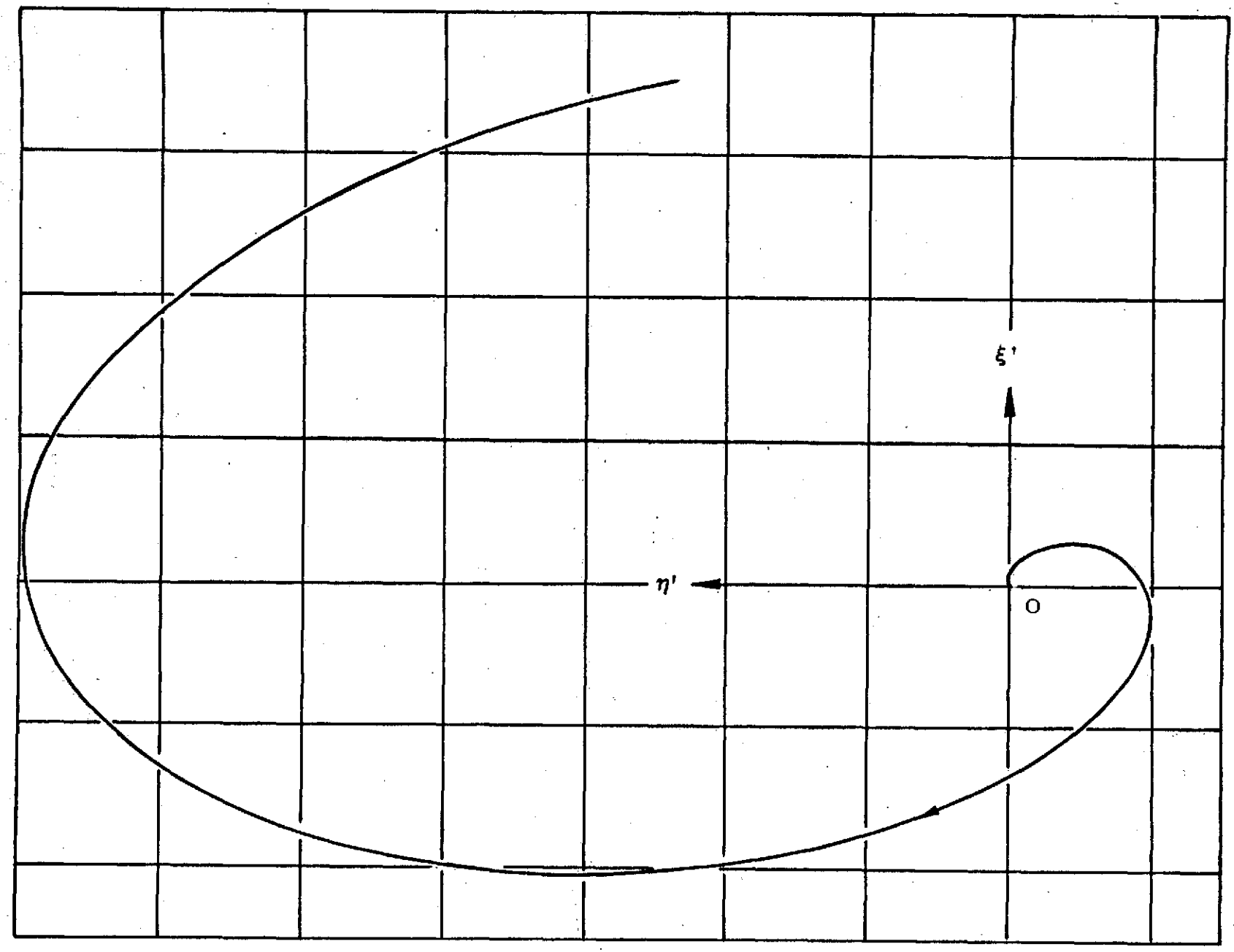


FIG. 15. Sketch of a typical, complete hodograph, referred to a rotating frame of reference, due to $\tau_{\Xi}$ and $\tau_{H}$ combined.

Once again, because of the details apparent to the construction, and those which would occur in developing the several trace components, only a composite figure will be shown on the figure below. (See Fig. 16).

Viewing these sketches one sees that (as before) the spiral, or divergent effect dominates the overall character of these traces. Of course to a large extent this is to be expected because of the physical nature of this problem. The constant applied (specific) force would necessarily cause a monotonic "growth" in the speeds so that, in time, this should be the dominating characteristic found.

The application of this same force system to the inertially defined state components will be studied next. In these following paragraphs displacement and hodograph traces are determined, and their geometries described and illustrated.

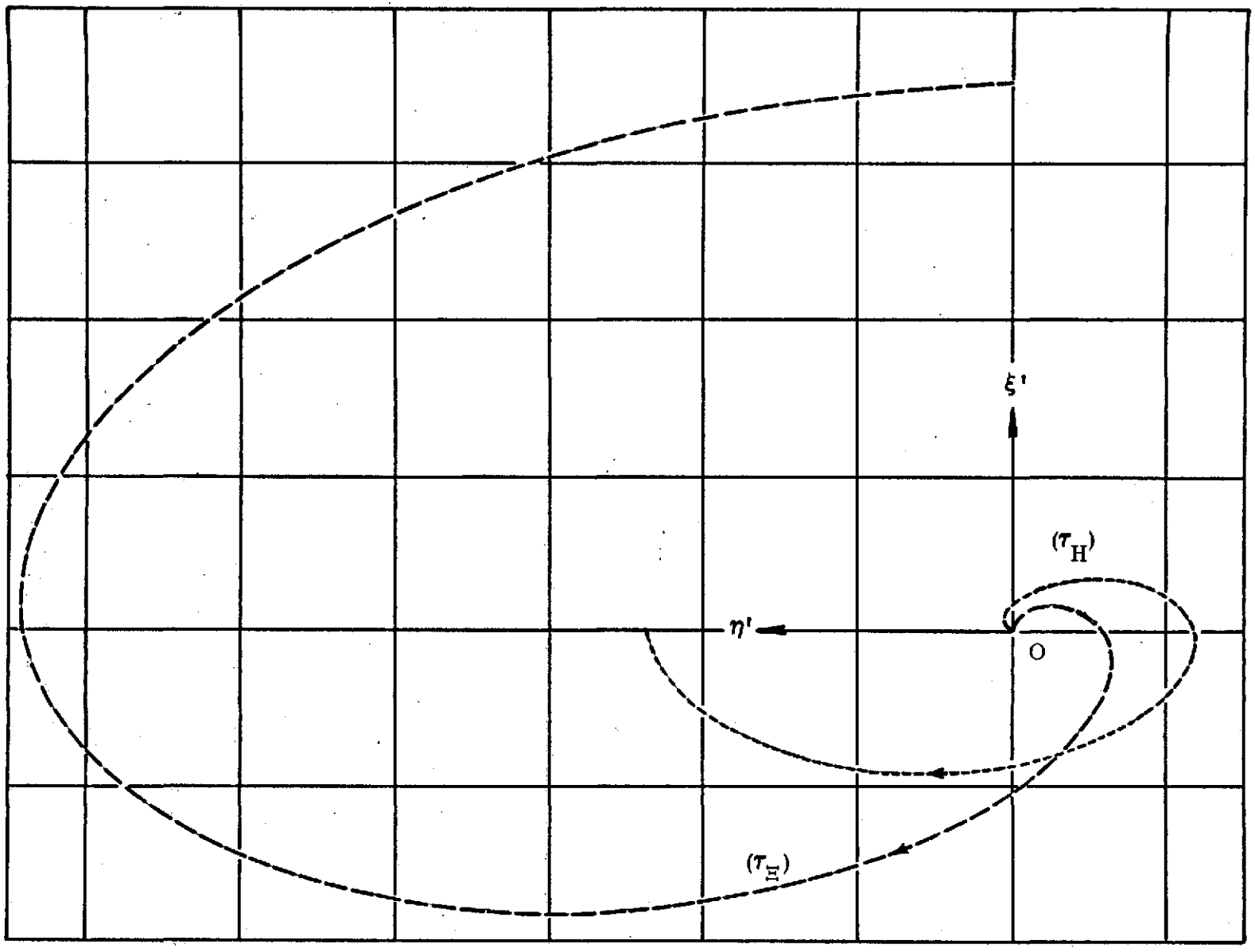


FIG. 16. Sketch of typical in-plane hodographs, referred to the rotating frame of reference, as described for $\tau_\Xi$ and $\tau_H$ applied independently. Note: Scale increments are equi-valued.

## IX. DISPLACEMENTS FOR THE INERTIAL FRAME OF REFERENCE

The displacement diagrams showing relative motion traces apparent to the inertially aligned frame of reference are developed from the appropriate analytical solution. This problem has considered a moving particle influenced by its own initial state, but additively subjected to a force system aligned with the inertial frame's axes. In fact this representation is analogous to the situation examined and discussed above. For reference purposes the equation which describes this motion has been previously obtained as:

$$I_2\bar{R}(\varphi) = \left\{T_2(2\varphi^-) + 3\left[J_2 - J_1\right]\right\}\left[A_{a_I}\right]_{i.v.} + T_2(\varphi^-)\left\{I_2 - \frac{3}{2}\varphi\left[B_2 J_1\right]\right\} K_{o_I} + T_2(\varphi^-)\left[\Phi_\tau \bar{\tau}_I\right], \tag{47}$$

wherein, $\left[A_{a_I}\right]_{i.v.}$ and $K_{o_I}$ are those quantities defined in Eqs. (26) and (27). Also, the matrix expression $\Phi_\tau$ is that described in Eq. (42), above.

Analogous to that case presented in the foregoing paragraphs the only quantities to be studied and analyzed here are those associated with the specific force, $\bar{\tau}_I$.

IX.1 The Zero Initial Value Problem. Restricting this discussion to terms in $\bar{\tau}_I$, then this particular partial solution is:

$$\delta\left[I_2\bar{R}(\varphi)\right] \equiv T_2(\varphi^-)\left[\Phi_\tau \bar{\tau}_I\right]. \tag{48}$$

Recalling the earlier partial solution and reviewing the matrix $\Phi_\tau$, above, it appears that the most descriptive breakdown for this case involves six component vectors. Each of these will be shown below in matrix format.

(1). The first vector component describes a point locus on the displacement ($\Xi$, H) plane. That is,

$$\begin{bmatrix} \delta_1{}^{\Xi} \\ \delta_1 H \end{bmatrix} \equiv \begin{bmatrix} 4 & 0 \\ 0 & \frac{13}{4} \end{bmatrix} \begin{bmatrix} \tau_{\Xi} \\ \tau_H \end{bmatrix} \quad . \tag{49a}$$

(2). The second partial solution defines a point moving along a line of fixed direction. This is described by:

$$\begin{bmatrix} \delta_2{}^{\Xi} \\ \delta_2 H \end{bmatrix} \equiv \frac{9}{4}\varphi \begin{bmatrix} 0 & -1 \\ 1 & 0 \end{bmatrix} \begin{bmatrix} \tau_{\Xi} \\ \tau_H \end{bmatrix} \quad . \tag{49b}$$

The trace is a locus with monotonically increasing distance between the point and the origin. Direction, per se, depends on the sgn $(\tau_i)$, and the rate is related to the magnitude of $\bar{\tau}_I$.

(3). The next vector defines loci which describe a circle on the displacement plane. That is,

$$\begin{bmatrix} \delta_3{}^{\Xi} \\ \delta_3 H \end{bmatrix} \equiv \begin{bmatrix} -2\cos\varphi & 5\sin\varphi \\ -2\sin\varphi & -5\cos\varphi \end{bmatrix} \begin{bmatrix} \tau_{\Xi} \\ \tau_H \end{bmatrix} \quad ; \tag{49c}$$

which is equivalent to the circle:

$$(\delta_3{}^{\Xi})^2 + (\delta_3 H)^2 = (2\tau_{\Xi})^2 + (5\tau_H)^2 . \tag{49d}$$

The composite trace obtained from the sum, $\bar{\delta}_1$, $\bar{\delta}_2$ and $\bar{\delta}_3$, would represent the circle $(\bar{\delta}_3)$, with a displaced center $(\bar{\delta}_1)$, whose peripheral loci are each continually being moved according to $\bar{\delta}_2$.

(4). One of these partial solution vectors is described in terms of the double frequency trigonometric functions above. This forms the positional loci:

$$\begin{bmatrix} \delta_4{}^{\Xi} \\ \delta_4 H \end{bmatrix} \equiv \begin{bmatrix} -2\cos 2\varphi & -\frac{7}{4}\sin 2\varphi \\ -2\sin 2\varphi & +\frac{7}{4}\cos 2\varphi \end{bmatrix} \begin{bmatrix} \tau_{\Xi} \\ \tau_H \end{bmatrix} \quad . \tag{49e}$$

The $\bar{\delta}_4$ vector traces out the circle,

$$(\delta_4{}^{\Xi})^2 + (\delta_4 H)^2 = (2\tau_{\Xi})^2 + (\frac{7}{4}\tau_H)^2 . \tag{49f}$$

(5). The next component vector ($\bar{\delta}_5$) describes a "spiral" situated in a modified coordinate space. The matrix for this vector is:

$$\begin{bmatrix} \delta_5{}^{\Xi} \\ \delta_5 H \end{bmatrix} \equiv 3\varphi \begin{bmatrix} -\sin\varphi & 0 \\ \cos\varphi & 0 \end{bmatrix} \begin{bmatrix} \tau_{\Xi} \\ \tau_H \end{bmatrix} , \tag{49g}$$

leading to the parametric expression:

$$\left[ \left( \frac{\delta_5{}^{\Xi}}{\tau_{\Xi}} \right)^2 + \left( \frac{\delta_5 H}{\tau_{\Xi}} \right)^2 \right]^{\frac{1}{2}} = 3\varphi , \tag{49h}$$

which defines an archimedian spiral.

(6). The last vector is defined in terms of double frequency trigonometric terms also. However, it leads to the spiral:

$$\begin{bmatrix} \delta_6{}^{\Xi} \\ \delta_6 H \end{bmatrix} \equiv \frac{3\varphi}{4} \begin{bmatrix} -\sin 2\varphi & \cos 2\varphi \\ \cos 2\varphi & \sin 2\varphi \end{bmatrix} \begin{bmatrix} \tau_{\Xi} \\ \tau_H \end{bmatrix} , \tag{49i}$$

described by the parametric expression:

$$(\delta_6{}^{\Xi})^2 + (\delta_6 H)^2 = \frac{3}{4}\sqrt{\tau_{\Xi}{}^2 + \tau_H{}^2}\ \varphi . \tag{49j}$$

From these six vectors the first one locates a fixed point ($\bar{\delta}_1$); two ($\bar{\delta}_3$, $\bar{\delta}_4$) are loci describing circles; another forms the line with "increasing" length; and, the remaining two vectors ($\bar{\delta}_5$, $\bar{\delta}_6$) generate spirals. For this total, three trace geometries show divergence while the others produce figures with bounded amplitudes of motion (fixed radii). Out of this description it should be evident that the general geometry here should be classed as "spiral-like". To the contrary, however, near the initial point these figures deviate from the more usual "smooth" character associated with other problems of this type. (See Fig. 17).

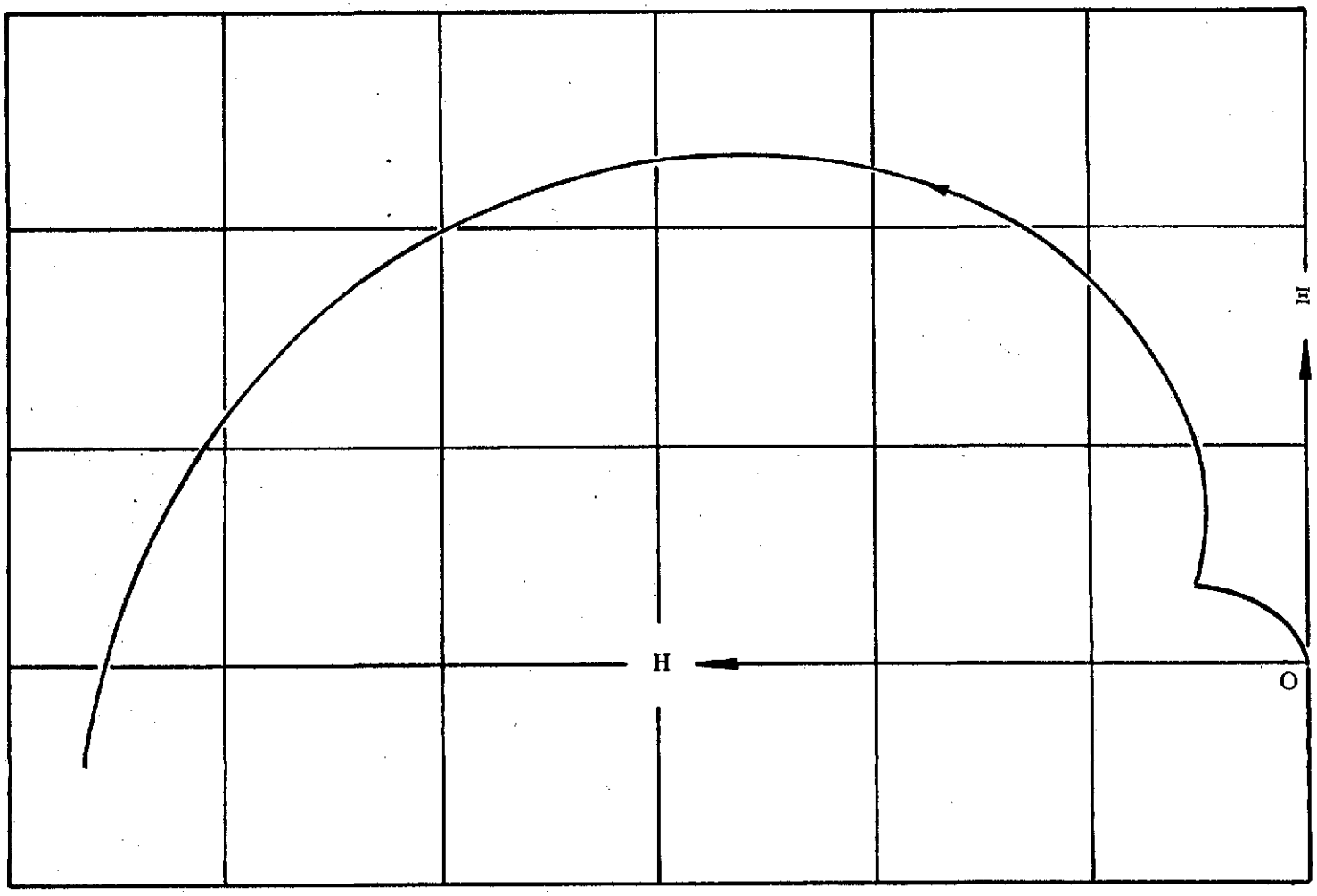


FIG. 17. Sketch of a ($\Xi$, H) trace geometry as produced by the application of a specific force $\bar{\tau}_I \equiv \bar{\tau}_I(\tau_\Xi, \tau_H)$. This composite figure is the combination of a six vector construction as described for this Zero-Initial-Values Problem.

IX.2 Special Cases. The only special cases of interest here would be those where only one force component at a time is considered. These traces, for this constrained condition, are also spirals. However, the spiral for $\tau_H$ (alone) produces the more classical figure (see Fig. 18). To the contrary, when $\tau_{\Xi} = 0$ the spiral ($\bar{\delta}_5$) vanishes but the other geometric characteristics are retained.

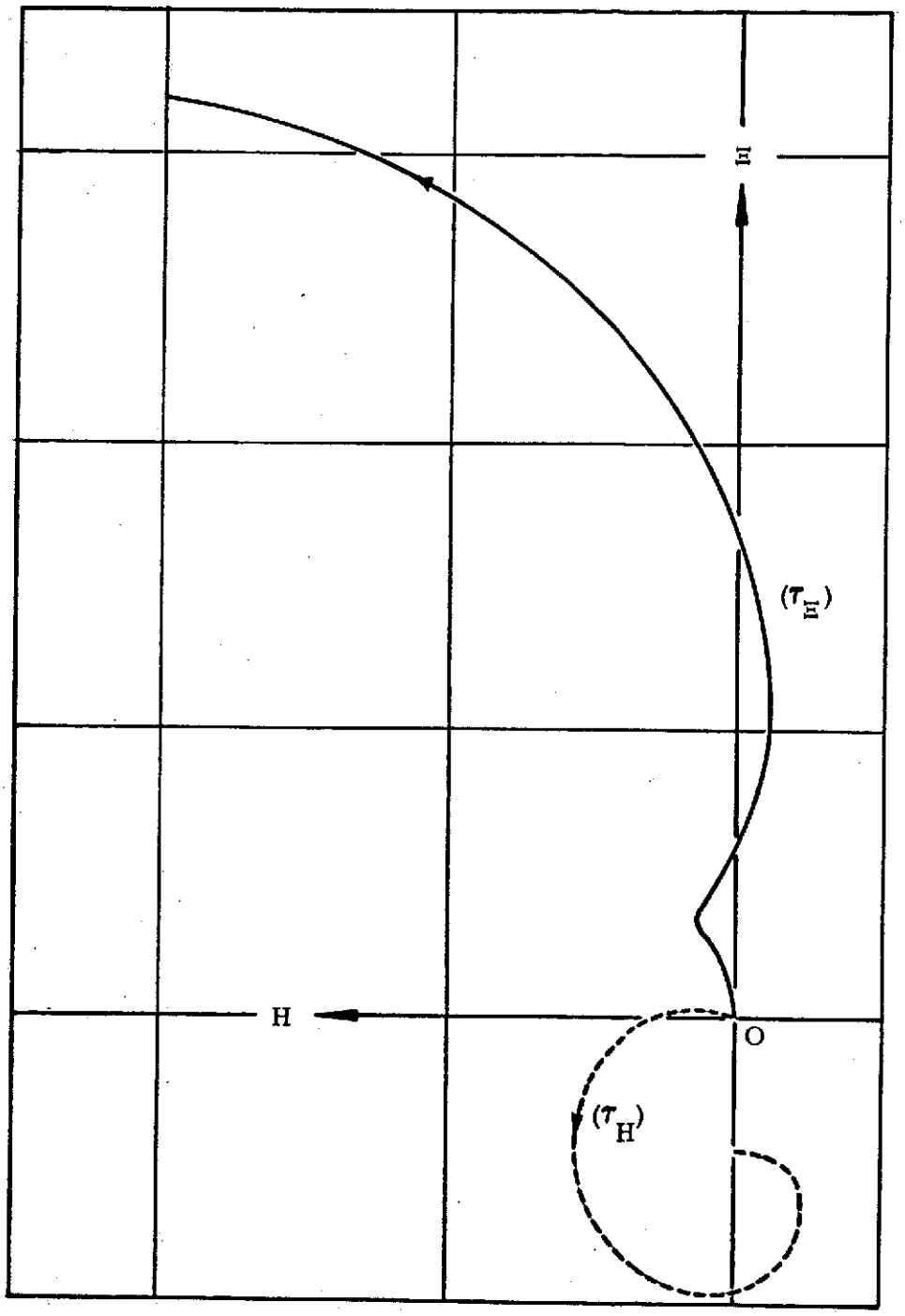


FIG. 18. Sketch of typical graphs of the in-plane displacement loci, referred to an inertially aligned frame of reference, as produced by the application of $\tau_{\Xi}$ and $\tau_H$, independently.

## X. THE HODOGRAPH IN THE INERTIAL FRAME OF REFERENCE

The general expression for this in-plane hodograph has been found to be:

$$I_2\bar{R}'(\varphi) \equiv B_2\left\{2\left[T_2(2\varphi^-)\right]\left[A_{a_I}\right]_{i.v.} + \frac{1}{2}T_2(\varphi^-)\left[2J_2 - J_1 - 3B_2J_1\varphi\right]K_{o_I}\right.$$

$$\left. + T_2(\varphi^-)\left[\Phi_\tau\bar{\tau}_I\right]\right\} + T_2(\varphi^-)\left[\Phi'_\tau\bar{\tau}_I\right], \tag{50}$$

wherein,

$$\Phi'_\tau \equiv -\left[2J_1 + 5J_2\right]B_2T_2(\varphi^+) + \frac{3}{2}\left[J_1 + 2J_2\right]\left[J_2B_2 + (I_2 - B_2\varphi)B_2T_2(\varphi^+)\right]$$

$$+ \frac{1}{4}\left[J_1 - 2J_2\right]B_2\left[T_2(\varphi^-) + T_2(\varphi^+)\right]. \tag{51}$$

Since the only part of this solution which is currently of interest is that involving $\Phi_\tau$ and $\Phi'_\tau$, then the needed descriptions will be developed accordingly. As a consequence, the partial solutions to be analyzed here are those obtained from:

$$\delta\left[I_2\bar{R}'(\varphi)\right] \equiv B_2\left[T_2(\varphi^-)\Phi_\tau\right]\bar{\tau}_I + T_2(\varphi^-)\left[\Phi'_\tau\right]\bar{\tau}_I, \tag{52}$$

(for definitions of $\Phi_\tau$ and $\Phi'_\tau$ see the expressions above).

X.1 The Partial Solution Due to $\bar{\tau}_I$ only. Equation (52) denotes the general expression to be examined here. Following the pattern established earlier that expression will be separated into its several (four, to be specific) sub-matrices. Each of these will be studied, individually, to ascertain the appropriate geometry from each. In the construction of a composite trace the several vectors would be summed.

It is demonstrated below that the full geometry on this hodograph plane is composed from a pair of circles and a pair of spirals. Specific descriptions for these will be acquired in the following paragraphs.

After several combinations and a rearrangement of terms the four vectors mentioned above are:

(1). A circle with its center located not at the coordinate origin, is developed from:

$$\begin{bmatrix} \delta_1 \Xi'(\varphi) \\ \delta_1 H'(\varphi) \end{bmatrix} \equiv \frac{1}{4} \begin{bmatrix} 13 \sin 2\varphi & -(9+11\cos 2\varphi) \\ (9-13\cos 2\varphi) & -11 \sin 2\varphi \end{bmatrix} \begin{bmatrix} \tau_\Xi \\ \tau_H \end{bmatrix} . \tag{53a}$$

The quadric expression for this figure is found to be:

$$(\delta_1 \Xi' + \frac{9}{4}\tau_H)^2 + (\delta_1 H' - \frac{9}{4}\tau_\Xi)^2 = (\frac{13}{4}\tau_\Xi)^2 + (\frac{11}{4}\tau_H)^2 . \tag{53b}$$

It is evident that the above expression is composed of two (2) vectors: one, a constant defining the fixed locus $(-\frac{9}{4}\tau_H, +\frac{9}{4}\tau_\Xi)$; and, a second vector locating points on the circle of radius $\sqrt{(\frac{13}{4}\tau_\Xi)^2 + (\frac{11}{4}\tau_H)^2}$. This geometry has a motion frequency which is twice that of the orbital frequency; and, the direction of motion is the same as that for the base orbit.

(2). Next, there is a circle of single orbit frequency described from:

$$\begin{bmatrix} \delta_2 \Xi' \\ \delta_2 H' \end{bmatrix} \equiv \begin{bmatrix} -\sin\varphi & 5\cos\varphi \\ \cos\varphi & 5\sin\varphi \end{bmatrix} \begin{bmatrix} \tau_\Xi \\ \tau_H \end{bmatrix} . \tag{53c}$$

This matrix leads to the parametric equation:

$$(\delta_2 \Xi')^2 + (\delta_2 H')^2 = \left[\tau_\Xi^2 + (5\tau_H)^2\right] . \tag{53d}$$

(3). The secular influence here provides a pair of archimedian spirals. One of these geometries is:

$$\begin{bmatrix} \delta_3 \Xi' \\ \delta_3 H' \end{bmatrix} = 3\varphi \begin{bmatrix} -\cos\varphi & 0 \\ -\sin\varphi & 0 \end{bmatrix} \begin{bmatrix} \tau_\Xi \\ \tau_H \end{bmatrix} ; \tag{53e}$$

or, in parametric form:

$$(\delta_3 \Xi')^2 + (\delta_3 H')^2 = (3\tau_\Xi)^2 \varphi^2 . \tag{53f}$$

This spiral ($r = k\varphi$), has its constant (k) defined in terms of $\tau_\Xi$ alone ($k \equiv 3\tau_\Xi$). Also, it has a "turning rate" equal to that of the base orbit.

(4). However, the second spiral has a double frequency; it is described in the matrix equation:

$$\begin{bmatrix} \delta_4 \Xi' \\ \delta_4 H' \end{bmatrix} = \frac{3\varphi}{2} \begin{bmatrix} -\cos 2\varphi & -\sin 2\varphi \\ -\sin 2\varphi & \cos 2\varphi \end{bmatrix} \begin{bmatrix} \tau_\Xi \\ \tau_H \end{bmatrix} . \tag{53g}$$

The archimedian spiral from the above equation can be represented by the quadric:

$$(\delta_4 \Xi')^2 + (\delta_4 H')^2 = \left(\frac{3\varphi}{2}\right)^2 (\tau_\Xi^2 + \tau_H^2). \tag{53h}$$

It is noted that the complete hodograph is acquired as the sum of these four vectors (Eqs. (53)). In order to illustrate this addition, a sketch, shown on Fig. 19, has been prepared. There, the initial vectors, $\bar{\delta}_i(0)$, and a representative set ($\bar{\delta}_i$) are included to illustrate typical loci. In addition, Fig. 20 has been included here to show a typical trace for the fixed specific force components ($\tau_\Xi$, $\tau_H$).

X.2 Special Cases. The special situations worthy of consideration at this point are those which consider only one force component ($\tau_\Xi$, $\tau_H$) in each example case.

When the $\tau_H$ component (of $\bar{\tau}_I$) is eliminated the trace geometry is not significantly altered (see Fig. 21). However, when $\tau_\Xi \equiv 0$ the $\bar{\delta}_3$ vector vanishes and that trace is significantly altered in scale and configuration. (The geometries shown on Fig. 21 are for a total angular displacement of one complete base orbit revolution).

It is easy to recognize what changes occur for the several component vectors ($\bar{\delta}_i$) here, when each of the $\bar{\tau}_I$ components is nulled. In Eqs. (53) the

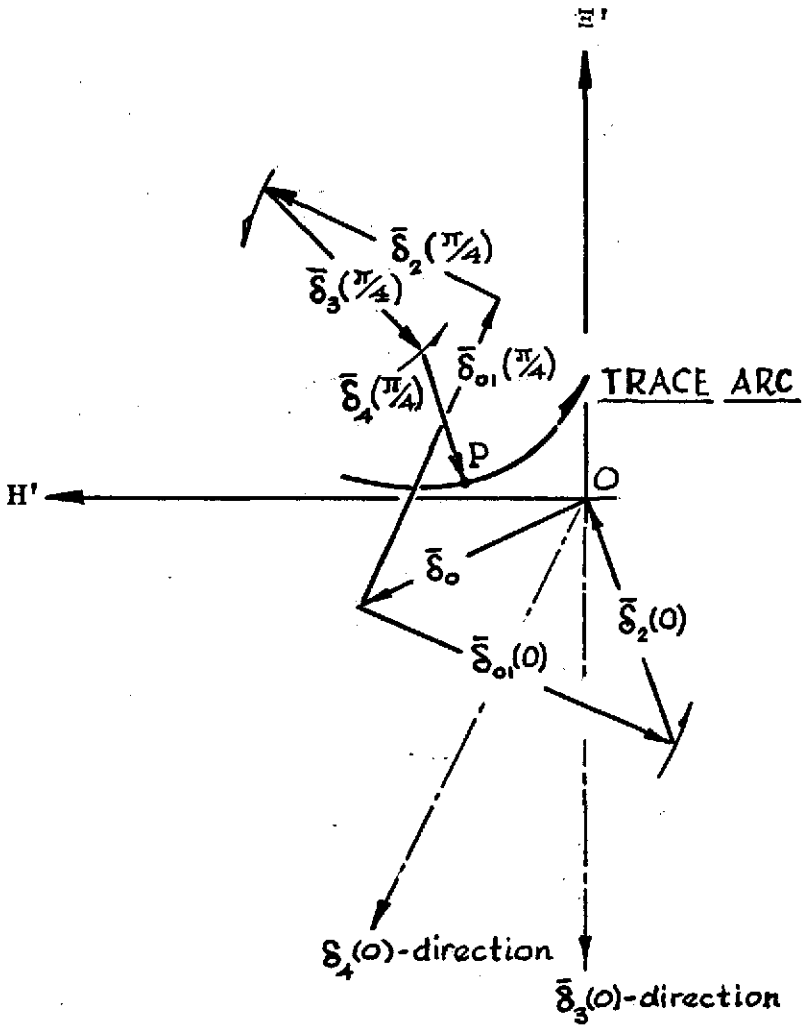


FIG. 19. A sketch depicting the construction for hodograph loci due to $(\tau_\Xi, \tau_H)$. Here $\bar{\delta}_0$ is the fixed component of $\bar{\delta}_1$ (see Eq. (53a)); $\bar{\delta}_2$ describes a circle (Eq. (53c)); while $\bar{\delta}_3$, $\bar{\delta}_4$ are spirals (see Eqs. (53e), (53g)). The two loci shown here (O, P) depict trace points for $\varphi = 0$ and $\varphi = \pi/4$, respectively.

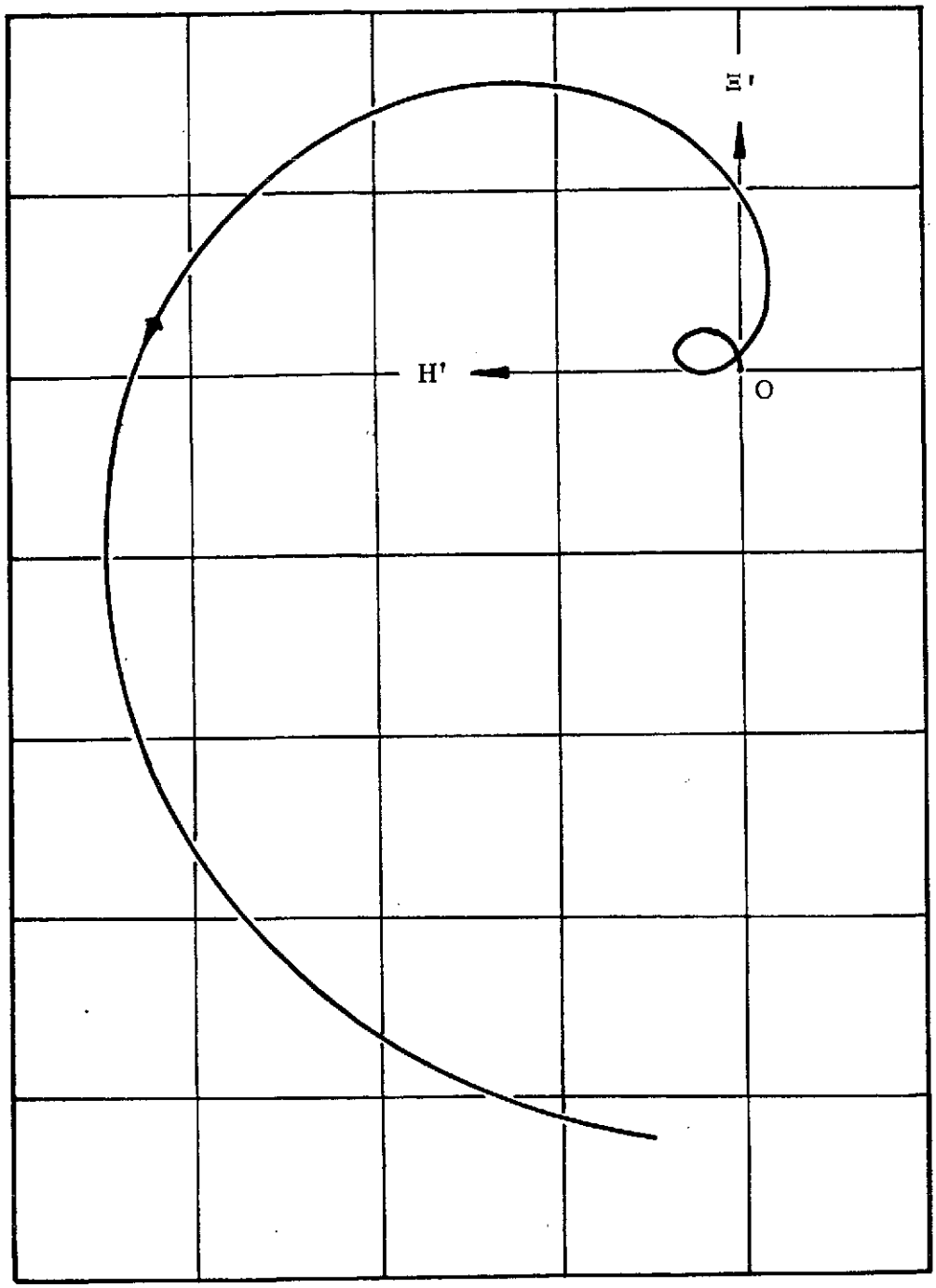


FIG. 20. A typical trace for the ($\Xi'$, H') hodograph plane as produced by the specific force components ($\tau_\Xi$, $\tau_H$). This figure is for loci in the range $0 \leq \varphi \leq 2\pi$ (referred to the base, circular orbit). Direction along the curve is as indicated; O describes the trace origin.

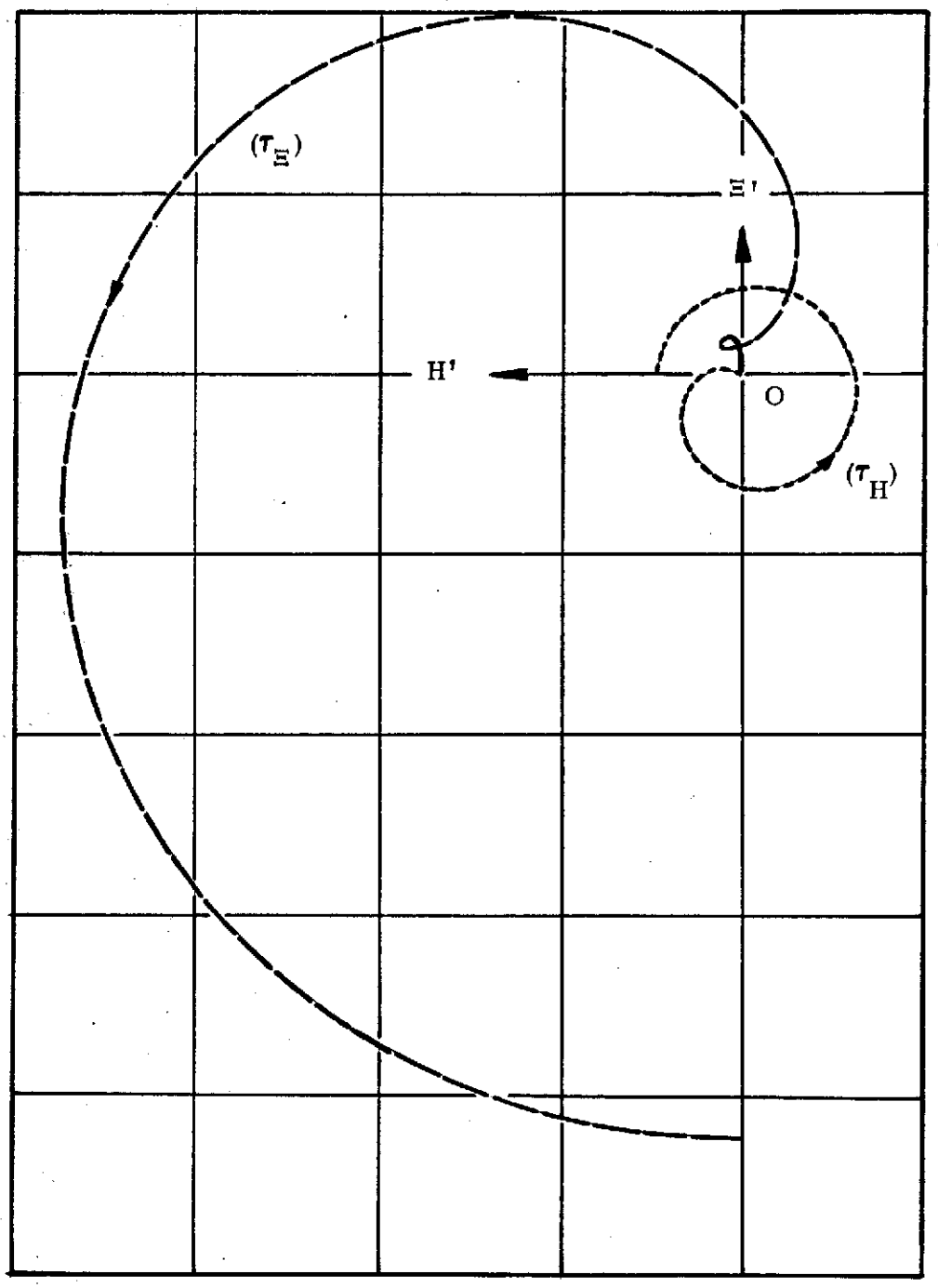


FIG. 21. Typical traces for the hodographs produced by the $\bar{\tau}_I$ components $(\tau_\Xi, \tau_H)$ applied independently. These figures correspond to a one orbit transit of the reference particle.

appropriate columns, in the matrices, could be replaced by zeros. Thus, the characteristic lengths of these geometries are altered (in scale) due to the components of $\bar{\tau}_I$ being removed. Also, there will be alterations in initial loci positioning for the same reasons. A comparing of Figs. 20 and 21 will show what variations have occurred for these implied special cases.

The remaining topic to be discussed, regarding the construction of trace geometries, is that represented by the out-of-plane state variables. The figures which will be formed and described, below, represents that situation; these will be for a particle in motion under the influence of an initial state and/or a specific force system.

## XI. OUT-OF-PLANE TRACE CONSTRUCTIONS

The general construction of trace geometries depicting out-of-plane motions cannot be as simply described as those for the in-plane cases. The primary reason for this is easily recognized when the reader examines the analytical, scalar equations for the appropriate state variables. On studying these expressions one finds that the uncoupling of these motion types leaves the equations expressed in terms of inconsistent parameters. That is, the initial state values, and/or the force components, which appear are not apparent to both of the plane's descriptive equations. Consequently the joining together of the solution equations, as was done for the in-plane traces, cannot be accomplished here. In fact the full range of "state" and/or "forcing" parameters will appear in these equations; this leads to a mathematical inhomogenity which does not accomodate the "building" of vectors for trace loci. Since a somewhat different approach is suggested now, it will be noted (below) that the traces are described in a slightly different manner. There, scalar expression will be presented and these -- rather than their vector counterparts -- will be discussed as the means for representing motion geometries.

It will be evident, also, that the consequence of having acquired a linearized solution is utilized. That is, the initial values problem is (again) considered separate from the "disturbing force" case. In this regard a major simplification is afforded; however, if the "coupled" influence of an initial state and a disturbing force is desired, then this is easily acquired through simple addition of appropriate coordinates for the displacements.

In order to present a complete representation of the out-of-plane displacements, and their corresponding hodographs, it is necessary to describe traces in both the local, rotating frame of reference and the inertial frame. For each set of geometries the several cases to be examined are those for the initial state and the applied, external force systems ($\bar{\tau}$, $\bar{\tau}_I$). The one added constraint, which is introduced here, is that all such motions originate from the origin (i.e., $\bar{\rho}_o$, $\bar{\Omega}_o \equiv 0$). Needless to say this restricts the generality of the initial state,as a disturbance, but does not affect the traces for the applied

forces (recall that these have been examined, throughout, as the "Zero-Initial Values Problem").

For consistency, the Initial Values Problem(s) will be described first; then the two applied force cases will be examined and illustrated.

## XII. DISPLACEMENTS FOR THE INITIAL-VALUES PROBLEM

(a) Local, Rotating Frame of Reference. The solution for this problem situation can be obtained from the general displacement equations:

$$I_2 \bar{\lambda}(\varphi) = \left[I_2 + 3(J_2 - J_1)\right] T_2(\varphi^-)\, A_a + \left[I_2 - \frac{3}{2}\varphi\, B_2 J_1\right] K_o + \Psi_\tau \bar{\tau}\,,$$

and (54)

$$J_3 \bar{\lambda}(\varphi) = J_3 \left\{ \bar{\lambda}_o \cos\varphi + \bar{\lambda}'_o \sin\varphi + \bar{\tau}(1 - \cos\varphi) \right\};$$

subject to the constraints:

$$\bar{\lambda}_o \equiv \bar{0} \quad \text{and} \quad \bar{\tau} \equiv \bar{0}.$$

One consequence of these restrictions is that coefficients (A, K) are reduced to:

$$A_a \equiv A_a(A_1, A_2), \text{ with}; \; A_1 = 2\eta'_o\,, \quad A_2 = \xi'_o\,;$$

and (55)

$$K_o \equiv K_o(K_1, K_2), \text{ wherein}; \; K_1 = 2\eta'_o, \quad K_2 = -2\xi'_o\,.$$

Rather than writing Eqs. (54) separately, return to Eqs. ( .22)* and from there show the matrix expansion as:

$$\begin{bmatrix} \xi(\varphi) \\ \eta(\varphi) \\ \zeta(\varphi) \end{bmatrix} = 2 \left\{ \begin{bmatrix} 0 & 1 & 0 \\ -1 & -\frac{3\varphi}{2} & 0 \\ 0 & 0 & 0 \end{bmatrix} + \begin{bmatrix} \frac{1}{2}\sin\varphi & -\cos\varphi & 0 \\ \cos\varphi & 2\sin\varphi & 0 \\ 0 & 0 & \frac{1}{2}\sin\varphi \end{bmatrix} \right\} \begin{bmatrix} \xi'_o \\ \eta'_o \\ \zeta'_o \end{bmatrix}. \tag{56}$$

The trace described on the $(\xi, \zeta)$-plane is expressed from the analytical, scalar expressions:

$$\xi(\varphi) = 2\eta'_o(1 - \cos\varphi) + \xi'_o \sin\varphi\,,$$

and (57a)

$$\zeta(\varphi) = \zeta'_o \sin\varphi\,.$$

Examining these equations one sees that the trace is composed as an ellipse and a line. These result in the skewed ellipse, given by the quadric:

*This expression appears, as noted, in Reference [2].

$$(\xi - 2\eta'_o)^2 + \zeta^2 = \frac{1}{2}\left\{\left[\xi'^2_o + 4\eta'^2_o + \zeta'^2_o\right] - \left[\xi'^2_o - 4\eta'^2_o + \zeta'^2_o\right]\cos 2\varphi\right\}$$

$$- 2\xi'_o \eta'_o \sin 2\varphi \,. \tag{57b}$$

A sketch of these traces appears below on Fig. 22. There, the reader will find the two component geometries and the full trace (Eq. (57b)).It should be evident that the skewed ellipse is described by the algebraic sum of the two sets of coordinates ($\xi$) (see Eq. (57a)).

The ($\eta$, $\zeta$) trace, from Eq. (56), is developed from:

$$\eta(\varphi) = 4\eta'_o \left(\sin\varphi - \frac{3\varphi}{4}\right) - 2\xi'_o (1 - \cos\varphi)$$

and

$$\zeta(\varphi) = \zeta'_o \sin\varphi \,. \tag{58a}$$

These two equations may be interpreted as: (1), an ellipse (due to $\xi'_o$, $\zeta'_o$); and (2) an s-shaped curve (due to $\eta'_o$, $\zeta'_o$). The full trace, on the ($\eta$, $\zeta$) displacement plane, is represented by the quadratic parametric equation:

$$(\eta + 2\xi'_o + 3\eta'_o\varphi)^2 + \zeta^2 = \frac{1}{2}\left\{\left[(2\xi'_o)^2 + (4\eta'_o)^2 + \zeta'^2_o\right] + \left[(2\xi'_o)^2 - (4\eta'_o)^2\right.\right.$$

$$\left.\left. - (\zeta'_o)^2\right]\cos 2\varphi\right\} + 8\xi'_o \eta'_o \sin 2\varphi \,. \tag{58b}$$

A sketch showing these two basic geometric curves and the full trace is found on Fig. 23 below. It is of some interest to recognize that the ellipse has its geometric center located away from the coordinate origin (at $\eta = -2\xi'_o$, $\zeta = 0$); and, that the s-curve is developed from a slant line coupled with a secular (or rate) component (proportional to $\varphi$).

The sketch, drawn to an arbitrary scaling, depicts a geometry where the "size" of the ellipse and the s-curve are selected to be the same. This selection leads to a displacement trace which closely approximates a cycloid - like geometry --one which would be repeated, sequentially, each orbit.

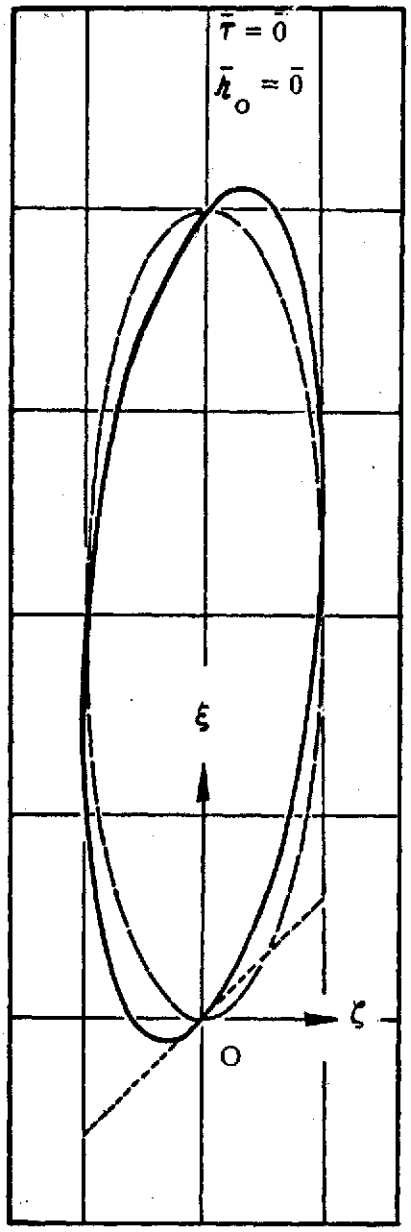


(FIG. 22)

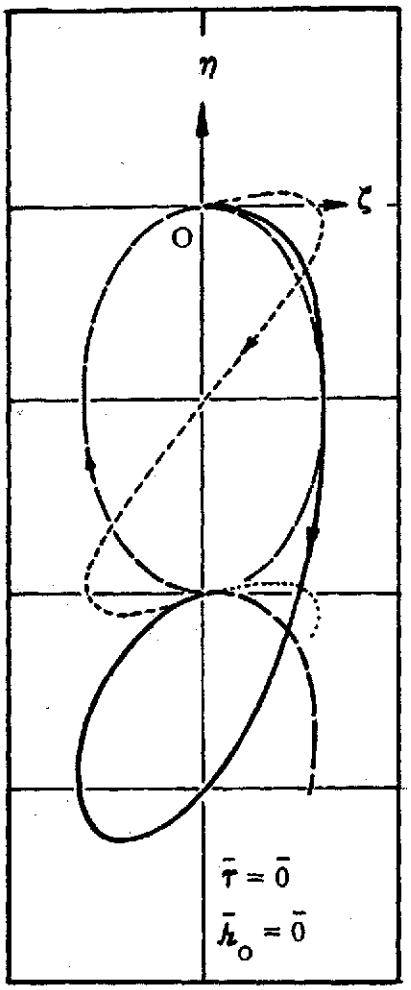


(FIG. 23)

FIG. 22. Sketch showing typical traces, on the $(\xi, \zeta)$-plane, for the Initial Values Problem. Dashed curves are the partial solutions; the skewed ellipse is the composite trace.

FIG. 23. Sketch, on the $(\eta, \zeta)$-plane, describing typical traces for the Initial Values Problem. Ellipse and s-curve are partial descriptions; the full line curve (and dashed extension) represent the composite geometry. (Solid line is for $0 \leq \varphi \leq 2\pi$).

(b) The Inertial Frame of Reference. Here the problem solution is obtained from the general analytical results:

$$I_2\bar{R}(\varphi)=\left[T_2(2\varphi^-)+3(J_2-J_1)\right]A_{a_I}+T_2(\varphi^-)\left\{\left[I_2-\frac{3}{2}\varphi B_2 J_1\right]K_{o_I}+\Psi_\tau\bar{\tau}\right\},$$

and

$$J_3\bar{R}(\varphi)=J_3\left\{\bar{R}_o\cos\varphi+\bar{R}'_o\sin\varphi+\bar{\tau}(1-\cos\varphi)\right\}; \tag{59}$$

subject to the constraints:

$$\bar{R}_o=\bar{0}, \quad \text{and} \quad \bar{\tau}=\bar{0}.$$

In agreement with these restrictions:

$$A_1=H'_o, \quad A_2=\frac{1}{2}\Xi'_o, \quad K_1=2H'_o \quad \text{and} \quad K_2=-2\Xi'_o. \tag{60}$$

Expressed in matrix form the displacements are given by:*

$$\begin{bmatrix}\Xi(\varphi)\\ H(\varphi)\\ Z(\varphi)\end{bmatrix}=2\left\{\begin{bmatrix}\sin\varphi & \cos\varphi+\frac{3\varphi}{2}\sin\varphi & 0\\ -\cos\varphi & \sin\varphi-\frac{3\varphi}{2}\cos\varphi & 0\\ 0 & 0 & 0\end{bmatrix}+\begin{bmatrix}-\frac{\sin 2\varphi}{4} & \frac{1}{2}(-3+\cos 2\varphi) & 0\\ \frac{1}{4}(3+\cos 2\varphi) & \frac{\sin 2\varphi}{2} & 0\\ 0 & 0 & \frac{\sin\varphi}{2}\end{bmatrix}\right\}\begin{bmatrix}\Xi'_o\\ H'_o\\ Z'_o\end{bmatrix}. \tag{61}$$

The traces appearing on both displacement planes are seen to have secular characteristics; and, both have contributing geometries which possess single and double orbit frequency. The rather complicated form of the scalar expressions describing these figures makes it difficult to ascribe names to each. Consequently, the sketch found on Fig. 24 will show contributions due to the individual speed components, and the full trace geometry (a summation of coordinates).

From these sketches, drawn for one orbital passage ($\varphi\cong 2\pi$), it is found that the only closed geometry is that due to $\Xi'_o$; and, on both displacement planes. If one would recall, this corresponds to the condition required to eliminate secular effects; i.e., $H'_o\equiv 0$. This same conditioning is brought out here in these trace component geometries.

*Instead of listing solution types separately, as in Eqs. (59), the operator (Eq. ( .13a), Ref. [2]) was applied to Eq. (56).

Note: Smallest divisions in vicinity of origin, for both scales, define equal coordinate increments.

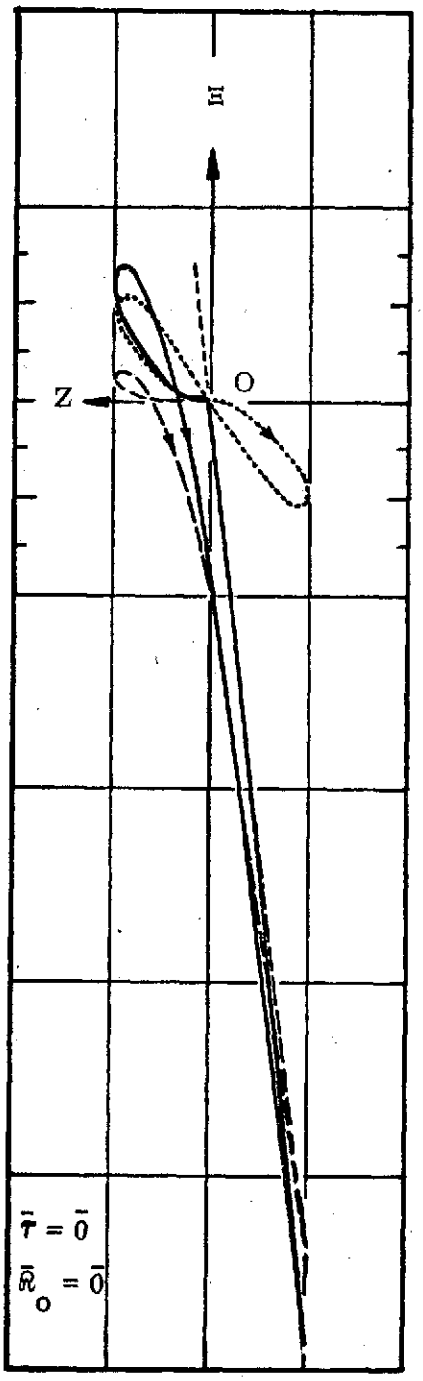


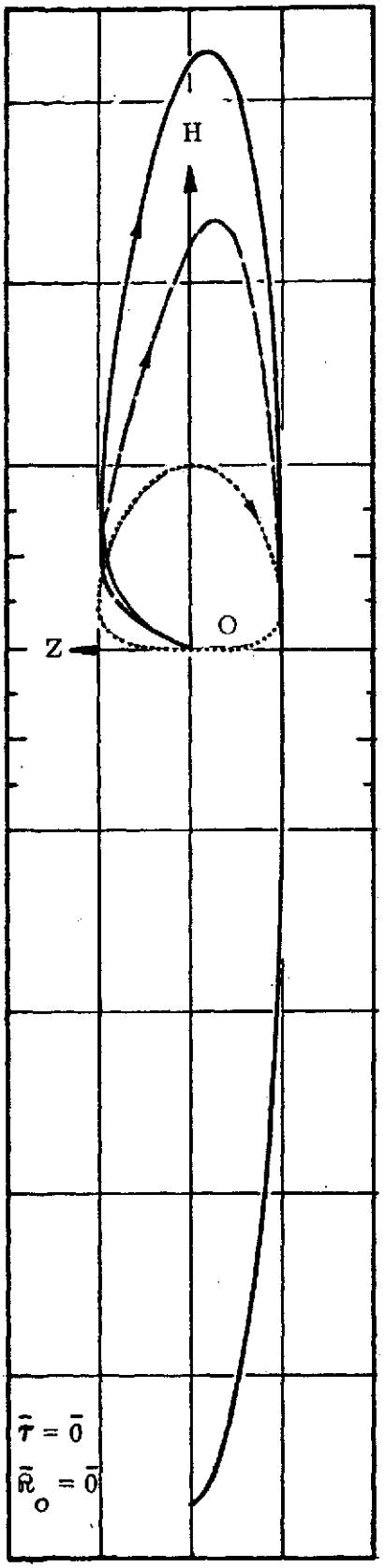


FIG. 24. Sketch of out-of-plane traces developed for the Initial-Values Problem in the inertially aligned frame of reference. Dotted curves are for $Z'_o$ alone; solid arcs are for both speeds.

## XIII. HODOGRAPHS FOR THE INITIAL VALUES PROBLEM

(a) Local, Rotating Frame of Reference. The hodograph equations are acquired from the general expressions:

$$I_2 \bar{h}'(\varphi) = \left[I_2 + 3(J_2 - J_1)\right] B_2 T_2(\varphi^-) A_a - \frac{3}{2}\left[B_2 J_1\right] K_o + \frac{\Psi'}{\tau}\bar{\tau} ,$$

and

$$J_3 \bar{h}'(\varphi) = J_3\left\{\bar{h}'_o \cos\varphi - \bar{h}_o \sin\varphi + \bar{\tau}\sin\varphi\right\} ; \tag{62}$$

wherein the constant coefficients (A, K) are those given in Eqs. (55). The hodograph equations for this problem may be obtained from (say) Eq. (56) as:

$$\begin{bmatrix} \xi'(\varphi) \\ \eta'(\varphi) \\ \zeta'(\varphi) \end{bmatrix} = 2\left\{ \begin{bmatrix} 0 & 0 & 0 \\ 0 & -\frac{3}{2} & 0 \\ 0 & 0 & 0 \end{bmatrix} + \begin{bmatrix} \frac{\cos\varphi}{2} & \sin\varphi & 0 \\ -\sin\varphi & 2\cos\varphi & 0 \\ 0 & 0 & \frac{\cos\varphi}{2} \end{bmatrix} \right\} \begin{bmatrix} \xi'_o \\ \eta'_o \\ \zeta'_o \end{bmatrix} . \tag{63a}$$

The two out-of-plane traces formed by these expressions are found to be skewed ellipses; the quadrics describing them are:

(1) in the $(\xi', \zeta')$-plane:

$$\xi'^2 + \zeta'^2 = \frac{1}{2}\left\{\left[\xi'^2_o + 4\eta'^2_o + \zeta'^2_o\right] + \left[\xi'^2_o - 4\eta'^2_o + \zeta'^2_o\right]\cos 2\varphi\right\} + 2\xi'_o\eta'_o \sin 2\varphi ; \tag{63b}$$

and, (2) in the $(\eta', \zeta')$-plane:

$$(\eta' + 3\eta'_o)^2 + \zeta'^2 = \frac{1}{2}\left\{\left[4\xi'^2_o + 16\eta'^2_o + \zeta'^2_o\right] - \left[4\xi'^2_o - 16\eta'^2_o - \zeta'^2_o\right]\cos 2\varphi\right\} - 8\xi'_o\eta'_o \sin 2\varphi . \tag{63c}$$

Both of these skewed ellipses are noted to be formed from a symmetric ellipse coupled with a slant line.

Because of the geometric similarity which is found here, the two hodographs may be represented by the single sketch found on Fig. 25. There, the directions of traverse, over the trace, will be different (position valued parameters have been assumed). Also, the scale of these two geometries would be different.

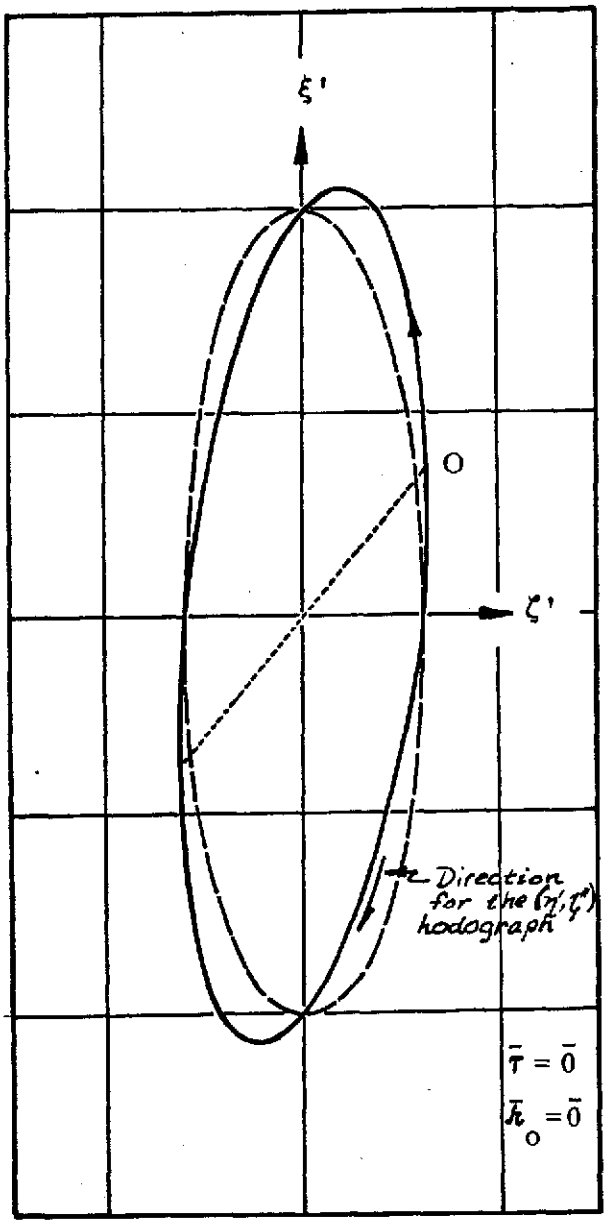


FIG. 25. Typical trace construction on the $(\xi', \zeta')$-plane, for an Initial-Values Problem with $\bar{\tau} = \bar{h}_o = 0$. The broken curves are for partial solutions; the full curve is the composite geometry. Note: A similar geometry is achieved on the $(\eta', \zeta')$-plane, however directions are reversed (as shown) and sizes could be altered.

Here, too, the skewed ellipse is recognized to be developed by summing coordinates used to describe the simple ellipse and the slant line (for both representations).

(b) Hodographs in the Inertial Frame of Reference. The general analytical results for this problem type have been acquired as:

$$I_2\bar{R}'(\varphi) = B_2\left\{\left[2T_2(2\varphi^-)\right]A_{a_I} + T_2(\varphi^-)\left[(I_2 - \frac{3}{2}\varphi B_2 J_1)K_{o_I} + \Psi_\tau\bar{\tau}\right]\right\}$$

$$+ T_2(\varphi^-)\left[\Psi'_\tau\bar{\tau} - \frac{3}{2}B_2 J_1 K_{o_I}\right], \qquad (64)$$

and

$$J_3\bar{R}'_o(\varphi) = J_3\left\{\bar{R}'_o\cos\varphi - \bar{R}_o\sin\varphi + \bar{\tau}\sin\varphi\right\}.$$

The constants which apply for the present case are those given by Eqs. (60). For reference purposes, the scalar expressions for these out-of-plane hodographs are obtained as:

$$\begin{bmatrix} \Xi'(\varphi) \\ H'(\varphi) \\ Z'(\varphi) \end{bmatrix} = 2\left\{\begin{bmatrix} \cos\varphi & \frac{1}{2}(\sin\varphi + 3\varphi\cos\varphi) & 0 \\ \sin\varphi & \frac{1}{2}(-\cos\varphi + 3\varphi\sin\varphi) & 0 \\ 0 & 0 & 0 \end{bmatrix}\right.$$

$$\left. + \begin{bmatrix} -\frac{\cos 2\varphi}{2} & -\sin 2\varphi & 0 \\ -\frac{\sin 2\varphi}{2} & \cos 2\varphi & 0 \\ 0 & 0 & \frac{\cos\varphi}{2} \end{bmatrix}\right\}\begin{bmatrix} \Xi'_o \\ H'_o \\ Z'_o \end{bmatrix}. \qquad (65)^*$$

These equations imply a general divergence for planar traces. This is noted (again) to be associated with the input parameter $H'_o$, and, as seen on the figure below, the geometry contributed by $\Xi'_o$ is a "closed" one (see Fig. 26). Unfortunately these traces are rather complicated and do not lend themselves to simple name descriptions. (Note that each figure shows the component traces and the final hodograph geometry).

*This equation is also obtained by differentiating Eq. (61).

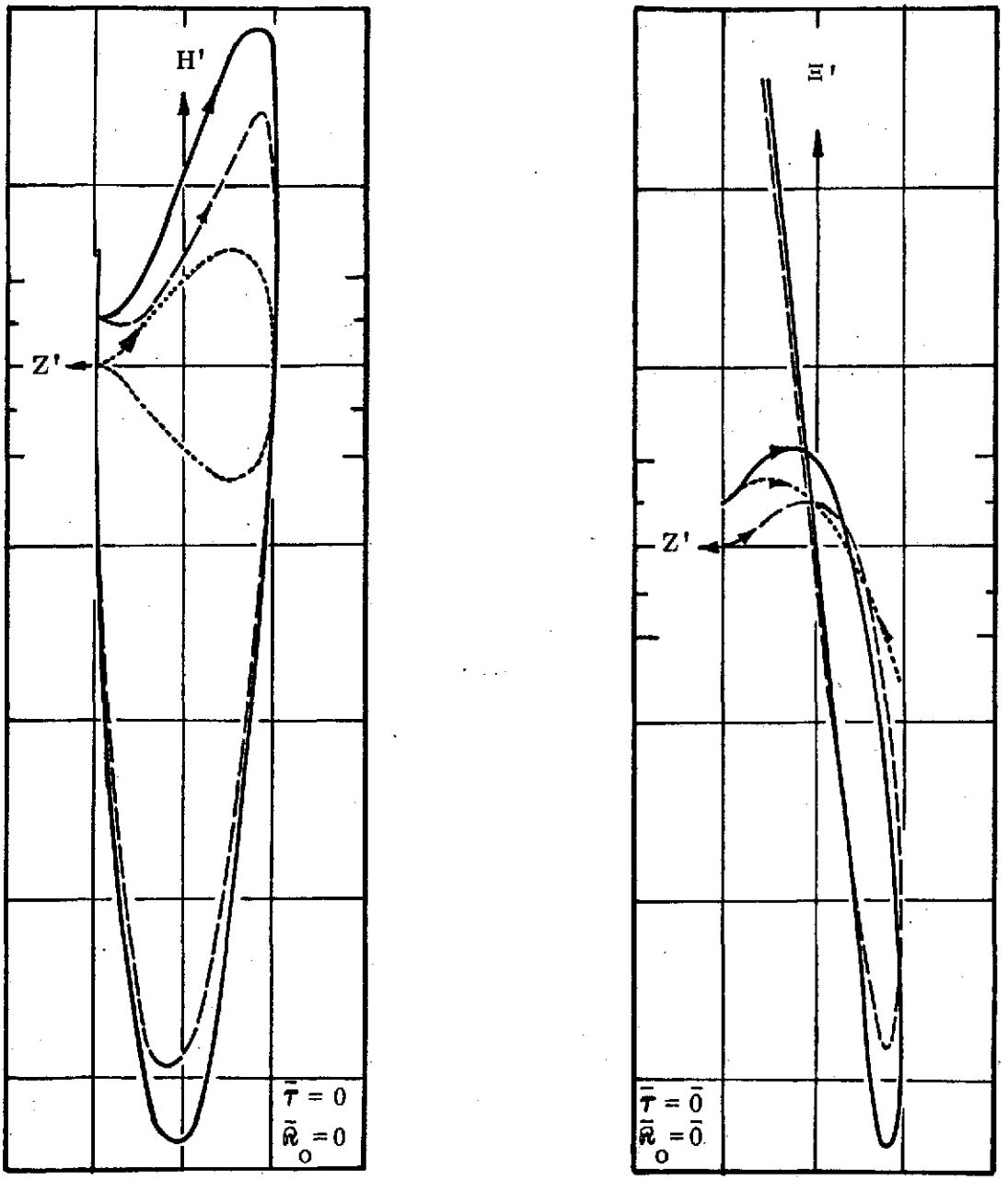


FIG. 26. Typical trace sketches, referred to the inertially aligned frame, for the Initial-Values Problem, with $\bar{\tau} = \bar{\mathcal{R}}_o = 0$. Dotted curves are figures for $\Xi'_o$ alone; dash arcs are for $H'_o$ alone; solid curves are composite hodograph traces.

Note: Smallest scale divisions in vicinity of origin are for equal coordinate increments.

In the following sections the zero-initial-value problems will be discussed. There, cases for the two disturbances ($\bar{\tau}$ and $\bar{\tau}_I$) will be developed separately; and, the displacement and hodograph geometries will be described in the two frames of reference.

## XIV. ZERO INITIAL VALUE PROBLEMS

(a) Local, Rotating Frame of Reference. The solution type to be described here is contained in the general equations denoted as Eqs. (54). The difference between this case and that described in Section XII is that now the disturbance is $\bar{\tau} \equiv \bar{\tau}(\tau_\xi, \tau_\eta, \tau_\zeta)$, rather than the Initial State. However, a direct development for the displacement matrix equation is obtained from Eq. ( .22a), Reference [2], as:

$$\begin{bmatrix} \xi(\varphi) \\ \eta(\varphi) \\ \zeta(\varphi) \end{bmatrix} = 2\left\{ \begin{bmatrix} \frac{1}{2} & 0 & 0 \\ 0 & 2 & 0 \\ 0 & 0 & \frac{1}{2} \end{bmatrix} + \varphi \begin{bmatrix} 0 & 1 & 0 \\ -1 & -\frac{3\varphi}{4} & 0 \\ 0 & 0 & 0 \end{bmatrix} - \begin{bmatrix} \frac{\cos\varphi}{2} & \sin\varphi & 0 \\ -\sin\varphi & 2\cos\varphi & 0 \\ 0 & 0 & \frac{\cos\varphi}{2} \end{bmatrix} \right\} \begin{bmatrix} \tau_\xi \\ \tau_\eta \\ \tau_\zeta \end{bmatrix} . \tag{66a}$$

Now, the trace geometry found on the $(\xi, \zeta)$-plane is obtained as the combination of a cycloid (due to $\tau_\eta$) plus a slant line (from $\tau_\xi$). Choosing these $\tau_i$-components to be positive valued the two contributing geometries, and the acquired total trace, could appear as shown by the sketches found on Fig. 27. Incidentally a quadratic form of the descriptive parametric equation for the full trace is found to be:

$$\left[\xi - (\tau_\xi + 2\tau_\eta\varphi)\right]^2 + \left[\zeta - \tau_\zeta\right]^2 = \frac{1}{2}\left\{\left[\tau_\xi^2 + 4\tau_\eta^2 + \tau_\zeta^2\right] + \left[\tau_\xi^2 - 4\tau_\eta^2 + \tau_\zeta^2\right]\cos 2\varphi\right\}$$
$$+ 2\tau_\xi\tau_\eta \sin 2\varphi . \tag{66b}$$

Looking at the full trace it seems reasonable to refer to it as a skewed cycloid.

In an analogous manner the trace appearing on the $(\eta, \zeta)$-plane could be described as an accelerating s-shaped curve. It is developed from a cycloid (provided by $\tau_\xi$) and a modified form of the s-curve (due to $\tau_\eta$). These component traces* are found on Fig. 28, along with the combination geometry shown there. Incidentally, the quadric expression for this full trace can be written as:

*The traces found on this figure are drawn for positive valued $\tau_i$ components. The reader can easily ascertain the consequence of changing the sign for the $\tau_i$ components. A change in magnitude is not as readily visualized.

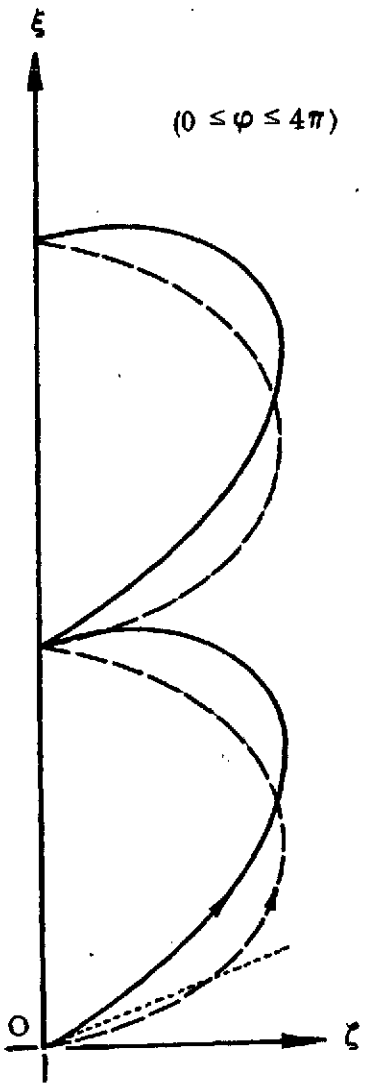


FIG. 27

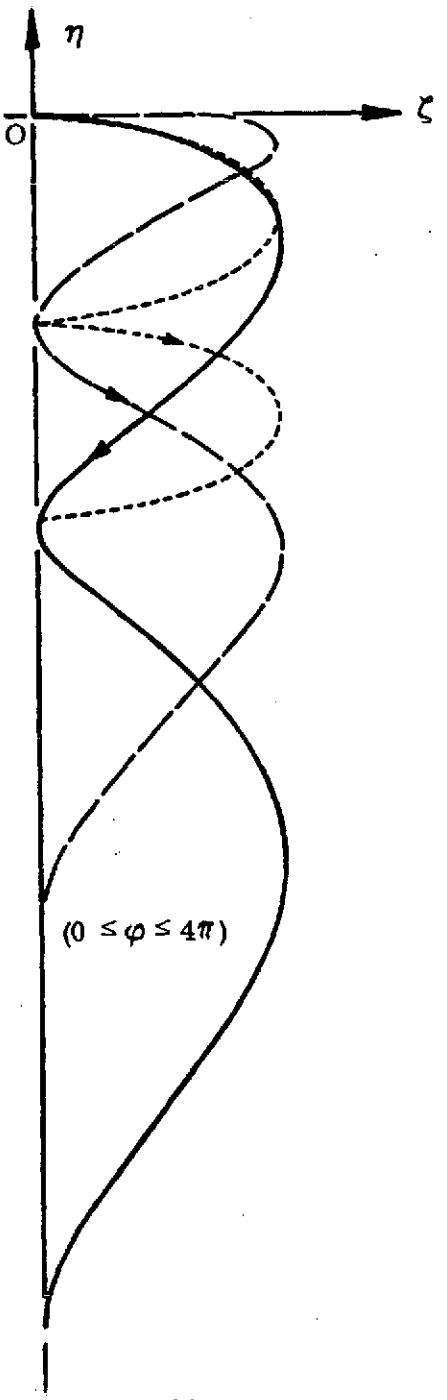


FIG. 28

FIG. 27, 28. Typical trace geometries developed for a Zero Initial-Values Problem ($\bar{h}_o = \bar{h}'_o = 0$). Disturbance provided by specific force components of $\bar{\tau}$. Solid curves are composite traces; broken arcs are for partial solutions.

$$\left[\eta - 4\tau_\eta\left(1 - \frac{3\varphi^2}{8}\right) + 2\tau_\xi\varphi\right]^2 + \left[\zeta - \tau_\zeta\right]^2 = \frac{1}{2}\left\{\left[4\tau_\xi + 16\tau_\eta^2 + \tau_\zeta^2\right]\right.$$

$$\left. - \left[4\tau_\xi^2 - 16\tau_\eta^2 - \tau_\zeta^2\right]\cos 2\varphi\right\} - 8\tau_\xi\tau_\eta \sin 2\varphi \,. \qquad (66c)$$

Again, it should be evident that the total displacement trace is composed as a summation of the component geometry coordinates. The transfer of this geometry to the inertial frame is discussed in the next sub-section.

(b) The Inertial Frame of Reference. A mathematical description of these out-of-plane traces was noted as Eqs. (59). However, for the specialization implied here the only coefficients of consequence are those proportional to the specific force $\bar{\tau}(\tau_\xi, \tau_\eta, \tau_\zeta)$.

As a matter of record the scalar expressions which evolve for this case study are:

$$\Xi(\varphi) + \frac{3}{2}\tau_\xi = \tau_\xi\left(\frac{1}{2}\cos 2\varphi + \cos\varphi + 2\varphi\sin\varphi\right) + \tau_\eta\left(\sin 2\varphi + 2\varphi\cos\varphi - 4\sin\varphi + \frac{3\varphi^2}{2}\sin\varphi\right),$$

$$H(\varphi) + 3\tau_\eta = \tau_\xi\left(\frac{1}{2}\sin 2\varphi + \sin\varphi - 2\varphi\cos\varphi\right) + \tau_\eta\left(-\cos 2\varphi + 2\varphi\sin\varphi + 4\cos\varphi - \frac{3\varphi^2}{2}\cos\varphi\right),$$

and

$$Z(\varphi) = \tau_\zeta(1 - \cos\varphi). \qquad (67)$$

Forming graphs from these expressions, a set of representative traces are found on Figs. (29, 30)*. There the two component geometries, and the full combination figure, are the results for positive values of the $\tau_i$. It should be evident that all component sketches suggest a divergence; the ($\Xi$, Z)-plane curves appear to close, however this is a consequence of the mathematical solution form only.

Once again the mathematical complexity of these expressions negates the possibility of affixing simple names to the corresponding geometric figures. For this reason only typical traces are displayed; no attempt has been made to separate the full analytical expressions into simpler component forms for graphic description.

*The traces, as shown, are for only one orbit of motion; i.e., $\Delta\varphi \cong 2\pi$.

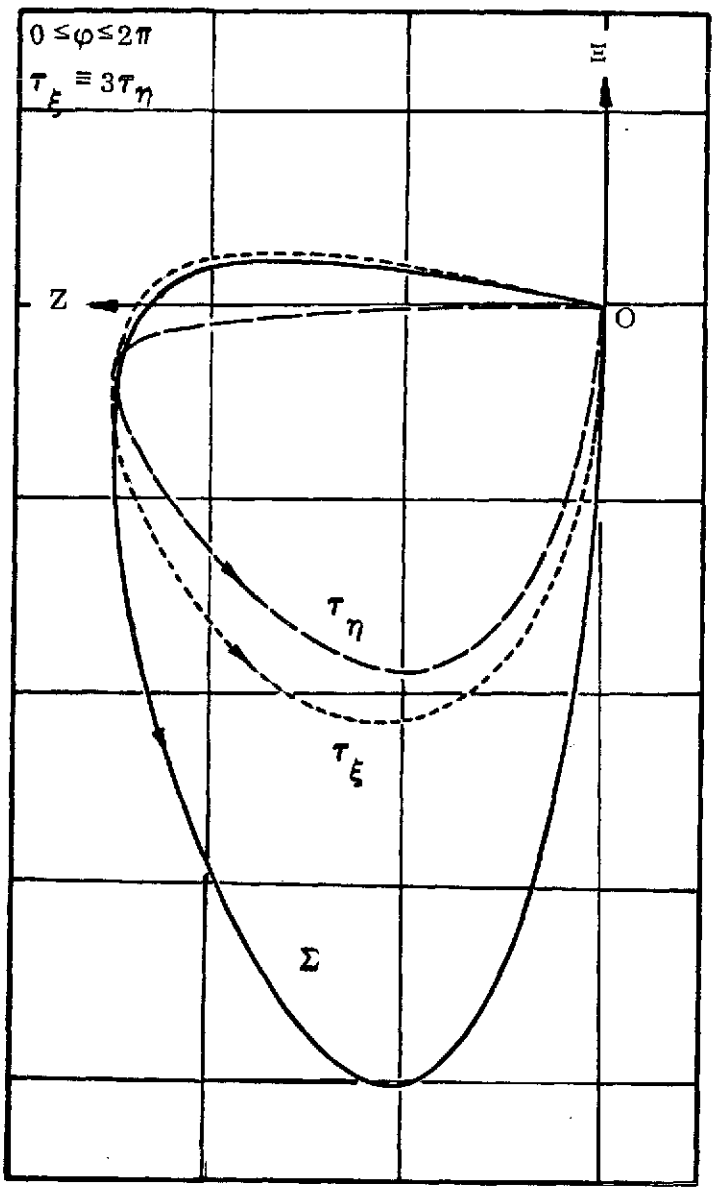


FIG. 29. Typical out-of-plane trace geometries developed for a Zero Initial-Values Problem. Note that individual ($\tau_i$, $\tau_\zeta$) influences are shown as well as the composite figure ($\Sigma$).

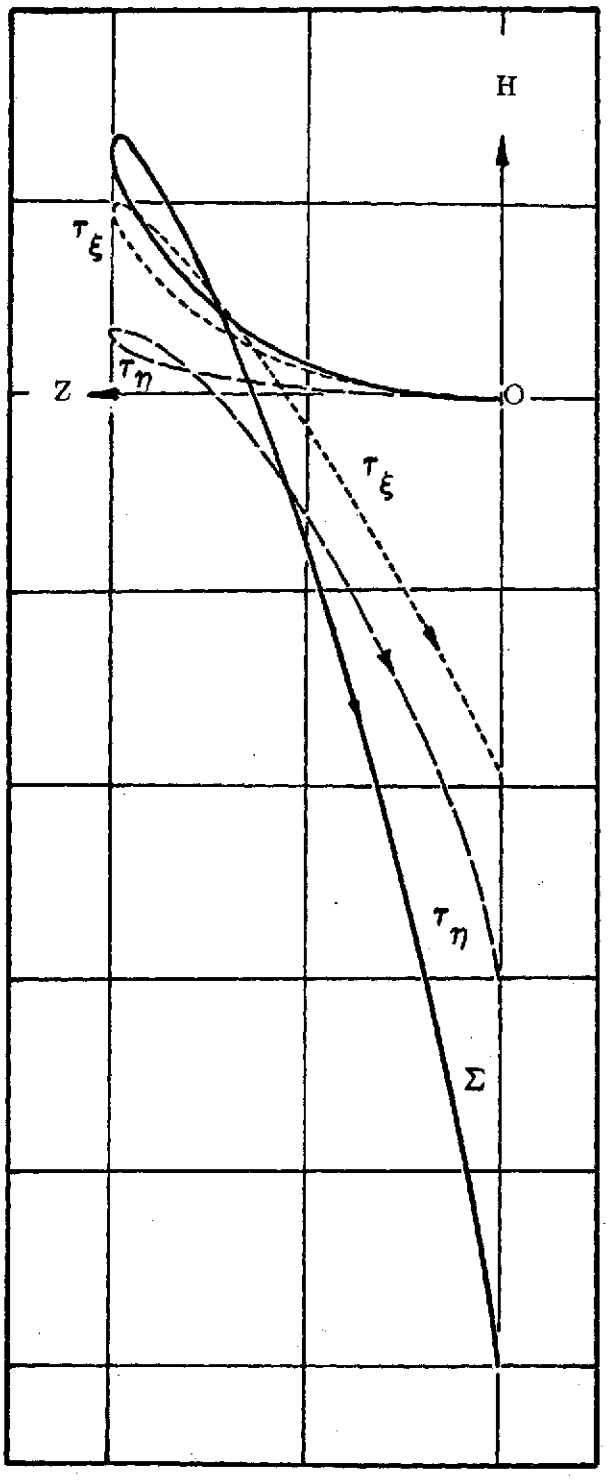


FIG. 30. Typical out-of-plane trace geometries developed by a Zero Initial-Values Problem. Note that individual ($\tau_i$, $\tau_\zeta$) traces are shown as well as the composite figure ($\Sigma$).

## XV. HODOGRAPHS FOR THE ZERO-INITIAL VALUES PROBLEM

(a) Local, Rotating Frame of Reference. The general hodograph equations for this case are expressed in Eqs. (62); however, these specific expressions require that all input parameters except the $\tau_i$ be removed. The scalar expression which result are:

$$\xi'(\varphi) = \tau_\xi \sin\varphi + 2\tau_\eta(1-\cos\varphi),$$

$$\eta'(\varphi) = 4\tau_\eta\left(\sin\varphi - \frac{3\varphi}{4}\right) - 2\tau_\xi(1-\cos\varphi),$$

and

$$\zeta'(\varphi) = \tau_\zeta \sin\varphi . \tag{68}$$

After examining these equations it is found that the geometries which would evolve here are identical in form to those found on Figs. (22) and (23). That is, Fig. 22 is typical of the $(\xi', \zeta')$ trace when the $\tau_i$ constant replace the initial values $(\xi_o', \eta_o')$*. Also, Fig. 23 has the same graphical form as would the trace on the $(\eta', \zeta')$-plane here. (Note that Eqs. (63a) are identical to those above when the $\tau_i$ replace corresponding initial values).

Due to this similarity in the sketches, those which would normally appear here will be deleted. The comparing of equation forms leads to an immediate recognition of the analogous component geometries, etc.

(b) Hodographs in the Inertial Frame of Reference. Returning to Eqs. (64) and recasting them in terms of the $\tau_i$ scalars, it is easy to show that the expressions for this situation are:

$$\Xi'(\varphi) = \tau_\xi\left[\sin\varphi + 2\varphi\cos\varphi - \sin 2\varphi\right] + \tau_\eta\left[\left(\frac{3\varphi^2}{2} - 2\right)\cos\varphi + \varphi\sin\varphi + 2\cos 2\varphi\right],$$

$$H'(\varphi) = \tau_\xi\left[-\cos\varphi + 2\varphi\sin\varphi + \cos 2\varphi\right] + \tau_\eta\left[\left(\frac{3\varphi^2}{2} - 2\right)\sin\varphi - \varphi\cos\varphi + 2\sin 2\varphi\right],$$

and

$$Z'(\varphi) = \tau_\zeta \sin\varphi . \tag{69}$$

*This argument supposes the $\tau_i$ are positive valued like the $(\xi_o', \eta_o', \zeta_o')$.

Typical graphs, constructed on the ($\Xi'$, Z') and (H', Z')-planes, are presented below as Figs. (31) and (32), respectively. From the sketch, and from Eqs. (69) it is readily seen that divergence is present and can only be removed when the in-plane force is removed (a trivial case). Shown on both figures are component traces, for each $\tau_i$-component, separately considered; and, the combined trace which is indicative of the hodograph for a general $\bar{\tau}$ application*. (These plots represent the hodograph for <u>one</u> orbital excursion. It is known that the linearized solution results are subject to deterioration even for this restricted range of the independent variable. However, the trends which are exhibited here do bear good resemblance to the more accurately acquired numerical results). One caution: the appearance of trace closure on the (H', Z') hodograph is (again) a consequence of the mathematics, not a consequence of the system's dynamic response.

In the next section out-of-plane traces are developed for the application of a specific disturbance force ($\bar{\tau}_I$), acting in directions parallel to the inertial frame of reference. These graphs will be found to be analogous to those above; hence, their complexity also reduces the discussions to generalities.

*These traces were constructed for the $\tau_i > 0$. When either or both components would have a sign change, the reversal in geometry is obvious. Changes in magnitude would simply magnify the coordinate displacements.

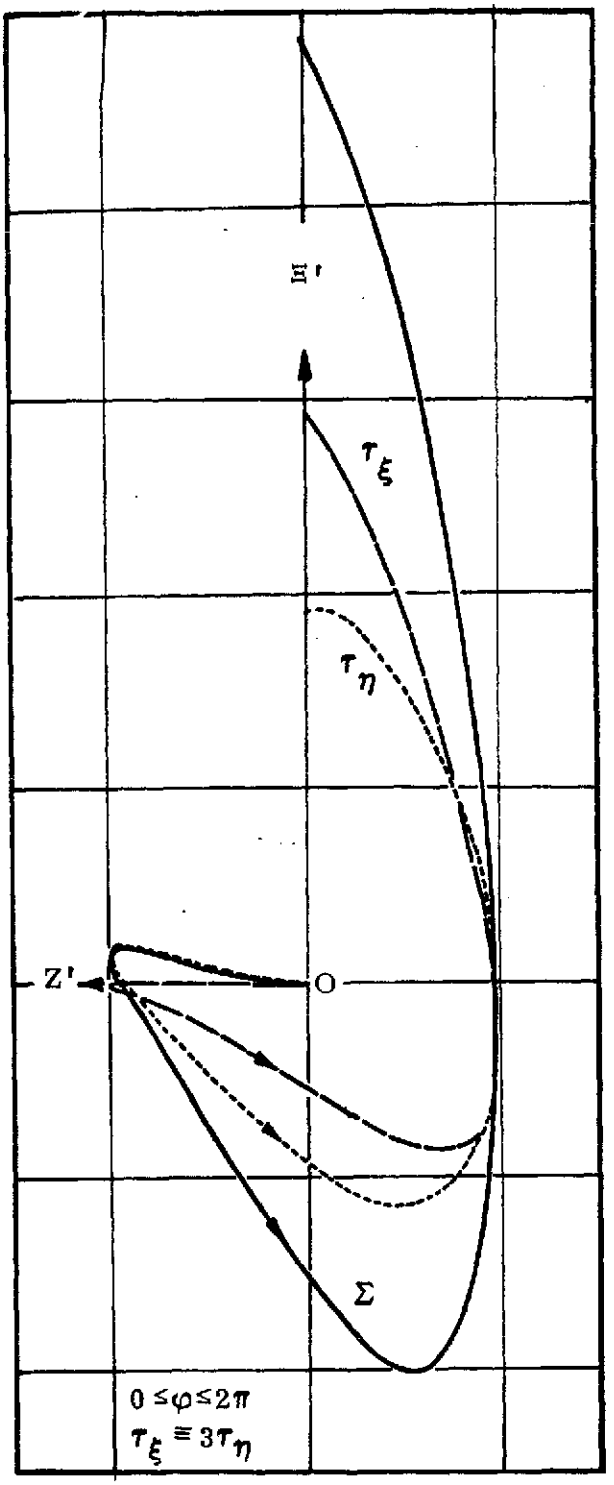


FIG. 31. Sketch showing out-of-plane hodograph traces due to $\tau_i$ components with $\bar{R}_0 = \bar{R}'_0 = \bar{0}$. Note that individual ($\tau_i$, $\tau_\xi$) traces are shown with the composite trace ($\Sigma$).

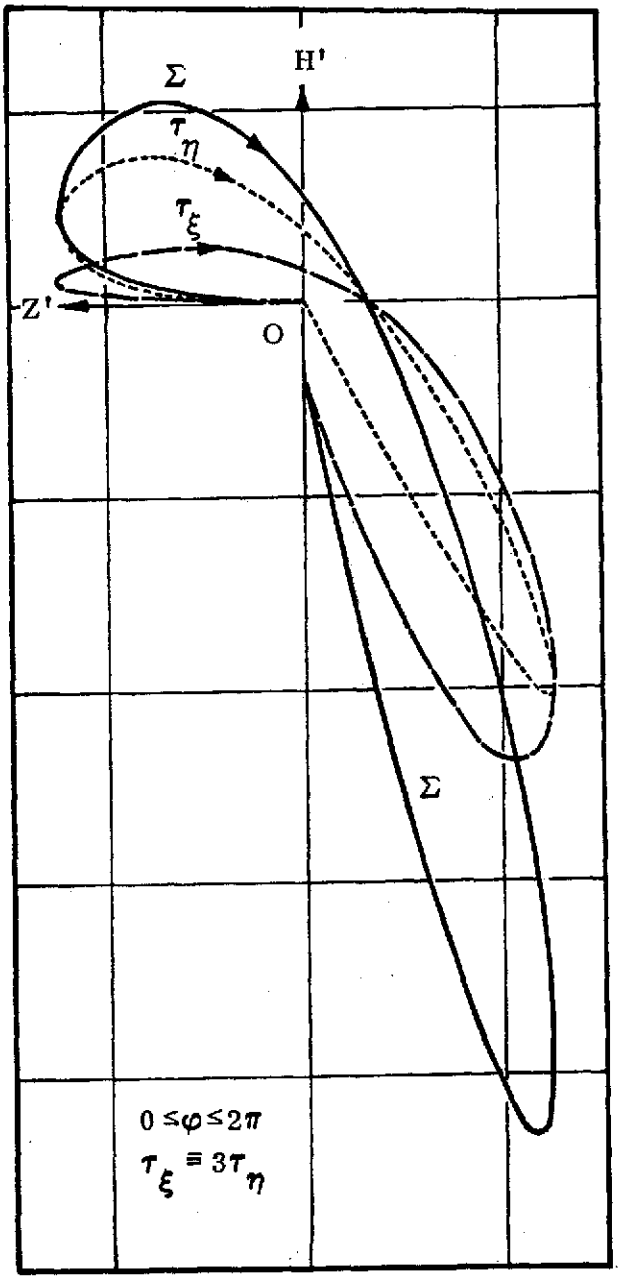


FIG. 32. Sketch for out-of-plane hodograph traces due to application of $\bar{\tau}$ components, with ($\bar{R}_o = \bar{R}'_o = 0$). Note that individual ($\tau_i$, $\tau_\zeta$) traces are shown in addition to the composite figure ($\Sigma$).

## XVI. OUT-OF-PLANE DISPLACEMENTS, DUE TO $\bar{\tau}_I$--

(a) Local, Rotating Frame of Reference. The analytical solution for displacements arising as a consequence of an applied force ($\bar{\tau}_I$) -- one aligned so that there are fixed components parallel to the inertial frame of reference -- provides only limited new information. This information arises solely in terms of $\bar{\tau}_I$ since coupling between it and other input disturbances is not apparent. As a consequence only incremental displacements will be described below; and, of course, the same arguments will hold for other descriptions (displacements and hodographs alike).

The general analytical solution for displacements referred to the local, rotating frame of reference, arising as a result of initial values and $\bar{\tau}_I (\equiv \bar{\tau}_I (\tau_\Xi, \tau_H, \tau_Z))$ has been expressed by:

$$\bar{\lambda}(\varphi) = \left[I_2 + 3(J_2 - J_1)\right] T_2(\varphi^-) \left[A_a\right]_{i.v.} + \left[I_2 - \frac{3}{2}\varphi B_2 J_1\right] K_o + \Phi_\tau \bar{\tau}_I$$
$$+ J_3 \left[\bar{\lambda}_o \cos\varphi + \bar{\lambda}'_o \sin\varphi + \bar{\tau}_I (1 - \cos\varphi)\right]. \tag{70}$$

Only the $\bar{\tau}_I$ parts of this result are of interest here; hence, only these partial solutions will be discussed below. Consequencly these partial displacements are noted by:

$$\Delta(I_2 \bar{\lambda}(\varphi)) \equiv \Phi_\tau \bar{\tau}_I = \left\{\left[2J_1 + 5J_2\right]\left[T_2(\varphi^+) - I_2\right] + \frac{3\varphi}{2}\left[J_1 + 2J_2\right]\left[J_2 B_2 + B_2 T_2(\varphi^+)\right]\right.$$
$$\left. + \frac{1}{4}\left[J_1 - 2J_2\right]\left[T_2(\varphi^-) - T_2(\varphi^+)\right]\right\} \bar{\tau}_I ;$$

and

$$\Delta(J_3 \bar{\lambda}(\varphi)) = J_3 \left\{\bar{\tau}_I (1 - \cos\varphi)\right\}. \tag{71}$$

For the construction of representative traces in this case, the format of the equations is such that simple curve forms are not easy to identify, throughout. Therefore, only the $\tau_i$ (component) traces are presented on the figures; yet,the reader can ascertain quickly the influence each component plays, the

effect of change in sign, and the approximate overall geometry produced by this disturbance force.

As an aid to visualizing these traces the scalar expressions from which they are developed are:

$$\xi(\varphi) = 2\tau_{\Xi}\left[\frac{3\varphi}{4}\sin\varphi - (1-\cos\varphi)\right] + \frac{3}{2}\,\tau_{H}\left[\sin\varphi - \varphi\cos\varphi\right],$$

$$\eta(\varphi) = 3\tau_{\Xi}\left[\varphi(1+\cos\varphi) - 2\sin\varphi\right] - 5\tau_{H}\left[(1-\cos\varphi) - \frac{3\varphi}{5}\sin\varphi\right],$$

and

$$\zeta(\varphi) = \tau_{Z}(1-\cos\varphi). \tag{72}$$

Fig. 33 (below) shows sketches of typical traces, due to $\tau_{\Xi}$ and $\tau_{H}$, on the $(\xi, \zeta)$-plane*. Though it may not be immediately evident, both traces are secular in both $\tau_i$ components. These sketches have been constructed for only one orbit of motion, hence they do not predict the trends for $\varphi > 2\pi$.

Fig. 34 has been constructed to illustrate the influence of $\tau_i$ on the geometric descriptions found for the $(\eta, \zeta)$-plane. Here, too, both trace geometries have a divergent characteristic arising from the force components $(\tau_{\Xi}, \tau_{H})$*. These geometries are drawn for only one orbital passage also $(\varphi \cong 2\pi)$.

As before all of these figures are constructed under the supposition that the $\tau_i$ components are positive constants. The reader can easily visualize the consequences of a sign change in either or both components. Also, it is not difficult to acquire some feeling for the shape of that trace which would result from an application of all $\tau_i$ components, simultaneously.

(b) Displacements in the Inertial Frame of Reference. With attention focused on the added displacements, brought about by the application of $\bar{\tau}_I$, it is found that (symbolically) these may be written as:

$$\Delta(I_2\bar{R}(\varphi)) \equiv T_2(\varphi^-)\,\Phi_{\tau}\,\bar{\tau}_I, \tag{73a}$$

*The $\bar{\tau}_I$ components are employed in pairs; i.e., both $\tau_{\Xi}$ and $\tau_H$ are applied separately, but each in conjunction with $\tau_Z$.

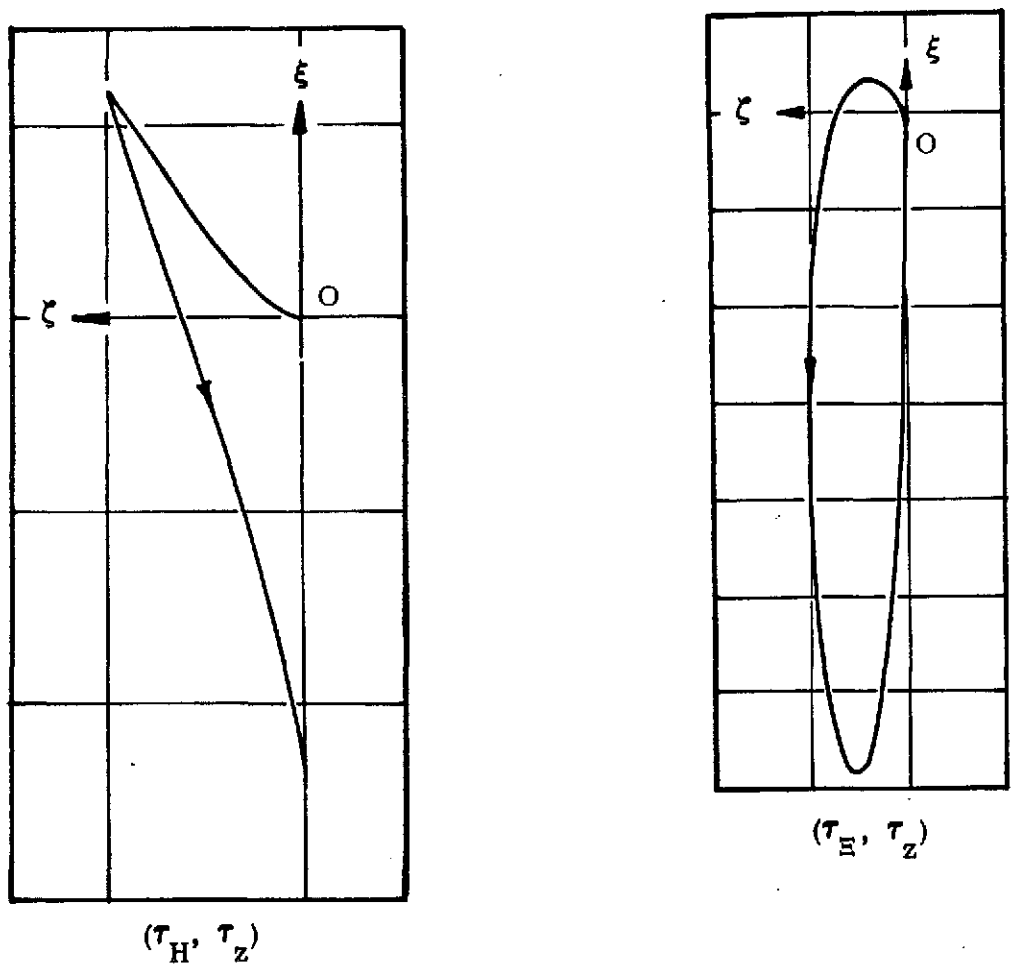


FIG. 33. Sketch for typical ($\xi$, $\zeta$) trace geometries due to $\bar{\tau}_I$ components. Each curve above is for paired components of the specific force. A composite figure is composed by summing coordinates.

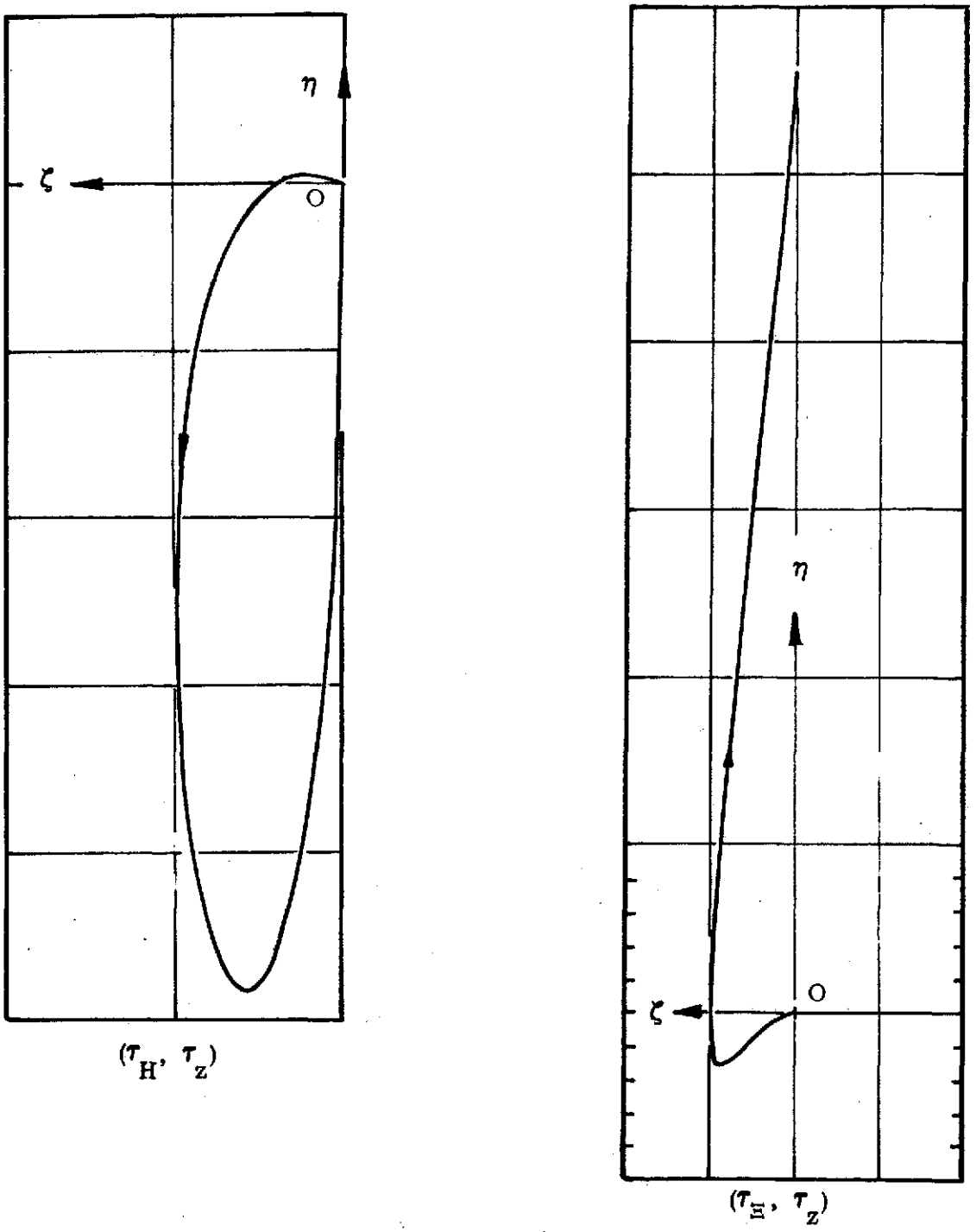


FIG. 34. This is the set of companion trace geometries for those shown on FIG. 33. Note: Each sketch is for the indicated pair of $\bar{\tau}_I$ components. Smallest scale divisions in vicinity of origin describe equal scale increments.

(see also Eqs. (72)); then the scalar expressions to be utilized are:

$$\Xi(\varphi) = 2\tau_{\Xi}\left[(1-\cos\varphi)+(1-\cos 2\varphi)-\frac{3\varphi}{2}\left(\sin\varphi+\frac{1}{4}\sin 2\varphi\right)\right]+\tau_{H}\left[-5\left(\varphi-\sin\varphi\right)\right.$$

$$\left.+\frac{7}{4}\left(\varphi-\sin 2\varphi\right)+\varphi\left(1+\frac{3}{4}\cos 2\varphi\right)\right],$$

$$H(\varphi) = -2\tau_{\Xi}\left[(\sin\varphi+\sin 2\varphi)-\frac{3\varphi}{8}\left(3+4\cos\varphi+\cos 2\varphi\right)\right]+\tau_{H}\left[5(1-\cos\varphi)-\frac{7}{4}(1-\cos 2\varphi)\right.$$

$$\left.+\frac{3\varphi}{4}\sin 2\varphi\right],$$

and

$$Z(\varphi) = \tau_{Z}(1-\cos\varphi). \tag{73b}$$

Out-of-plane displacements from these expressions, treating each of the $\tau_i$ as separate actions, have been determined*. These appear on Fig. (35) and (36) for the ($\Xi$, Z)- and (H, Z)-planes, respectively. For the description of a full trace (one produced by $\bar{\tau}_I(\tau_{\Xi}, \tau_H, \tau_Z)$), it is only necessary to sum coordinates from the two representations shown below (for example).

Once again it should be recognized that these traces have divergent geometric characteristics arising from both $\tau_{\Xi}$ and $\tau_H$. Hence it is not possible to acquire a closed relative motion figure for these disturbances. Also, the complicated form of these displacement expressions does not lend to describing these component curves by simple and familiar names.

*The $\tau_i$ have been arbitrarily chosen as positive constants here. The consequence of sign change and magnification follows easily, by inspection.

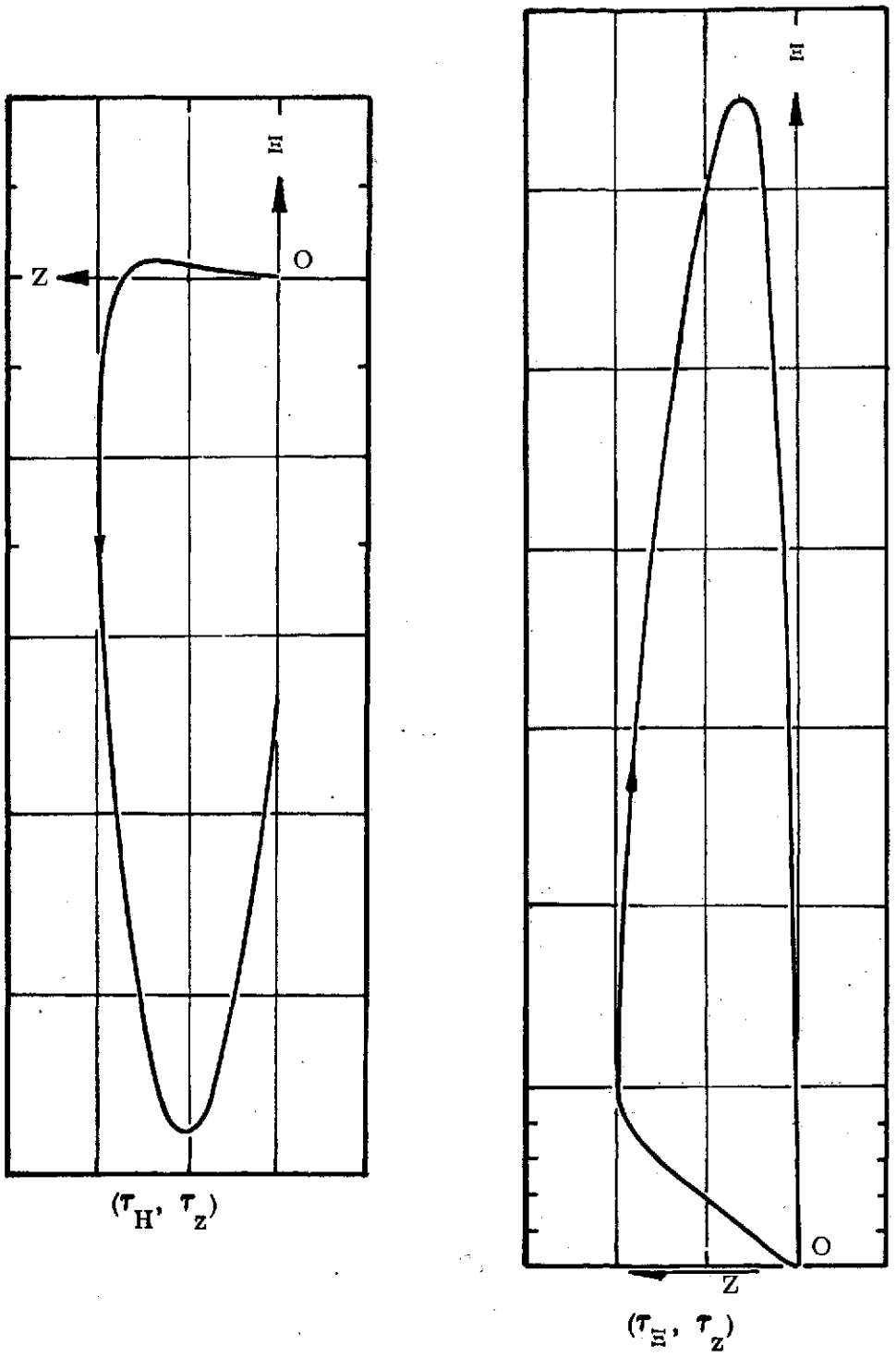


FIG. 35. Sketch of out-of-plane geometries described for typical paired values of $\bar{\tau}_I$. The composite figure would be acquired by adding ordinates. Smallest scale divisions in vicinity of origin define equal scale increments.

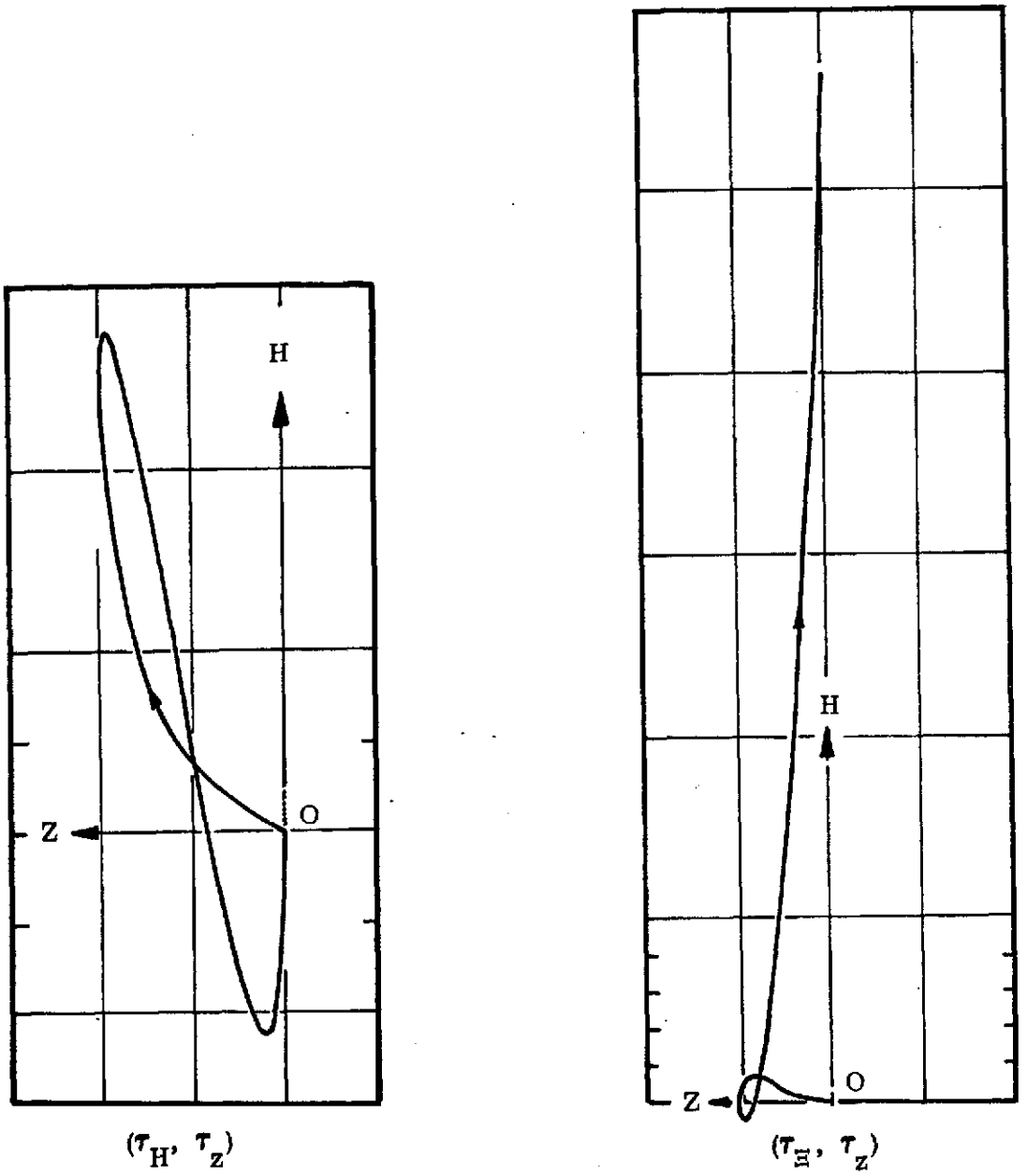


FIG. 36. Typical out-of-plane geometries described by application of $\bar{\tau}_I$ components alone. Note each graph is for a paired set of specific force components. The full trace, for $\bar{\tau}_I$, is obtained by adding ordinates. Also, smallest scale divisions in vicinity of origin describe equal coordinate increments.

## XVII. OUT-OF-PLANE HODOGRAPHS, DUE TO $\bar{\tau}_I$

(a) Local, Rotating Frame of Reference. Hodographs for this situation may be acquired by (say) differentiating the expressions in Eqs. (71). When this is done one finds, as a result:

$$\Delta(I_2\bar{\lambda}'(\varphi)) \equiv \Phi'_{\tau}\bar{\tau}_I = \left\{-\left[2J_1+5J_2\right]B_2T_2(\varphi^+)+\frac{3}{2}\left[J_1+2J_2\right]\left[J_2B_2+(I_2-B_2\varphi)B_2T_2(\varphi^+)\right]\right.$$
$$\left.+\frac{1}{4}\left[J_1-2J_2\right]\left[B_2T_2(\varphi^-)+B_2T_2(\varphi^+)\right]\right\}\bar{\tau}_I ,$$

and

$$J_3\bar{\lambda}'(\varphi) \equiv J_3\bar{\tau}_I\sin\varphi . \tag{74a}$$

These expressions lead directly to hodographs which are produced by the external force system $\bar{\tau}_I$, and for which the examples shown on Figs. (37) and (38) are plotted. There, as before, the $\tau_i$ components are assumed to be positive constants; hence the sketches reflect this constraint*. For convenience, the scalar format of the expressions above may be shown to be:

$$\xi'(\varphi)=\frac{1}{2}\tau_{\Xi}\left[-\sin\varphi+3\varphi\cos\varphi\right]+\frac{3\tau_H}{2}\left[\varphi\sin\varphi\right],$$

$$\eta'(\varphi)=3\tau_{\Xi}\left[(1-\cos\varphi)-\varphi\sin\varphi\right]-2\tau_H\left[\sin\varphi-\frac{3\varphi}{2}\cos\varphi\right],$$

and

$$\zeta'(\varphi)=\tau_z\sin\varphi . \tag{74b}$$

(b) Inertial Frame of Reference. The hodographs to be mentioned here are those analogous to the case above, except that the planes for description are now referred to an inertial triad, as indicated. Taking account of the expressions in Eq. (74) and recalling Eqs. (71), then it follows that:

$$\Delta(I_2\bar{R}'(\varphi)) \equiv T_2(\varphi^-)\left[B_2\Phi_{\tau}+\Phi'_{\tau}\right]\bar{\tau}_I ,$$

and

$$J_3\bar{R}'(\varphi) = J_3\bar{\tau}_I\sin\varphi . \tag{75a}$$

*Sign changes and magnifications can be visualized by an inspection of the graphs and descriptive equations.

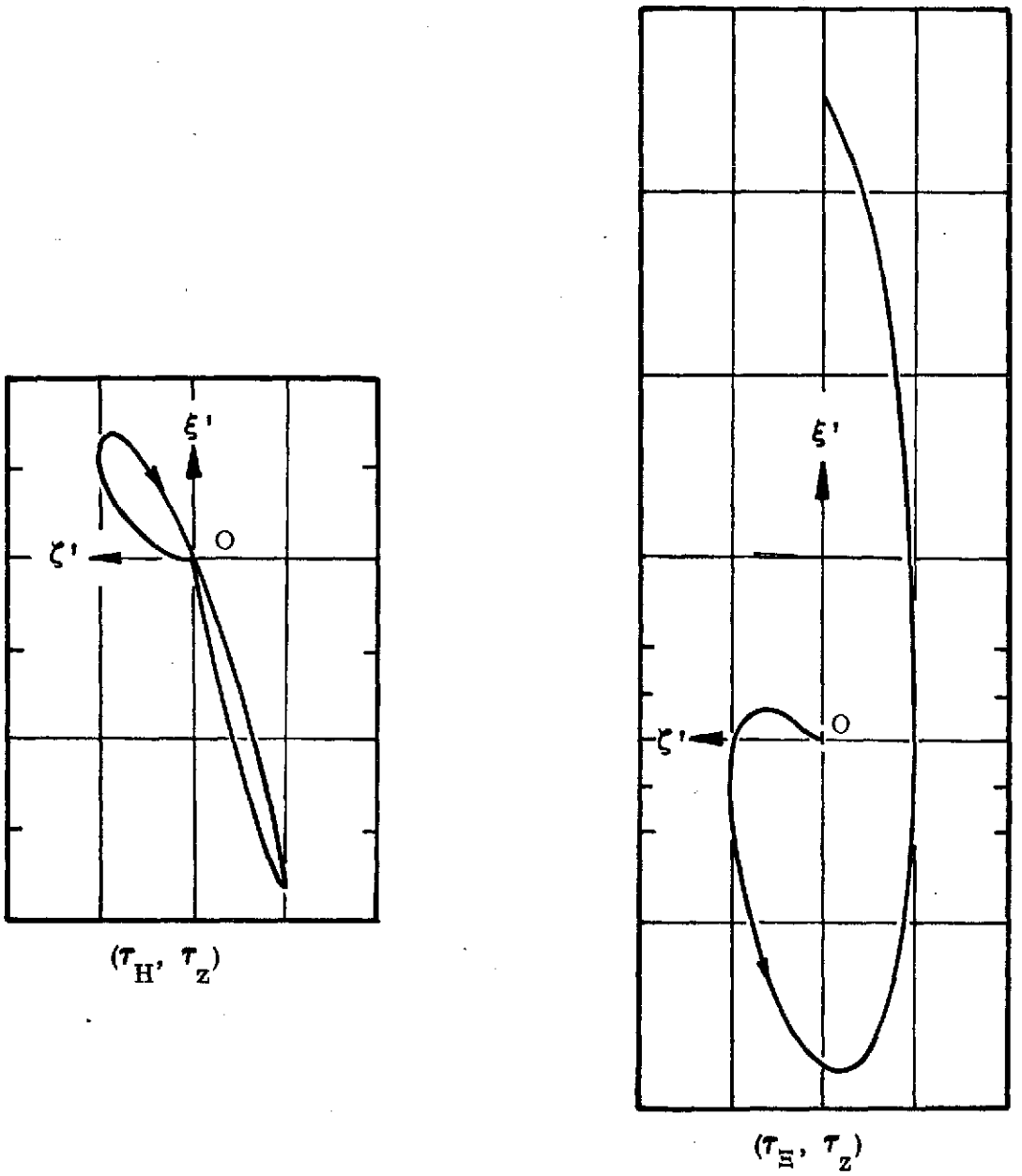


FIG. 37. Typical out-of-plane hodograph traces due to paired specific force ($\bar{\tau}_I$) components. Note: Each graph is for the specified pair of $\tau_i$-values shown. A full hodograph figure, for $\bar{\tau}_I$ proper, is obtained by summing ordinates. Smallest scale divisions, in vicinity of origin, represents equal coordinate increments.

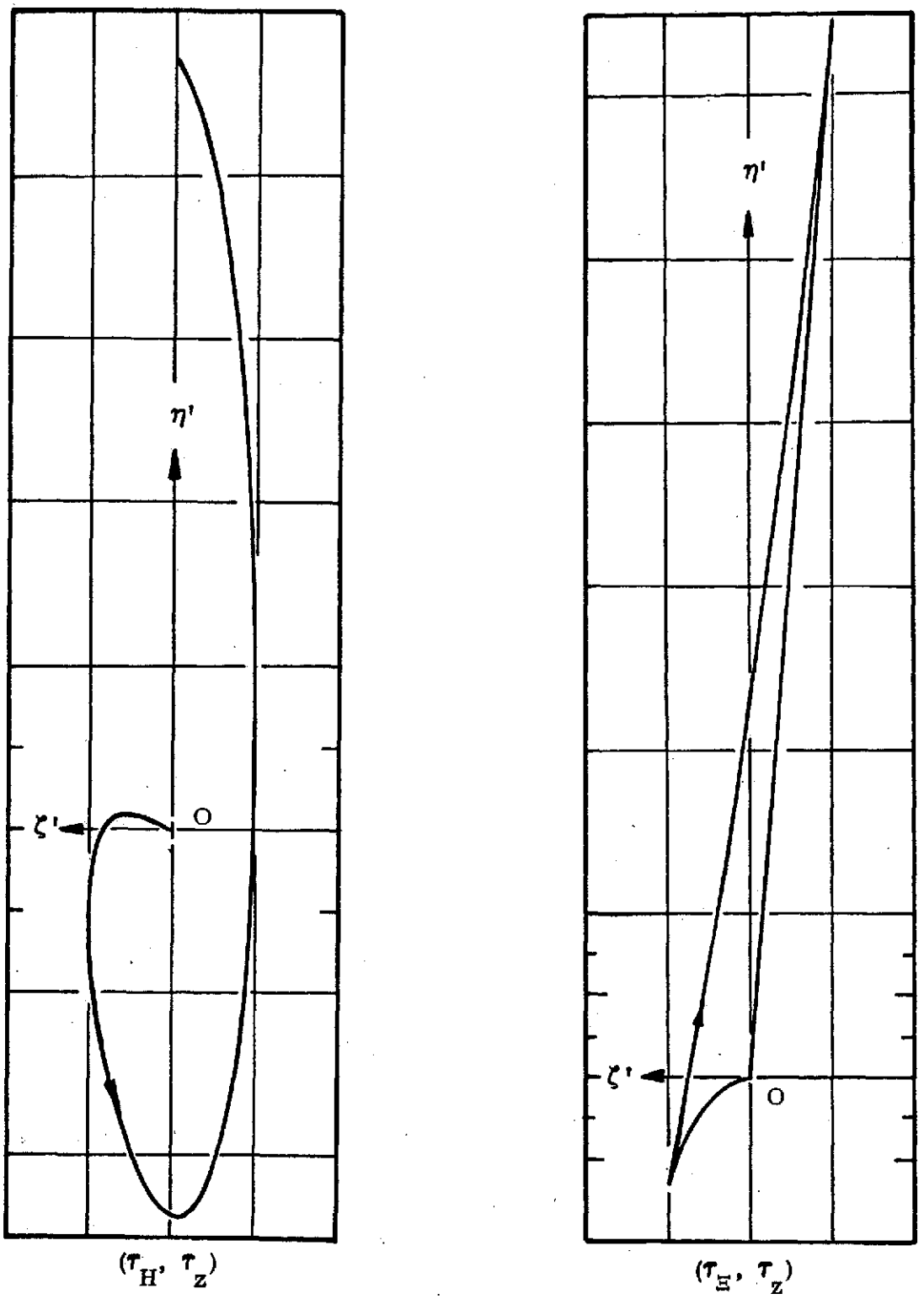


FIG. 38. Hodograph traces, due to the application of specific force paired components, as noted. The full hodograph can be obtained by summing ordinates. Note: Smallest scale divisions, in vicinity of origin, denote equal coordinate increments.

When these matrices are expanded, and scalar expressions acquired, it is found that an appropriate set (here) is:

$$\Xi'(\varphi) = -\tau_{\Xi}\left[\sin\varphi - \frac{13}{4}\sin 2\varphi + 3\varphi(\cos\varphi + \frac{1}{2}\cos 2\varphi)\right] - \tau_{H}\left[5(1-\cos\varphi) - \frac{11}{4}(1-\cos 2\varphi) + \frac{3\varphi}{2}\sin 2\varphi\right],$$

$$H'(\varphi) = -\tau_{\Xi}\left[(1-\cos\varphi) - \frac{13}{4}(1-\cos 2\varphi) + 3\varphi(\sin\varphi + \frac{1}{2}\sin 2\varphi)\right] + \tau_{H}\left[5\sin\varphi - \frac{11}{4}\sin 2\varphi + \frac{3\varphi}{2}\cos 2\varphi\right],$$

and

$$Z'(\varphi) = \tau_{Z}\sin\varphi\,. \tag{75b}$$

Sketches of the trace geometries describing these analytical results are found on Figs. (39) and (40), below. Those figures, being compatible with all others contained here, are mainly presented to illustrate trends which will be found for this disturbance type. The secularity for these coordinates is evident, again; also, this character cannot be removed without an elimination of the force, per se.

Throughout much of the work noted in these latter sub-sections it has become more and more evident that the complexities of the inertial frame representations, and referenced disturbances, lead to geometric difficulties. These difficulties relate to problems not so much mathematical, as semantic, in nature. The traces produced for the out-of-plane situations are difficult to name; they do not lead to elegant representations; and, finally, they do not fit a pattern of predictability which one would hope to achieve. For these reasons, primarily, a familarity with these problem conditions is needed if one is to be able to estimate a priori results.

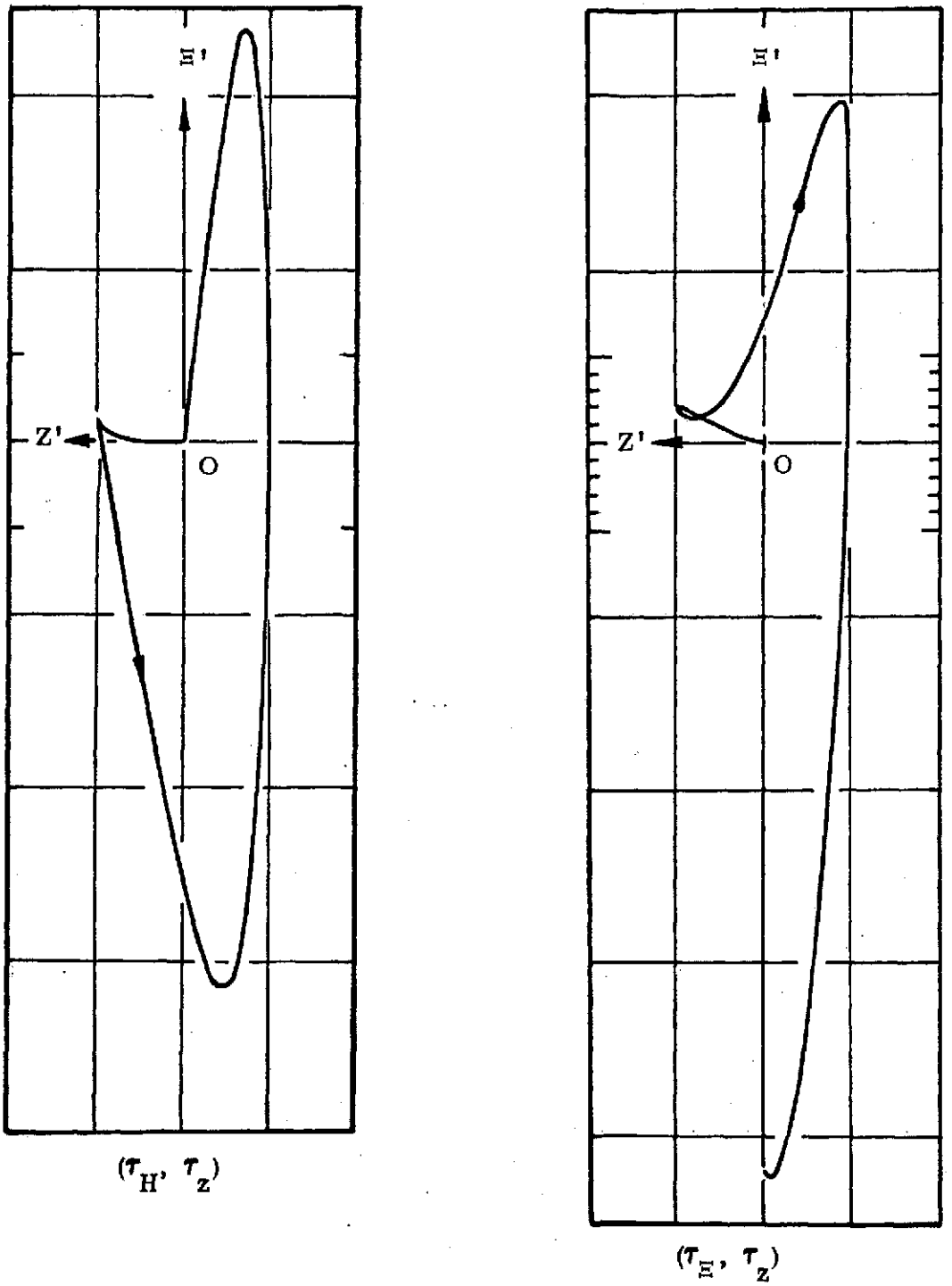


FIG. 39. Typical hodograph traces developed by the application of specified paired $\bar{\tau}_I$ components, as noted. The full figure, due to $\bar{\tau}_I$, is described by summing ordinates. Smallest scale divisions, in vicinity of origin, denotes equal coordinate increments.

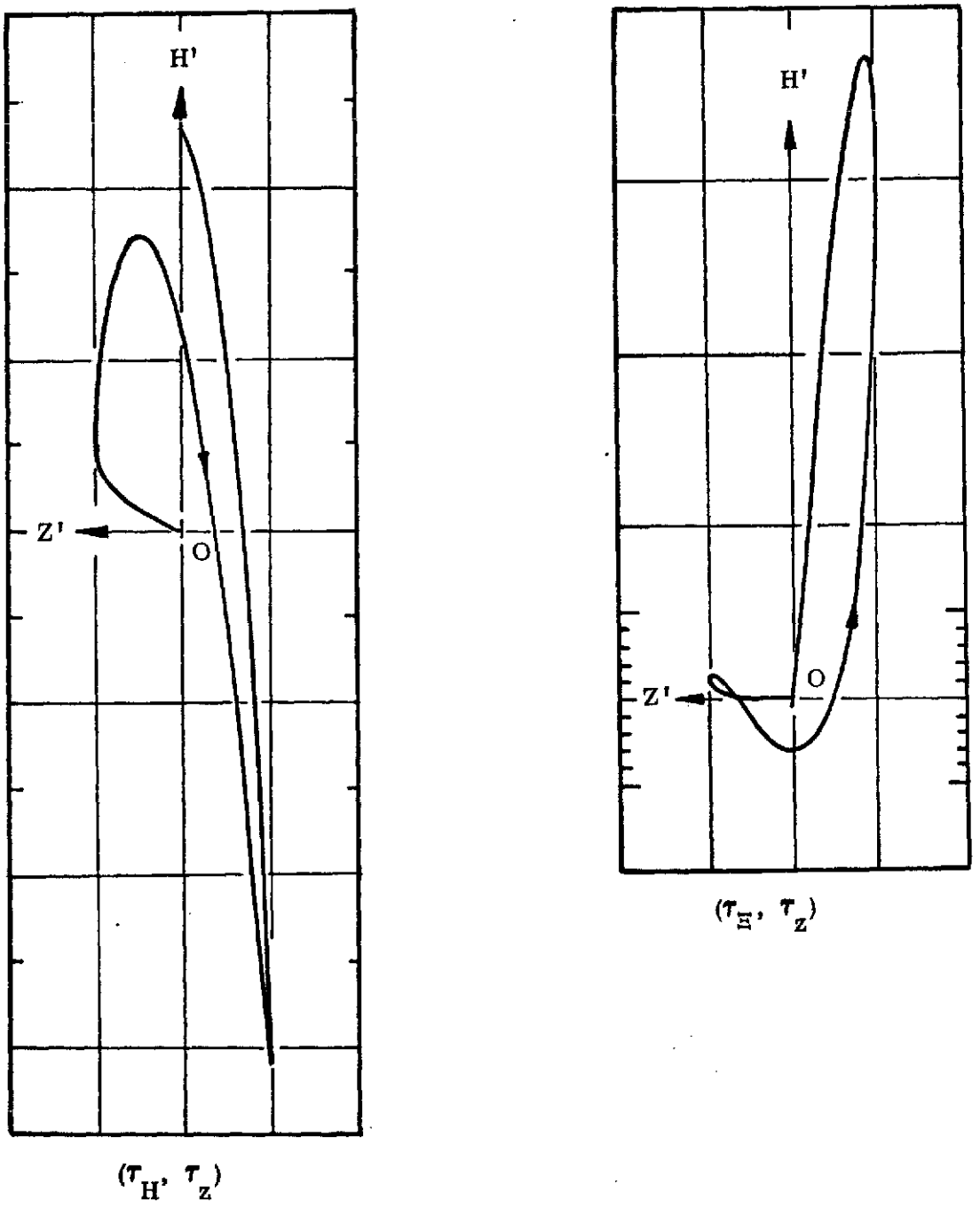


FIG. 40. Trace geometries developed through the application of paired $\bar{\tau}_I$ components, as noted. A composite hodograph figure is obtained by summing ordinates. Note: Smallest scale divisions, in vicinity of the origin, denote equal coordinate increments.

## XVIII. SUMMARY

It has been shown, here, that, in general, geometric traces can be simply constructed to illustrate the relative motions experienced by particles in a number of problem situations. These diagrams will describe the displacements and hodographs which arise as a consequence of initial value inputs and selected disturbance (force) conditions.

Due to the linearization which has been imposed on the mathematical formulation there has been a separation of the in-plane and out-of-plane coordinate solutions. This, in turn, uncoupled results to the extent that the out-of-plane geometries are not as elegantly described as the in-plane one. Also, this has led to some loss in generalization, compared to the in-plane situations. In effect, then, the construction of in-plane traces is easier to represent and to visualize. The out-of-plane geometries are the more complicated cases and generally need some added specializations in order to acquire figures which have some degree of symmetry and simplicity.

It is of interest here to note that traces, representative of motion in the local, rotating frame of reference, are composed from functions which have a frequency equal to that of the base orbit. However, the geometries referred to the inertial frame incorporate single and double frequency functions. Needless to say this adds some complexity to the interpretation of trace geometries; and adds to the difficulties of properly "naming" these various components. Aside from the obvious secular (or divergence) terms which arise for the fixed thrusting cases, there are secular effects which come about through the initial value inputs. Generally, these latter influences can be removed only by the elimination of certain terms, or combination of terms, as dictated (and noted) in the appropriate sections of the documentation. As a general observation it has been found that the secular nature of the traces (in particular, the displacement diagrams) can be eliminated by the removal of initial velocity components which are parallel

to the base orbit velocity vector. That is, so long as there are only initial velocity vectors which are orthogonal to the reference (base orbit) vector, then there will not be a secular characteristic for these traces.

A second, interesting observation is that the in-plane displacement traces progress in opposite directions, depending on the frame of reference. Specifically, for in-plane traces, referred to the inertial frame, the motion over the relative displacement trace follows the base orbit motion. And, contrary to this, the displacements, referred to the rotating frame, have a trace motion which is opposed to the base orbit's direction. One rather simple explanation of this lies in the fact that these frames of reference has a "rotation" relative to each other. That is, the rotating frame (itself) has a rotation, equal to the base orbit's rotation, when it is viewed from inertial space. In this regard, as an example, a point fixed in the inertial relative frame would appear to rotate backward (against the orbit) in the rotating frame. Of course, the converse is true when the two frames of reference switch roles.

Also, herein, it has been demonstrated that the full in-plane traces may be described by a summing of vectors, each of which is described in the general equations. Each vector is selected on the basis of that geometric figure which it described during each circuit of the base orbit. In this fashion, then, the sum of these vectors is described by a sequence of geometrics, all of which lead to those loci which describe the overall trace geometry. Unfortunately this same device cannot be used in the construction of out-of-plane traces. Some of those traces have a relatively simple interpretation, others do not; consequently, this elegance of definition is largely absent for the out-of-plane cases.